TECHNISCHE UNIVERSITÄT MÜNCHEN

Lehrstuhl für Tierhygiene

Isolation and characterisation of peptide aptamers targeting the prion protein

Sabine Gilch

Vollständiger Abdruck der von der Fakultät Wissenschaftszentrum Weihenstephan für Ernährung, Landnutzung und Umwelt der Technischen Universität München zur Erlangung des akademischen Grades eines

Doktors der Naturwissenschaften

genehmigten Dissertation.

Vorsitzende:	Univ.-Prof. A. Schnieke, Ph. D.
Prüfer der Dissertation:	1. Univ.-Prof. Dr. Dr. h. c. J. Bauer
	2. Univ.-Prof. Dr. H. Schätzl
	3. Univ.-Prof. Dr. M. Schemann

Die Dissertation wurde am 07.01.09 bei der Technischen Universität München eingereicht und durch die Fakultät Wissenschaftszentrum Weihenstephan für Ernährung, Landnutzung und Umwelt am 12.03.09 angenommen.

1. Summary

1.1 English version

Prion diseases are rare and obligatory fatal neurodegenerative disorders of humans and animals. The pathogenic event in these diseases is the structural transition of the host-encoded cellular prion protein (PrP^c) into an aberrantly folded pathological isoform PrP^{Sc}. According to the most common models describing the prion conversion process, a direct interaction of both PrP isoforms, possibly in complex with cellular co-factors, is required. Subsequently, the mainly α-helical PrP^c is converted into a molecule with a high content of β-sheets that is prone to aggregate and therefore accumulates within neurons. This finally leads to neurodegeneration, although the exact mechanisms remain largely enigmatic.

The prophylactic and therapeutic regimens against prion diseases are highly limited. Several classes of molecules have been characterized, including e. g. chemical compounds, inhibitors of signalling molecules or β-sheet breaker peptides. Only a few have an effect on the progression of prion disease when administered to infected animals by various routes.

Peptide aptamers comprise a class of molecules consisting of a variable peptide sequence inserted within a constant scaffold protein. The variable peptide sequence is linked N- and C-terminally to the scaffold. Thereby, its conformational freedom is reduced compared to free peptides or peptides fused terminally to a carrier protein, leading to a more stable fold, an increased affinity for their target molecules and an increased stability. Peptide aptamers are of use for inhibition or activation of target proteins, the identification of protein-protein interactions and they can be exploited as a basis for rational drug design. Usually, they are selected by yeast-two hybrid (Y2H) screening of combinatorial peptide aptamer libraries. As scaffold protein, the bacterial thioredoxin A (trxA) is most commonly used. Here, the random peptide moieties are inserted into its active-site loop, thereby destroying the enzymatic activity of trxA.

We generated a constrained peptide library with a complexity of ~ 10^6 individual sequences. In a Y2H screen employing full-length murine PrP (aa 23-231) as a bait three peptide aptamers which reproducibly bind to PrP were selceted. Treatment of prion-infected cells with recombinantly expressed aptamers abolished PrP^{Sc} conversion with an IC_{50} value below 1 µM. For expression in eukaryotic cells, peptide aptamers were fused to N- and C-terminal signal peptides for entry of the secretory pathway and addition of a glycosyl-phosphatidyl-inositol-(GPI-) anchor, respectively. Upon transient transfection, the peptide aptamers were transported to the cell surface and were associated with lipid rafts. However, only one peptide aptamer slightly reduced PrP^{Sc} accumulation in persistently infected cells. To

improve the anti-prion activity of the peptide aptamers, further modifications were introduced. The C-terminal GPI-anchoring signal was replaced either by a KDEL sequence that mediates ER retention or by the transmembrane and cytosolic domain of LAMP-I. The latter protein is directly transported from the trans-Golgi network to lysosomes. Expression of these peptide aptamer versions reduced the amount of PrP^{c} at the cell surface. Dependent on peptide sequence and C-terminal modification, the accumulation of PrP^{Sc} was decreased upon transient expression in persistently infected cells. Furthermore, *de novo* infection with prions can be prevented.

For the first time, it is demonstrated that trxA-based peptide aptamers can be targeted to the secretory pathway and are able to bind to their target protein despite a different environment for binding and post-translational modifications of the target protein. This study expands the possibilities of application of peptide aptamers. Regarding prion diseases, structure determination of PrP-binding peptide aptamers might provide the basis for rational drug design and thereby offer new possibilities to combat prion diseases.

1.2 Deutsche Version

Prion-Erkrankungen sind seltene und unweigerlich tödlich verlaufende Krankheiten, die bei Mensch und Tier vorkommen können. Das pathogene Ereignis bei diesen Erkrankungen ist die strukturelle Umwandlung des wirtseigenen zellulären Prion Proteins (PrP^{c}) in seine pathologische Isoform PrP^{Sc}. Den am weitesten akzeptierten Modellen zufolge, die den Prion-Konversionsprozess beschreiben, ist ein direkte Interaktion zwischen den beiden PrP Isoformen, möglicherweise im Komplex mit zellulären Ko-Faktoren, für die Umfaltung notwendig. Dadurch wird das überwiegend α-helikal gefaltete PrP^{c} in ein Molekül mit hohem β-Faltblatt Anteil umgewandelt, das die Tendenz hat zu aggregieren und deshalb in Neuronen akkumuliert. Dieser Prozess führt letztendlich zur Neurodegeneration, obwohl die genauen Mechanismen bislang nicht eindeutig aufgeklärt sind.

Die prophylaktischen und therapeutischen Möglichkeiten, um gegen diese Krankheiten vorzugehen, sind sehr begrenzt. Einige Molekülklassen wurden bereits auf ihre inhibitorische Wirkung auf die Prion-Konversion hin untersucht, z. b. chemische Substanzen, Inhibitoren von Signalkaskaden oder *β-sheet-breaker* Peptide. Nur sehr wenige zeigten einen Effekt auf den Verlauf der Prion-Erkrankung bei der Anwendung nach experimenteller Infektion von Versuchstieren.

Peptid-Aptamere sind eine Klasse von Molekülen, die aus einer variablen Peptid-Sequenz bestehen, die von einem konstanten Gerüstprotein präsentiert wird. Die Peptid-Sequenz ist N- und C-terminal mit dem Gerüstprotein fusioniert. Dadurch wird die konformationelle

Freiheit im Vergleich zu nativen Peptiden reduziert, was zu einer stabileren intrinsischen Faltung und zu einer erhöhten Affinität für das Zielprotein führt. Peptid-Aptamere werden für die Inhibition oder Aktivierung ihrer Zielmoleküle, die Identifizierung von Protein-Protein-Interaktionen oder als Basis für das Massschneidern chemischer Moleküle verwendet. Gewöhnlich werden sie mittels Yeast-two hybrid Screen einer kombinatorischen Peptid-Aptamer Bibliothek identifiziert. Das bislang am häufigsten verwendete Gerüstprotein ist Thioredoxin A (trxA) aus *E. coli*. Die Zufalls-Peptidbibliothek wird hier in das aktive Zentrum inseriert, dadurch wird die enzymatische Aktivität von trxA blockiert.

Wir haben eine Zufalls-Peptidbibliothek mit einer Komplexizität von etwa 10^6 unterschiedlichen Sequenzen generiert. Mittels Yeast-two hybrid Screen gegen das murine PrP (AS 23-231) als Zielprotein wurden 3 Peptid-Aptamere isoliert, die reproduzierbar an PrP binden. Durch Behandlung mit rekombinant in *E. coli* exprimierten und aufgereinigten Peptid-Aptameren konnte die PrP^{Sc} Konversion in persistent mit Prionen infizierten Zellen mit einem IC_{50}-Wert < 1 µM verhindert werden. Um die Expression der Peptid-Aptamere an der Plasmamembran von eukaryotischen Zellen zu ermöglichen, wurden die Sequenzen N- und C-terminal mit Signalpeptiden fusioniert, die die Translokation in das ER bzw. die Anheftung eines Glycosyl-Phosphatidyl-Inositol (GPI) Ankers vermitteln. Nach transienter Transfektion wurden die Peptid-Aptamere zur Zelloberfläche transportiert, wo sie in *lipid rafts* lokalisiert waren. Jedoch konnte nur eines der Peptid-Aptamere die PrP^{Sc}-Bildung in infizierten Zellen reduzieren. Um die anti-Prion Aktivität der Moleküle zu verbessern, wurden weitere Modifikationen eingeführt. Das C-terminale GPI-Signalpeptid wurde entweder durch ein KDEL ER-Retentionssignal oder durch die transmembrane und cytosolische Domäne des Proteins LAMP-I ersetzt. LAMP-I wird direkt vom Trans-Golgi-Netzwerk zu Lysosomen transportiert. Es zeigte sich, dass die Expression dieser Versionen der Peptid-Aptamere die Expression von PrP^c an der Zelloberfläche reduziert. Abhängig von Peptid-Sequenz und C-terminaler Modifikation konnte die Akkumulierung von PrP^{Sc} in persistent infizierten Zellen bzw. die Neuinfektion durch transiente Expression verhindert werden.

Es wird hier zum ersten Mal gezeigt, dass Peptid-Aptamere im Gerüstprotein trxA im sekretorischen Transportweg exprimiert werden können und dass sich dadurch die Bindungseigenschaften trotz veränderter Bedingungen für die Bindung oder posttranslationaler Modifikationen des Zielproteins nicht verändern. Diese Studie erweitert damit die Anwendungsmöglichkeiten von Peptid-Aptameren. In Bezug auf Prion-Erkrankungen könnte die Bestimmung der Struktur PrP-bindender Peptid-Aptamere die Grundlage für rationales Drug Design bilden und neue Möglichkeiten bieten, um Prion-Erkrankungen zu bekämpfen.

2. Introduction

2.1 Prion diseases

Spongiform degeneration and neuronal loss are characteristical histopathologic hallmarks found in the brains of individuals suffering from transmissible spongiform encephalopathies (TSE) or prion diseases (**Fig. 1**). TSEs are inevitably fatal and occur in humans and animals and can, under certain circumstances, be transmitted within or even between species (Weissmann 1996; Prusiner 1998). Although in humans these disorders were already described in the early 1920s (Creutzfeldt, 1920; Jakob, 1921), the etiology of the causative agent remained enigmatic for many decades. Due to their long incubation times this group of diseases was initially classified as slow-virus infections. However, no virus could be isolated from patients and an immune response, which one would expect upon viral infection, was absent. It became obvious that the causative agent could not be inactivated by methods that destroy nucleic acids like UV-radiation. Infectivity could only be reduced by processes that hydrolysed or denatured proteins, like treatment with sodium hydroxide or urea (Alper et al., 1967).

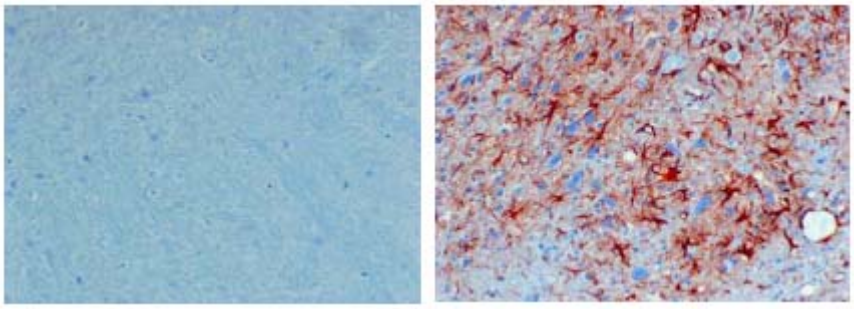

Fig. 1. Immunohistochemistry of murine brain sections for detection of pathological alterations in prion disease. Right picture depicts deposition of PrP^{Sc} aggregates (red), astrogliosis (blue; staining of glial fibrillar acidic protein GFAP) and vacuolation. Left picture: brain section of non-infected animal.

In 1982, S. Prusiner and coworkers were able to isolate a protease-resistant glycoprotein from brains of diseased hamsters that obviously represented the infectious fraction (Prusiner, 1982). Prusiner postulated the 'protein-only' hypothesis, which signifies that the pathogen causing prion diseases consists solely of protein and propagates without genetic information encoded by nucleic acids. To clearly restrain this new group of infectious agents from classical pathogens like viruses, he termed the word 'prion' by combining '***pro***teinaceous ***in***fectious particle' (Prusiner et al., 1984). Further investigations revealed that prions are composed of an abnormally folded isoform, PrP^{Sc} (Bolton et al., 1982), of a host-encoded

protein, the cellular prion protein PrP^c (Oesch et al., 1985). PrP^{Sc} accumulates within the central nervous system and thereby neuronal death is provoked. For proposing and elucidating the protein-only hypothesis, Stanley Prusiner was awarded the Nobel Prize for medicine in 1997.

The composition of the infectious unit exclusively of protein was controversially discussed during the following decades. Recently, profound support for the trueness of the protein-only hypothesis was provided by studies reporting on the *in vitro* generation of prion infectivity out of prion protein expressed recombinantly in *E. coli* (Legname et al., 2004) or of brain-derived PrP^c (Castilla et al., 2005).

2.1.1 Prion diseases of humans

In humans, TSEs can occur in three different ways: sporadic, hereditary or infectiously acquired (**Table 1**). Symptoms are variable but commonly include progressive dementia with personality changes, depression, lack of coordination, myoclonus, insomnia, confusion and memory problems. In late stages patients are unable to e. g. move or speak.

Table 1. Human prion diseases

Etiology	***Disease***	***Causation***
Sporadic	Sporadic CJD (sCJD)	Somatic mutations in PrP? Spontaneous conversion of PrP^c into PrP^{Sc}?
Inherited	Familial CJD (fCJD)	Germline mutations in *PRNP*
	Gerstmann-Sträussler-Scheinker-Syndrome (GSS)	Germline mutations in *PRNP*
	Fatal Familial Insomnia (FFI)	Germline mutations in *PRNP*
Acquired	Iatrogenic CJD (iCJD)	Contaminated tissue or neurosurgery instruments
	Variant CJD (vCJD)	Ingestion of BSE contaminated food
	Kuru	Ritualistic cannibalism

The most frequent human prion disease, accounting for 85 - 90 % of all cases, is **sporadic** Creutzfeldt-Jakob disease (sCJD; Creutzfeldt, 1920; Jakob, 1921), that occurs with an incidence of 1:1.000.000 worldwide (Brown et al., 2000). It is characterised by a long incubation period and a short clinical phase. Interestingly, unlike in Alzheimer's disease there is no increased probability of developing sCJD if more advanced in years. Symptoms arise typically at the age of 45 - 65, and patients usually die within 3 - 6 months. Sporadic CJD can be classified in at least six subtypes (Parchi et al., 1999, Hill et al., 2003). The subtypes and respective clinicopathological characteristics are mainly determined by the genotype (methionine or valine) at the polymorphic codon 129 of the prion protein and the molecular features of PrP^{Sc} (Parchi et al., 1996; 1997; 1999; 2000). Since no pathological mutations within the *PRNP* gene are present, the causation of PrP^{Sc} accumulation is discussed to be a spontaneous conformational change in PrP^{c} or a somatic *PRNP* mutation (Collinge, 1997).
Autosomal dominant mutations in the *PRNP* gene which inevitably lead to the development of **inherited** prion disease, build a proportion of 10 - 15 % of all human cases. More than 30 pathogenic *PRNP* mutations have been described (Collinge, 2001; Wadsworth et al., 2003; Mead, 2006) including insertions, nonsense and missense mutations (**Fig. 2**). According to the clinical syndrome, inherited prion diseases are classified into three subdivisions. Gerstmann-Sträussler-Scheinker (GSS) syndrome (Gerstmann et al., 1936) is mainly caused by the *PRNP* mutation P102L, the mean age at clinical onset is 45 years and the clinical duration can be between 2 and 17 years.

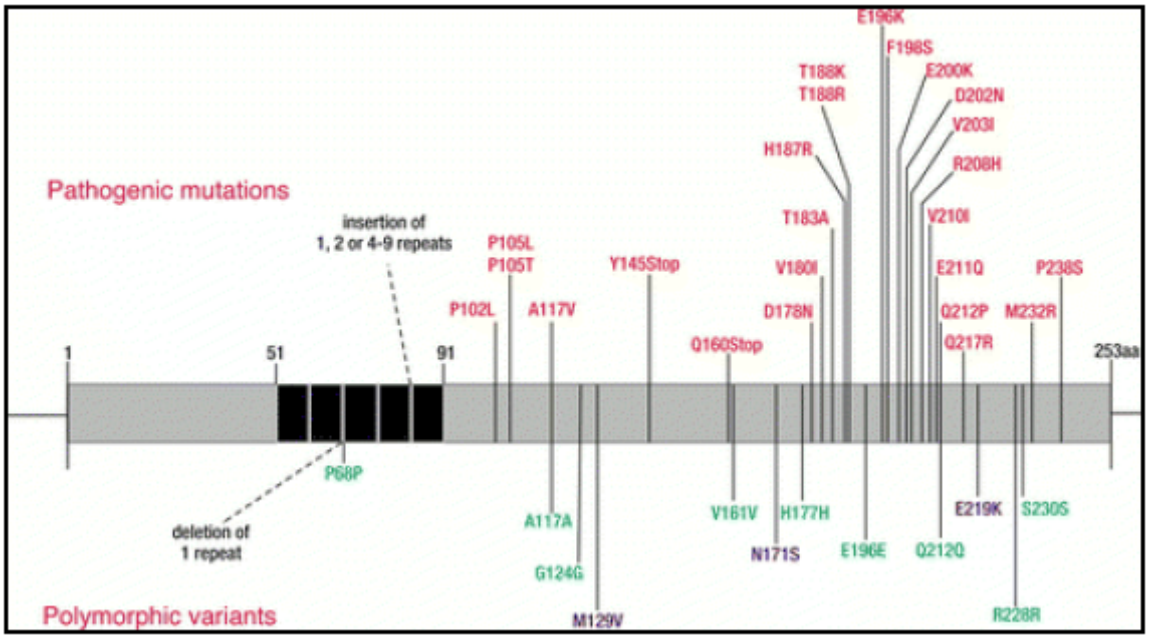

Fig. 2. Pathogenic mutations and polymorphisms of the human *PRNP* gene (from Collinge et al., 2001).

The most recently described inherited prion disorder Fatal Familial Insomnia (FFI) (Lugaresi et al., 1986) is caused by a missense mutation at codon 178 (D178N) and is extremely rare. However, occurrence of FFI is modulated by the polymorphism at codon 129. At this position, either valine or methionine is encoded, and homozygosity for either valine or methionine seems to genetically predispose humans for the development of sporadic or acquired CJD. FFI only appears if on the *PRNP* allele with the D178N mutation a valine is encoded at position 129. Otherwise, with a methionine in connection with D178N, the patient develops familial CJD (fCJD),

Acquired prion diseases in humans encompass Kuru, iatrogenic CJD (iCJD) and variant CJD (vCJD). Kuru, described for the first time in 1957 (Gajdusek & Zigas, 1957), arose among the Fore people in Papua Neuguinea. As a form of worship, parts of dead bodies including the brain were eaten by the tribespeople, thereby ingesting infectious prions. In the mid 1950s, this ritual cannibalism was prohibited and the chain of infection was completely interrupted. However, more than 40 years after cession of cannibalism insular cases of Kuru were still reported (Collinge, 2001), which were infected before.

Iatrogenic CJD spread mainly by the administration of growth hormone extracted from the hypophyses of human cadavers, the transplantation of cornea or dura mater grafts or the use of inadequately decontaminated neurosurgery instruments (Davanipour et al., 1985; Lueck et al., 2000; Head et al., 2002).

In 1995, a novel human prion disease appeared, basically in the UK, but later also in several other European countries (Will et al., 1996; Collinge & Rossor 1996). Mainly teenagers and younger people were affected, in sharp contrast to sCJD, and the disease was denominated variant Creutzfeldt-Jakob disease (vCJD). vCJD is characterised by early onset and a prolonged clinical phase (2 – 3 years), with a predominance of ataxia and psychiatric disturbances without early dementia symptoms (Zeidler et al., 1997, Hill et al., 1999, Belay 1999). Histopathologically, vCJD can be distinguished from sCJD by the presence of florid plaques (**Fig. 3;** Wadsworth & Collinge, 2007), which are similar to those found in brains of cattles affected with bovine spongiform encephalopathy (BSE). Local and chronological coincidence of vCJD with the BSE epidemic were the first indications that BSE might be the cause of vCJD. This assumption was supported by transmission studies of BSE and vCJD to transgenic mice expressing human PrP (Bruce et al., 1994, Hill et al., 1997) and macaques (Lasmezas et al., 1996), and molecular strain typing (Collinge et al., 1996a).

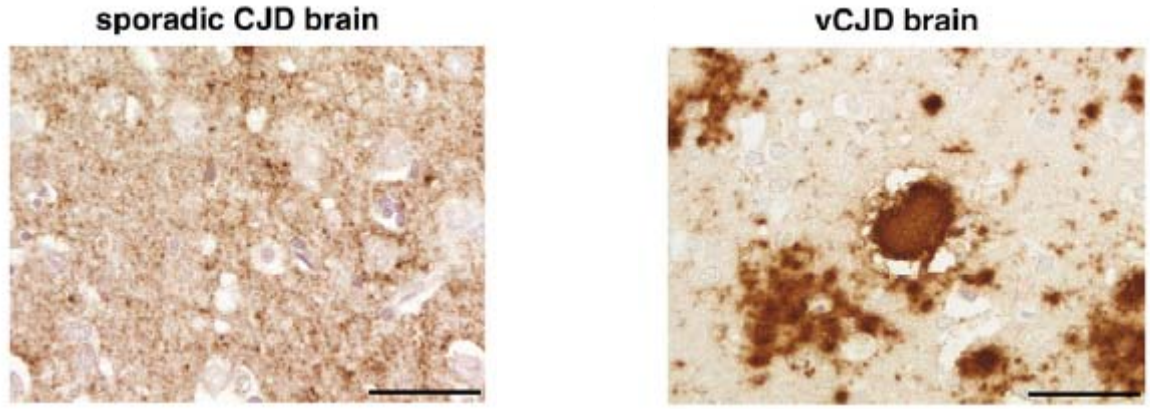

Fig. 3. Histopathological comparison of sCJD and vCJD brain lesions. The left panel depicts abnormal PrP^{Sc} deposition appearing as diffuse synaptic staining. In vCJD (right panel) florid plaques are visible. They are characterised by the presence of an amyloid core surrounded by a ring of spongiform vacuoles (from Wadsworth & Collinge, 2007).

To date, it is commonly accepted that vCJD arose because of the consumption of BSE contaminated food. So far, more than 200 cases of vCJD are known and statistics suggest that the number of individuals affected by vCJD during the next years may range between hundreds and thousands (Donnelly et al., 2002; Ghani et al., 2002). Remarkably, all clinical vCJD cases reveal homozygosity for methionine at *PRNP* codon 129 (Collinge et al., 1996). In vCJD, PrP^{Sc} is not only present within the brain, but also distributed throughout the lymphoreticular system (Wadsworth et al., 2001). This opens the possibility for lateral transfer, and indeed lateral transmission via blood transfusion has been described, giving rise to secondary vCJD (Llewelyn et al., 2004; Peden et al., 2004).

2.1.2 Prion diseases of animals

Besides humans a wide variety of mammals can be affected by TSEs (**Table 2**). In fact, scrapie of sheep and goats was described as early as 1732 (McGowan 1914). Scrapie, the name of which was assigned due to excessive scratching of the affected animals, is transmitted horizontally and vertically (Brotherston et al., 1968; Dickinson et al., 1974).

Table 2. Animal prion diseases

Disease	*Species*	*Causation*
Scrapie	Sheep and goat	Vertical and horizontal transmission Spontaneous
TME (transmissible mink encephalopathy)	Mink	Ingestion of contaminated food
FSE (feline spongiform encephalopathy)	Cat and big cat	Ingestion of contaminated food
CWD (chronic wasting disease)	Deer, elk and moose	Vertical and horizontal transmission Sporadic (?)
BSE (bovine spongiform encephalopathy)	Cattle	Ingestion of contaminated food Sporadic (?)

Bovine spongiform encephalopathy (BSE; Wells et al., 1987) with its epidemic dimension arising in the 1990s in the UK and later in many countries worldwide and subsequent zoonotic occurrence of vCJD in humans caused sensation of the general public, since it became obvious that prion diseases can be transmitted between species (cross species transmission). Symptoms of BSE are similar to scrapie, however the scratching is mainly missing. BSE cases were also reported in other European countries, therefore in Germany BSE tests for beef cattle older than 24 months were dictated in 2000/2001. The origin of BSE was probably a changed protocol for the fabrication of meat and bone meal by which prions from sheep and cattle were not inactivated anymore (Wilesmith & Wells 1998; Prusiner 2001). An alternative explanation is that BSE resulted from sporadic BSE cases which were processed to meat and bone meal and subsequently used as fodder for cattle. Further examples for animal TSEs are transmissible mink encephalopathy (TME; Burger & Hartsough, 1965), and feline spongiform encephalopathy (FSE; Wyatt et al., 1991), both occuring in captive animals and probably induced by feeding with prion-contaminated meat.
Animal TSEs described above are diseases of captive animals. In contrast to these, animal prion diseases can also occur in free-ranging wild-life animals. Chronic wasting disease

(CWD) is a prion disease of captive and free-ranging elk, mule deer, white-tailed deer and moose only occurring in North America and South Korea (Williams & Young, 1980; Kahn et al., 2004; Kim et al., 2005). Despite minimal international testing for CWD in Germany an active survey on thousands of deers was performed which were all tested negative for CWD (Schettler et al., 2006). In diseased animals prion infectivity is distributed extensively in the central nervous system and extraneural tissues including lymphoid tissues, pancreas adrenal gland or skeletal muscle (Sigurdson et al., 1999, 2001; Angers et al., 2006). Such an involvement of extra-neural organs in other natural TSEs is only known from vCJD, scrapie and TME (Hadlow et al., 1982; Hadlow et al., 1987; Head et al., 2003). As a specific characteristic, CWD prions are sercreted in saliva which was demonstrated to transmit the disease (Mathiason et al., 2006). This adds to the compelling evidence that CWD is transmitted horizontally (Miller & Williams, 2003) which might be enabled by spread via direct contact among animals or environmental exposure through grazing in areas contaminated by prion-infected secretions, excretions or tissues. Transmission to humans has not been reported so far and there appears to exist a species barrier between cervid prions and human PrP, when assessed in transgenic animal models.

2.1.3 Mechanisms of neurodegeneration in prion diseases

Transmission of prion diseases is mediated by prions which mainly consist of the pathological prion protein isoform PrP^{Sc} that accumulates in the brain. The mechanisms, however, that lead to neuronal cell death remain largely enigmatic. Usually, PrP^{Sc} is equated with neurotoxicity, but the amount of PrP^{Sc} detected in brains of affected individuals did not necessarily correlate with the degree of neurodegeneration. Application of PrP^{Sc} into brains of $PrP^{0/0}$ mice did not induce neuronal cell death despite high amounts of inoculated PrP^{Sc} (Brandner et al., 1996), indicating that PrP^{c} is required for transmission of a neurotoxic signal or that prion conversion has to occur that produces toxic intermediates. Along this line, post-natal depletion of neuronal PrP^{c} in prion-infected mice could prevent disease and revert neurodegeneration although in these mice PrP^{Sc} was present in high amounts within the brains and possibly was propagated by non-neuronal cell types (Mallucci et al., 2003). Interestingly, upon expression of a secreted form of PrP^{c} lacking the GPI-anchoring signal deposition of high amounts of amyloid plaques was discovered upon inoculation with prions. Despite this, clinical manifestations were minimal but disease could be accelerated by co-expression of wild-type PrP^{c} (Chesebro et al., 2005). Indeed, small PrP^{Sc} oligomers that might be formed during the conversion process were more toxic to various cell types than amyloid fibrils composed of PrP^{Sc} (Novitskaya et al., 2006, Simoneau et al, 2007). Such oligomers also appear to represent the most infectious unit in prion diseases, at least for the

scrapie strain RML (Silveira et al., 2005). All these data described above point out that PrP^{Sc} is not necessarily neurotoxic. Critical factors for neurodegeneration appear to be the expression of PrP^{c} in neurons and probably the neuron-associated *de novo* conversion of PrP^{c} into PrP^{Sc}.

Furthermore, the innate immune system represented mainly by microglial cells within the brain might play a fundamental role in neurodegeneration observed in prion diseases. Release of reactive oxygen species (ROS) or pro-inflammatory cytokines may contribute to neuronal damage (Brown, 2001; Perry, 2004) However, also the role of microglia in neurodegeneration is controversial since these cells have the capacity to degrade PrP^{Sc}. Altogether, these conflicting data do not outline a clear mechanism how neurodegeneration occurs.

2.2 The prion proteins

The prion protein gene family comprises three members: *PRNP* encoding the prion protein (Basler et al., 1986), *PRND* for doppel (Moore et al., 1999), and the recently characterised *SPRN* (Premzl et al., 2003) standing for shadoo (shadow) of the prion protein. Doppel is usually not expressed in the brain and has a predicted role in male fertility (Behrens et al., 2002). Yet it is responsible for the neurodegenerative phenotype observed in certain $PrP^{0/0}$ mouse lines, in which expression of doppel was accidentally triggered (Moore et al., 1999). Shadoo is expressed within the brain mainly complementary to PrP and its function in physiology and pathology is so far unknown (Watts et al., 2007).

2.2.1 Cellular prion protein PrP^{c}

For development of prion disease, *Prnp* expression is absolutely required (Bueler et al., 1993). The gene product, the cellular isoform of the prion protein PrP^{c} is a glycoprotein expressed in many extraneural tissues (Bendheim et al., 1992), but with highest levels in the central nervous system (CNS), specifically in neurons (Kretzschmar et al., 1986). It occurs in several topologies. The most abundant form is located at the cell surface where it is attached by a GPI-anchor (Stahl et al., 1992). Furthermore, two transmembrane forms were described in which the central hydrophobic domain (HD; aa 110 – 135) sticks in the membrane. ^{Ntm}PrP is a stop-transfer mutant of PrP^{c} with the amino-terminal part located in the lumen of the ER. In ^{Ctm}PrP the transmembrane region is reverted to produce a PrP with a luminal C-terminal part and a cytosolic amino-terminus (Hegde et al., 1998). The latter is implicated in neurotoxicity and linked to certain mutations that cause an increased formation of ^{Ctm}PrP, e.

g. A117V leading to development of GSS (Hegde et al., 1998). Cytosolic PrP (PrPcyto), which was only discovered in a subset of neurons (Mironov et al., 2003), has been further investigated in cell culture and transgenic mice and these studies suggested neurotoxic activity of this mislocated protein (Ma et al., 2002a; 2002b, Rambold et al., 2006).

2.2.1.1 The prion protein gene structure

The prion protein gene is highly conserved in mammals, birds, amphibia and fishes (Schätzl et al., 1995; Wopfner et al., 1999; Strumbo et al., 2001; Suzuki et al., 2002; Rivera-Milla et al., 2003). It is located at the short arm of human chromosome 20 and the corresponding region of chromosome 2 in mice (Robakis et al., 1986, Sparkes et al., 1986). Human *PRNP* consists of two, murine *Prnp* of three exons. Exon 2 has no homologue in human *PRNP*, and the entire open reading frame (ORF) is encoded in exon 3, eliminating the possibility of alternative splicing within the ORF (Basler et al., 1986; Westaway et al., 1994) (**Fig. 4**).

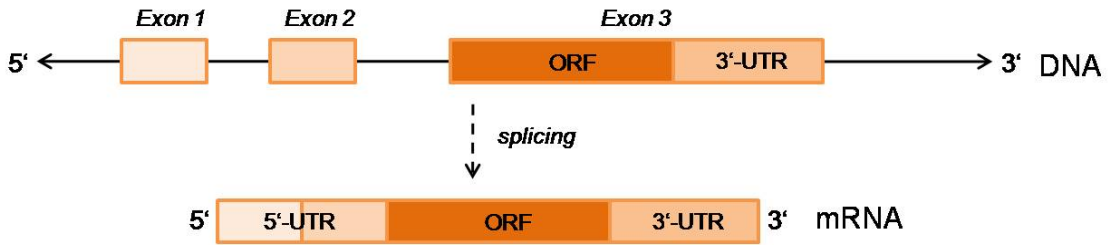

Fig. 4. Structure of murine *Prnp*. Murine *Prnp* consists of the short exons 1 and 2 and the long exon 3. The entire open reading frame (ORF) is encoded in exon 3, followed by a long 3' untranslated region (3'UTR).

The transcribed mRNA is between 2,1 and 2,5 kb in size and the translation product PrP^c consists of ~ 250 amino acids, depending on the species. The promoter lacks a typical TATA-box and contains potential binding sites for transcription factors of the SP1-family and AP-1 (Basler et al., 1986). Transcription factors SP1 and MTF-1 indeed appear to be involved in regulation of PrP^c expression (Bellingham et al., 2008). Interestingly, some insulinoma and pheochromocytoma cell lines down-regulate PrPc expression on the mRNA level in response to challenge with prion infected brain homogenates which confers some resistance to prion infection on those cells (Aguib et al., 2008).

2.2.1.2 Cell biology of PrP^c

The primary sequence of PrP^c consists of 254 amino acids in mice and 253 amino acids in humans. It contains a N-terminal signal peptide of 22 amino acids conferring translocation of the nascent polypeptide chain into the endoplasmic reticulum (ER) via the translocon (**Fig. 5**). The N-terminal signal peptide is co-translationally cleaved off by a signal peptide peptidase (Oesch et al., 1985). The posttranslational addition of a

glycosylphosphatidylinositol (GPI-) anchor mediating membrane linkage of PrP^c is promoted by a C-terminal signal peptide which is post-tranlationally removed (Stahl et al., 1992). Two N-linked carbohydrate moieties can be added at amino acid positions N180 and N196, giving rise to either di-, mono- or unglycosylated PrP. Upon misfolding, at least a small portion of PrP^c might be retro-translocated to the cytosol and is subjected to proteasomal degradation (Ma & Lindquist, 2002a).

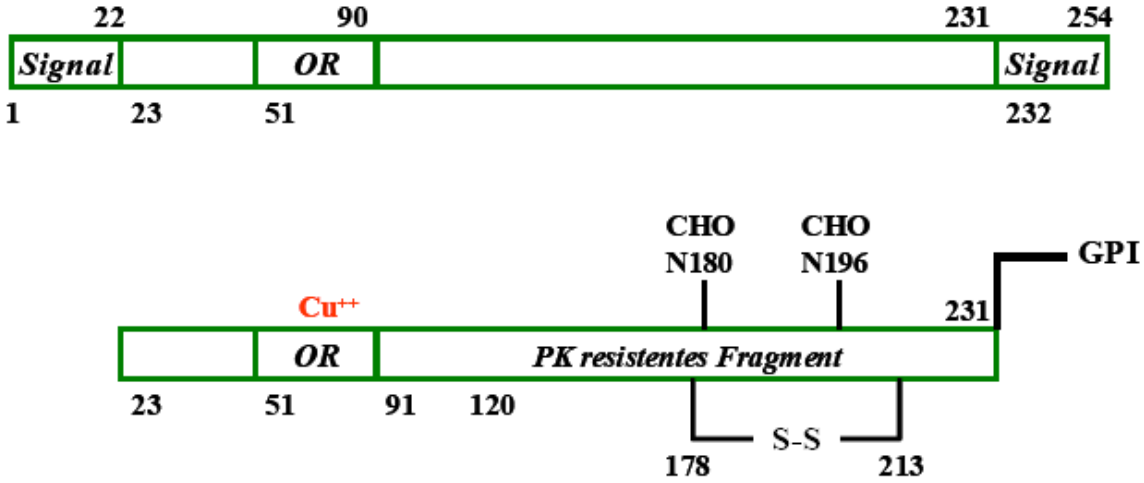

Fig. 5. Primary structure of murine PrP^c. The primary translation product (upper panel) with 254 amino acids (aa) contains a N-terminal (aa 1 – 22) and a C-terminal (aa 232 – 254) signal peptide. The N-terminal half of PrP^c comprises the octarepeat region (OR; aa 51 - 90), consisting of 5 repetitions of a G/P-rich octapeptide. In mature PrP^c (lower panel), both signal peptides are cleaved off and at the C-terminus, a glycosylphosphatidyl-inositol (GPI-) anchor is covalently linked to serine 231. The protein can be modified by two N-linked carbohydrate moieties at N180 and N196 (CHO), and an intramolecular disulfide bond is formed between C178 and C213. The C-terminal portion (aa 91 – 231) encompasses the PK resistant fragment in the PrP^{Sc} isoform. Copper ions (Cu^{2+}) can coordinatively bind to the octarepeat region.

Within the ER, one intramolecular disulfide bridge is built between residues C178 and C213. PrP^c transits through the secretory pathway to the plasma membrane (**Fig. 6**) where it is located in lipid rafts (Taraboulos et al., 1995; Vey et al., 1996; Madore et al., 1999), membrane microdomains with a high cholesterol and sphingolipid content. However, PrP^c can also be shedded (Parkin et al., 2004; Heiseke et al., 2008) and has been found to be associated with exosomes (Fevrier et al., 2004; Vella et al., 2007). Several studies highlight the importance of plasma membrane localisation and in particular lipid raft association for prion conversion (Caughey & Raymond, 1991; Taraboulos et al., 1995; Kaneko et al., 1997). The mechanism by which internalisation occurs is still under debate, and may either result from clathrin-mediated endocytosis (Sunyach et al., 2003), caveolin-dependent pathways (Prado et al., 2004; Peters et al., 2003) or through lipid rafts (Taraboulos et al., 1995). Complexation of copper ions with the octapeptide repeat domain within the PrP^c amino-terminus promotes its clathrin-mediated internalisation (Shyng et al., 1995). By interaction

with the N-terminal domain of PrP^c, the low-density lipoprotein receptor-related protein 1 (LRP1) appears to support transport of PrP^c through the secretory pathway. Knock-down of LRP1 led to retention of PrP^c in biosynthetic compartments (Parkyn et al., 2008), which is paralleled by the observation that deletion of N-terminal PrP (aa 23 – 90) decelerated the transport of PrP^c through the secretory pathway to the cell surface (Nunziante et al., 2003). Further transmembrane receptors supposed to promote PrP^c internalisation are the 37 kDa/67-kDa laminin receptor (LRP/LR; Hundt et al., 2001) or glycosaminoglycans (GAGs; Pan et al., 2002). Following internalisation PrP^c can recycle from endosomes back to the plasma membrane (Vey et al., 1996). Eventually, PrP^c is transported to lysosomes for degradation, and it has a half-life in N2a neuroblastoma cells of ~ 3 - 4 hours (Borchelt et al., 1990; Caughey & Raymond, 1991).

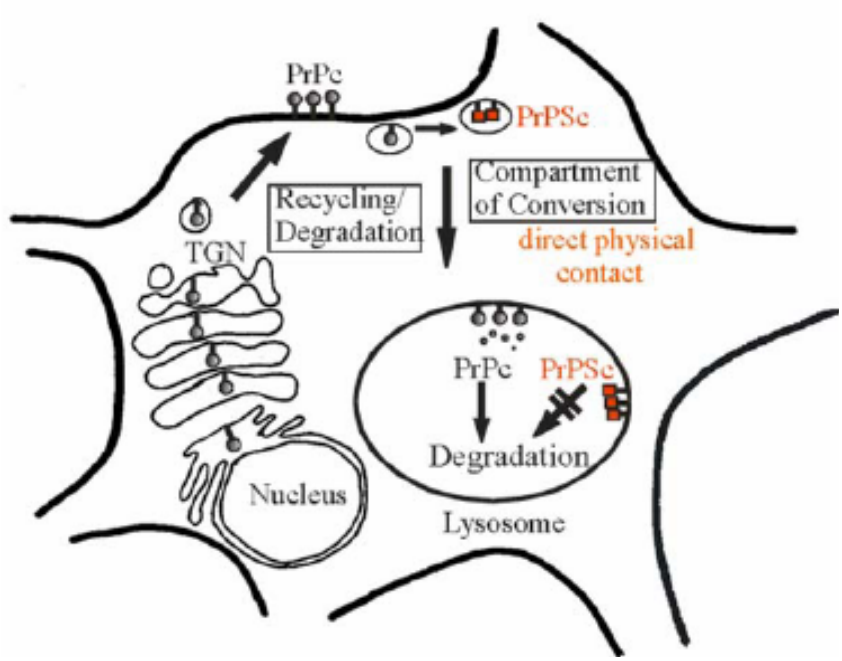

Fig. 6. Subcellular trafficking of PrP. PrP^c is imported into the endoplasmic reticulum (ER) and transported along the secretory pathway to the plasma membrane. It is internalised and can be recycled to the plasma membrane, before it is finally routed to lysosomes for degradation. In prion-infected cells, a portion of PrP^c interacts with PrP^{Sc} in a so far unknown compartment of conversion. PrP^{Sc} is degraded very slowly and accumulates in lysosomes.

2.2.1.3 Functions of the cellular prion protein

The definite function of PrP^c could not be elucidated so far. High expression in neurons (Kretzschmar et al., 1986) and evolutionary conservation in many species (Schätzl et al., 1995; Wopfner et al., 1999) indicate an important biological role. *Prnp* gene knock-out in mice did not display a prominent phenotype but suggests that PrP^c may function in

neurotransmission (Manson et al., 1994; Colling et al., 1996), regulation of circadian activity rhythms and sleep patterns (Tobler et al., 1996). Copper ions can bind coordinatively to the octarepeat region of PrP^c, and this binding stimulates its internalisation, pointing at a role in copper homeostasis (Hornshaw et al., 1995; Brown et al., 1997; Pauly & Harris, 1998). Lipid rafts are domains in which protein interactions resulting in signal transduction events are favoured due to the spatial proximity of proteins. PrP^c as a lipid raft protein might play a role in signalling, supported by observations in neuronal cells. Here, cross-linking of PrP^c led to the activation of the tyrosine kinase Fyn (Mouillet-Richard et al., 2000). Several interactors of PrP^c are implicated in signal transduction, like synapsin Ib and grb-2 (Spielhaupter & Schätzl, 2001). Further candidate proteins identified to bind to PrP^c are the anti-apoptotic Bcl-2 protein (Kurschner & Morgan, 1996), Hsp-60 (Edenhofer et al., 1996), the 37 kDa transmembrane laminin receptor precursor (LRP; Rieger et al., 1997) and neuronal cell adhesion molecules (NCAM; Schmidt-Ulms et al., 2001). However, most compelling evidence exists that PrP^c has neuroprotective properties. It protects cells against oxidative stress (Brown & Besinger, 1998; Haigh & Brown, 2006; Dupiereux et al., 2007), and an anti-apoptotic function is under debate (Roucou et al., 2003; 2005; Nishimura et al., 2007; Rangel et al., 2007; Rambold et al., 2008). Of note, the stress-protective function of PrP^c is impaired by the presence of PrP^{Sc} (Rambold et al., 2008).

The only fact which is definitely true is that PrP^c expression is necessary for onset of prion disease (Bueler et al., 1992) and for development of the neurotoxic phenotype that parallels TSEs (Mallucci et al., 2003).

2.2.2 Models of prion conversion

The pathogenic prion protein isoform PrP^{Sc}, which is, according to the protein-only hypothesis, the only infectious component of prions (Prusiner, 1998), arises from PrP^c by structural re-folding. Yet, the exact mechanisms leading to the marked changes in secondary and tertiary structure of the protein are not fully understood. To date, two models how the conversion process can be explained exist. The heterodimer model was proposed by Cohen and Prusiner (Prusiner et al., 1990; Cohen et al., 1994). Here, an equilibrium of PrP^c with a folding intermediate PrP* is proposed. PrP* is a partially unfolded PrP^c molecule, however unfolding is reversible, and the conformation of PrP^c is favoured. PrP* can form heterodimers with PrP^{Sc} and thereby adopts PrP^{Sc} structure to build a homodimer, a process which might be supported by other cellular factors, e. g. molecular chaperones. The homodimer dissociates and the released PrP^{Sc} monomers can re-fold further PrP* molecules, leading to an autocatalytic propagation of PrP^{Sc}. Since this process is a very rare event, spontaneous

disease only appears in elder people or upon destabilisation of PrP^c by mutations which lower the energy barrier for the structural transitions.

The second and now most widely accepted model is the nucleation dependent polymerisation model postulated by Lansbury and Caughey (**Fig. 7**; Come & Lansbury 1993; Caughey et al., 1995).

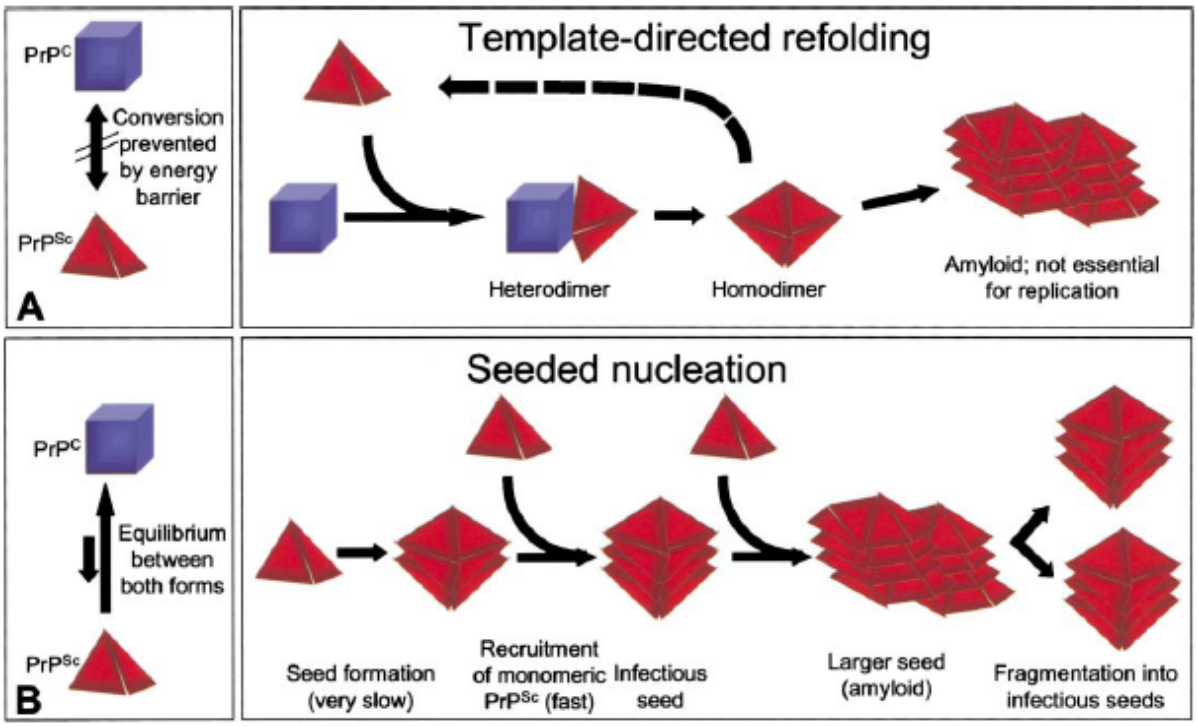

Fig. 7. Current models of prion conversion. Upon template-directed refolding, PrP^c forms a heterodimer with PrP^{Sc}. This leads to refolding of PrP^c to PrP^{Sc}. The resulting homodimer dissociates or forms amyloid aggregates, which are not essential for replication. In seeded nucleation, an equilibrium between PrP^c and PrP^{Sc} conformers exists. PrP^{Sc} molecules can form seeds, which is a rare process. If seeds are formed, more PrP^{Sc} monomers are recruited, amyloid is formed that breaks into smaller fragments which act as infectious seeds (from Aguzzi & Polymenidou, 2004).

Here an equilibrium between PrP^c and PrP^{Sc} is suggested, lying on the side of PrP^c. In a rare event, PrP^{Sc} molecules can form infectious oligomers, which serve as nucleation seed for the rapid deposition of further PrP^c molecules which then are re-folded to the conformation of PrP^{Sc}. Thereby, high molecular weight PrP^{Sc} aggregates are formed which break up and can form new seeds for further acquisition of PrP^c molecules. Interestingly, the most infectious unit are indeed oligomeric PrP^{Sc} units consisting of 14 to 28 PrP^{Sc} molecules, at least for prion strain RML (Silveira et al., 2005). Although suggesting different mechanisms, with both models all manifestation forms of prion diseases can be explained.

2.2.3 Biochemical and structural characteristics of PrP^c and PrP^{Sc}

Independent of the model conversion of PrP^c into PrP^{Sc} is associated with pronounced structural changes leading to distinct biochemical characteristics of the two PrP isoforms which do not differ in primary structure and posttranslational modifications (Pan et al., 1993). So far, no crystal structures are available, neither for PrP^{Sc} nor for PrP^c. However, the structure of PrP^c has been resolved by nuclear magnetic resonance (NMR) analysis of PrP23 - 231 resembling mature PrP^c, purified upon recombinant expression in *E. coli* (Riek et al., 1996; 1997). To the N-terminal part (aa 23-120) no defined structure could be assigned, suggesting that this part of the protein is highly flexible. This might be altered upon binding of metal ions to the octarepeat region spanning about amino acid positions 50 – 90, depending on the species (Schätzl et al., 1995; Wopfner et al., 1999). The results delineated for aa 121 – 231 propose a defined globular structure with 3 α-helices and two short antiparallel β-strands. Helix B and C are stabilised by an intramolecular disulfide bridge (**Fig. 8**).

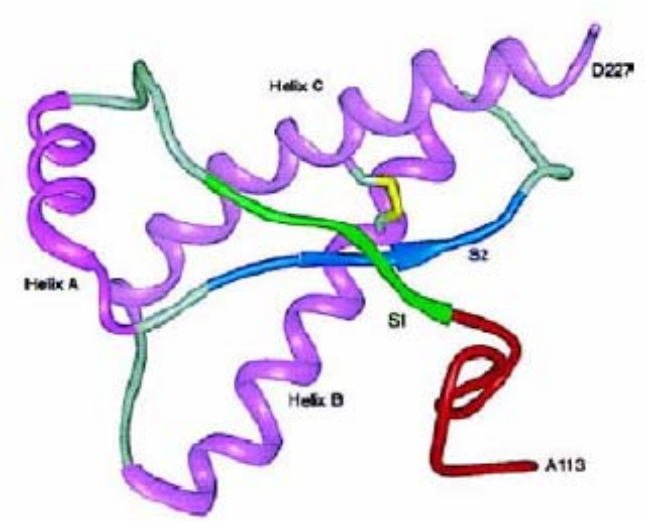

Fig. 8. NMR model of PrP^c structure. NMR analysis suggest that PrP^c contains 3 α-helices (purple) and two β-sheets (blue and green) preceded by a flexible N-terminal part (red). The intramolecular disulfide bond stabilising helices B and C is depicted in yellow (from Prusiner, 1998).

Overall, PrP^c consists of about 42 % α-helices and 3 % β-sheets, in contrast to PrP^{Sc} with 30 % α-helices and 45 % β-sheets (Pan et al., 1993; Gasset et al., 1993). More detailed structural predictions for PrP^{Sc} were obtained by the analysis of 2D-crystals in electron microscopy and molecular modelling (Wille et al., 2002; Govaerts et al., 2004). PrP^{Sc} most probably forms trimers with left-handed β-helices between aa 89 – 175, whereas the C-terminal α-helices and the disulfide linkage are retained (**Fig. 9**).

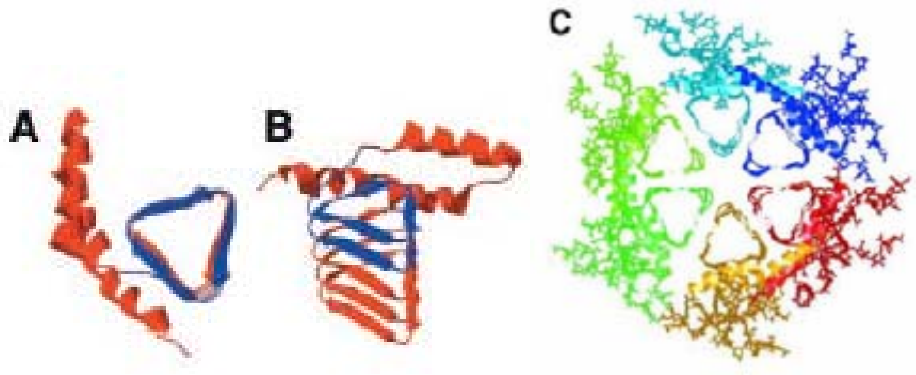

Fig. 9. β-helical model of PrP^{Sc} obtained by 2D-electron microscopy. A and B: top and side view of the protein core of monomeric PrP^{Sc}. Helix B and C are retained whereas aa 89 – 175 are refolded. C: top view of a dimer of trimers model for PrP^{Sc}. Left-handed β-helices form the core, surrounded by helices B and C and the carbohydrate moieties (from Wille et al., 2002).

The described structural transitions account for biochemical differences between PrP^{c} and PrP^{Sc}, which can be exploited for diagnostic purposes. Most remarkably, the C-terminal part of PrP^{Sc} (aa 90-231) is resistant to treatment with proteinase K (PK) (Prusiner et al., 1984; Oesch et al., 1985), giving rise to a N-terminally truncated PrP upon proteolytical digestion, by contrast to the complete degradation of PrP^{c} by PK. The occurrence of PK resistant PrP serves as a surrogate marker for prion infection. Further biochemical differences which can be used for diagnostic purposes are summarised in **Table 3.**

Table 3. Structural and biochemical differences of PrP isoforms.

	PrP^{c}	**PrP^{Sc}**
Infectivity	No	Yes
Secondary structure	Mainly α-helical	Mainly β-sheet
PK resistance	No	Yes (partially)
Detergent solubility	Yes	No

2.2.4 Species barrier and prion strains

Prion diseases can be transmitted within and also between species, the latter giving rise to the zoonotic transfer of BSE to humans and the appearance of vCJD. Though, inter-species transmission is restricted by the species barrier. This term refers to the observation that upon infection of one species with prions from another species incubation times of disease are prolonged in most cases, compared to incubation times monitored later upon intra-species transfer (Pattison, 1965). Nevertheless, prions can adapt to another host by serial infections. Species barrier is mainly predicted by the degree of homology between the PrP sequences of two species and the position of the amino acid exchanges (Scott et al., 1989; 1992; 1993; Telling et al., 1994; Schätzl et al., 1995; Priola, 2001). In addition, species-specific co-factors interacting with PrP^{Sc} appear to play a role (Telling et al., 1995). For instance, hamster prions do not cause disease in mice and *vice versa* (Scott et al., 1989; 1992; 1993; Priola, 1999). If transgenic mice expressing hamster PrP in addition to endogenous mouse PrP are infected, species barrier can be overcome and mice generate disease with prion titers comparable to hamsters and equal infectivity. Thereby, inubation times and expression levels of hamster PrP were inversely correlated (Scott et al., 1989; 1992; 1993; Prusiner et al., 1990). However, subclinical infection of wild-type mice with hamster prions was also demonstrated (Hill et al., 2000). This fuels the discussion whether species barrier really is an absolute event or whether PrP^{Sc} is propagated but the host dies before symptoms can occur. In this case, possibly prions can be transmitted.

The existence of prion strains represents a conundrum. Prion strains describe the phenomenon that despite identical primary structure different pathologies can be elicited which was initially described when mink prions were transmitted to hamsters and induced two distinct syndromes (Bessen et al., 1992). Prion strains can be characterised by glycoform profiling, fragment size of PrP^{Sc} upon PK digestion and different lesion profiles within the brain or incubation periods (Collinge et al., 1996, Safar et al., 1998). Strain properties are obviously imprinted in the PrP^{Sc} conformation (Telling et al., 1996; Scott et al., 1997) and can be propagated (Dickinson et al., 1968, Bruce et al., 1991), in case of BSE strain even between many species (Will et al., 1996; Collinge & Rossor, 1996). In humans, several prions strains are noted giving rise to different CJD phenotypes (Collinge et al., 1996; Parchi et al., 1996; Telling et al., 1996).

2.2.5 Cell culture models for prion infection

Detailed analysis of molecular and cellular requirements for prion infection or screening of putative anti-prion compounds are two common applications for cell culture models of prion

infection. During the last decade, the diversity of available cell models was strongly growing. However, they differ in the susceptibility for infection with different strains, their origin (neuronal *vs*. non-neuronal), the ability to stably or only transiently propagate prions, and can be either primary cells or permanent cell lines. Although sometimes transient prion propagation can be observed in certain cell lines, this is not a guarantee for establishment of stable infection (Vorberg et al., 2004).

The classical and most widely used cell line is the neuroblastoma line N2a (Butler et al., 1988; Race et al., 1987) and many information regarding cell biology of PrP^{c} and PrP^{Sc} was obtained by studying subcellular localisation or kinetics of synthesis and degradation in these cells (Borchelt et al. 1992; Taraboulos et al., 1994; Vey et al. 1996; Caughey & Raymond 1991; Nunziante et al., 2003). One drawback of this cell line is that it does not exhibit morphological characteristics of prion infection. Such a model was introduced by H. Schätzl with the murine hypothalamic cell line ScGT1 (Schätzl et al., 1997). This cell line can undergo apoptosis and vacuolation upon prion infection similar to neurons in infected brains. Recently, primary cerebellar granular cells (CGN) were reported to be amenable to different prion strains of 3 species, including human CJD (Cronier et al., 2004; 2007).

Cell lines expressing no or undetectable levels of PrP^{c} like the rabbit epithelial line RK13 or cell lines derived from mice devoid of the PrP gene as Hpl3-4 cells (Sakudo et al., 2005) could be stably reconstituted with PrP^{c} (Vilette et al., 2001; Maas et al., 2007). In RK13, heterologous ovine PrP^{c} expression enabled infection with sheep scrapie (Vilette et al., 2001). This was the first report to demonstrate that non-neuronal cells expressing heterologous PrP^{c} can be infected with prions homologous to the introduced PrP^{c}. However, in these cells the expression of tiny and undetectable amounts of endogenous PrP^{c} which might influence prion infection cannot be excluded. Therefore, even more useful due to the deletion of the *Prnp* gene, is the hippocampal Hpl3-4 cell line, which was shown to be susceptible to different mouse scrapie strains upon retroviral transduction with the mouse PrP gene (Maas et al., 2007). Further non-neuronal models are rat pheochromocytoma cells PC12 (Rubenstein et al., 1984), 3T3 and L929 fibroblasts (Vorberg et al., 2004), C2C12 muscle cells (Dlakic et al., 2007) or microglial cells derived from PrP-overexpressing mice (Iwamaru et al., 2007). Although CWD prions can be modestly propagated in cell culture (Raymond et al., 2006), to date no model for BSE prions is available.

Infection of cell cultures with prions usually is an ineffective process and most frequently cells are subcloned prior to in infection in order to isolate clones that are highly susceptible to prion infection (Bosque & Prusiner, 2000; Klöhn et al., 2003). The rate of PrP^{c} converted steadily into PrP^{Sc} is low, for example in RML infected N2a cells only approximately 1 – 5 % of PrP^{c} is converted to PrP^{Sc} (Borchelt et al., 1992). Prions can be transmitted to cell cultures

either by application of infected brain homogenates, cell lysates of infected cells or transfer of culture medium derived from certain infected cell lines (Schätzl et al., 1997; Maas et al., 2007). PrP^{Sc} can similar to PrP^{c} be released in association with exosomes (Fevrier et al., 2004; Vella et al., 2007) which might explain transmission by culture medium (Schätzl et al., 1997). The mechanism by which PrP^{Sc} is internalised remains largely enigmatic, but it does not depend on the expression of PrP^{c} (Magalhaes et al., 2005). GAGs, polysaccharides linked to a protein backbone are constituents of the extracellular matrix and might serve as co-receptors for prions, since heparan sulfate as one representative of GAGs is required for initial internalisation of PrP^{Sc} (Hijazi et al., 2005; Horonchik et al., 2005). The transmembrane protein LRP/LR appears to promote uptake of PrP^{Sc} in certain cell lines (Morel et al., 2005; Gauczynski et al., 2006). In experiments monitoring the uptake of fluorescently labelles purified PrP^{Sc} preparations in the murine septum cell line SN56 most of the PrP^{Sc} was detected in late endosomes and lysosomes (Magalhaes et al., 2005), confirming earlier immuno-electron microsopic studies that revealed localisation of PrP^{Sc} in secondary lysosomes (Laszlo et al., 1992). Despite predominant late endosomal/lysosomal localisation of PrP^{Sc} it can hardly be degraded by the cells and has a rather long half-life of > 24 hours (Ertmer et al., 2004).

The identification of the compartment of prion conversion is still a major challenge in prion research. The conformational changes appear to occur at the cell surface or in the early endocytic pathway (Caughey & Raymond, 1991; Borchelt et al., 1992). Increased retrograde transport to the ER induced experimentally by overexpression of certain mutant rab proteins can enhance PrP^{Sc} formation in N2a cells (Beranger et al., 2002). Cholesterol depletion by various means including inhibition of synthesis and complexation or extraction from the plasma membrane is deleterious for PrP^{Sc} propagation in several cell lines infected with RML prions (Taraboulos et al., 1995; Mange et al., 2000). Therefore, it was assumed that association of PrP^{c} with lipid rafts is crucial for prion conversion.

2.3 Therapy and prophylaxis of prion diseases

2.3.1 Strategies for identification of anti-prion compounds

In numerous efforts of identifying compounds useful against prion diseases, a variety of test systems was established. Based on the respective read-out, drugs with very distinct modes of action were found, also by virtue of library screens. In a high-throughput screen utilizing scanning for intensively fluorescent targets (SIFT) compounds were identified which interfere *in vitro* with the PrP^{c}-PrP^{Sc} interaction (Bertsch et al., 2005). Here, PrP^{Sc} aggregates purified from CJD brains were incubated with recombinant PrP and drugs out of a library comprising

10.000 compounds were tested with respect to inhibition of aggregate growth. Another semi-automated assay monitored the accumulation of amyloid recombinant PrP by thioflavin T staining (Breydo et al., 2005). Although such sole *in vitro* systems are undoubtedly useful for high-throughput screening and automation, a major drawback is that prion conversion in single cells or whole organisms appears to be much more complex than is attachment of recombinant PrP to PrP^{Sc} seeds. So far, *in vitro* generation of *bona fide* infectious prions from recombinant PrP, in this case N-terminally truncated PrP, has been demonstrated only once (Legname et al., 2004), and even here obviously only a tiny fraction of the inoculated material was indeed composed of infectivity. Other studies are based on conversion of recombinant PrP into molecules with PrP^{Sc}-like properties (e. g. partial PK resistance, insolubility, altered secondary structure (Riesner, 2003) which were not associated with infectivity in bioassays. Therefore, it is indispensable to confirm anti-prion activity of identified compounds by cell-based assays and finally in bioassays (**Fig 10**).

Given the drawbacks of *in vitro* methods for screening of anti-prion compounds, the most commonly used model is to select novel drugs by treatment of persistently prion-infected cells and subsequent analysis of their PrP^{Sc} load, which serves as a surrogate marker for prion infectivity. In this more physiological system, cellular requirements for prion conversion, in addition to the physical interaction between both PrP isoforms, are considered. These include for example the proper subcellular localisation and turn-over of PrP^{c} as well as the degradation kinetics of PrP^{Sc}. With this system, library screening in a 96-well format is possible if PrP^{Sc} amounts are measured e.g. by dot blot analysis (Kocisko et al., 2003). Different cell lines infected with various prion strains have been used (Kocisko et al., 2003; 2006).

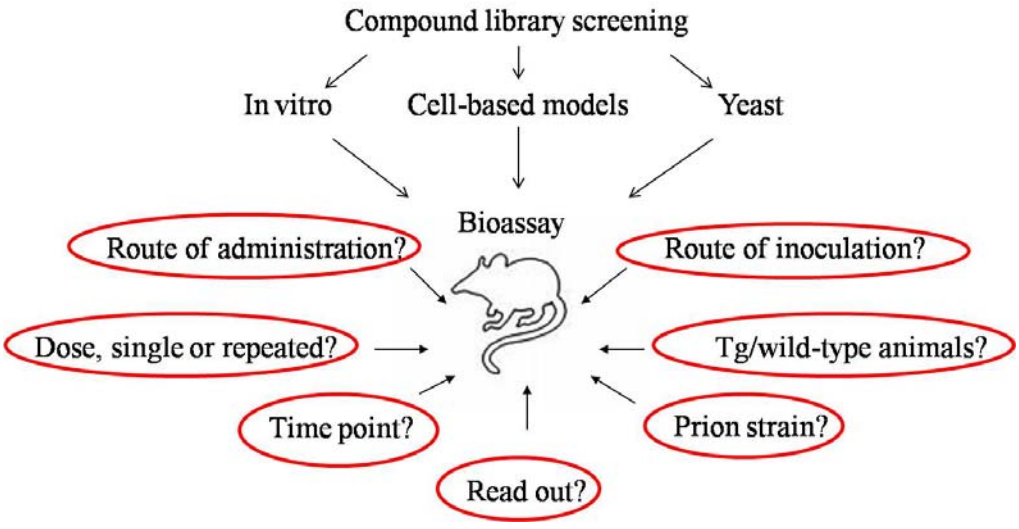

Fig 10. Screening strategies for anti-prion compounds. The most economical method to identify novel anti-prion agents is to screen libraries by either of the mentioned method. However, the effects of any substance need to be evaluated in bioassays. The outcome of bioassays is significantly influenced by numerous experimental parameters.

However, anti-prion activity in persistently infected cell cultures does not necessarily ensure benefits in an *in vivo* situation, mainly due to inadequate bioavailability within the central nervous system or toxicity of the drugs. Very recently, a cell culture system has been generated employing primary cerebellar granular neurons derived from transgenic mice over-expressing PrP^c of different origin, including human PrP (Cronier et al., 2007). Of note, in this study the first system useful for testing substances for inhibition of biosynthesis of human CJD prions was described. With regard to anti-prion activity of substances tested with these cells, results might be more closely related to the *in vivo* situation than upon testing in established cell lines like the neuroblastoma line ScN2a. Nevertheless, any compound selected by cell culture screens needs to be further evaluated in bioassays. Here, the read-out is usually incubation time to prion disease. However, the activity of drugs depends on parameters like route of prion inoculation, prion strain or timing and duration of drug administration (**Fig. 10**).

Although the exact mechanism of prion conversion has not been elucidated to date, the current models offer several points of intervention in this process (**Fig. 11**). It can be distinguished between strategies targeting *de novo* synthesis and degradation of PrP^{Sc}, respectively. *De novo* synthesis can be inhibited for example by knock-down of PrP^c expression using siRNA or by preventing plasma membrane localisation of PrP^c by application of the drug suramin. Furthermore, the interaction between the two PrP isoforms can be prevented by application of anti-PrP antibodies. Alternatively, degradation of PrP^{Sc} can be enhanced which is achived e. g. by imatinib treatment.

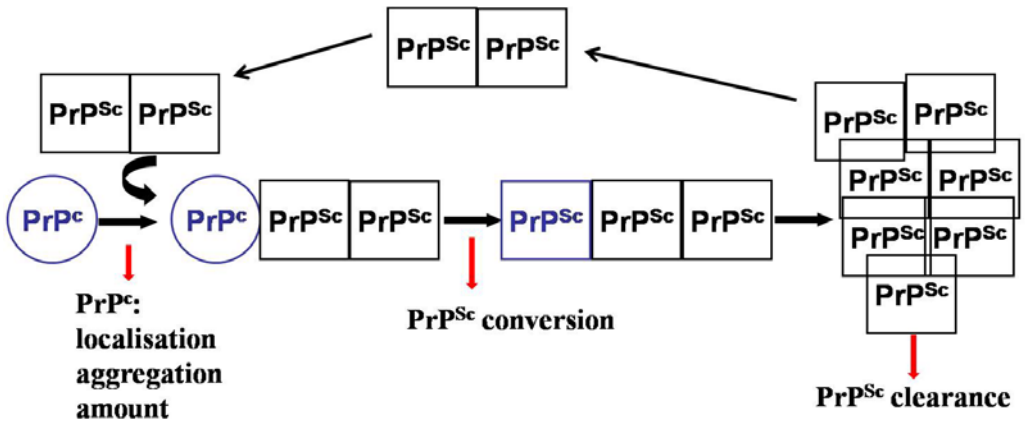

Fig. 11. Possible molecular mechanisms of anti-prion compounds. As targets can serve PrP^c, the interaction of PrP^c and PrP^{Sc} or the degradation of PrP^{Sc}.

2.3.2 Chemical compounds

Most of the known anti-prion drugs are small chemical molecules identified in cell-based assays addressing inhibition of prion conversion. The mode of action is quite divers, and for such compounds interference with every step of the conversion reaction (see **Fig. 11**) was theoretically demonstrated. Sulfated glycans like pentosan polysulphate (PPS) or dextran sulphate 500 (DS500) interfere presumably with binding of PrP to GAGs, known to act as co-receptors for prion protein and/or stimulate endocytosis of PrP^{c} (Shyng et al., 1995; Horonchik et al., 2005; Hijazi et al., 2005). Thereby, PrP^{Sc} levels in prion infected cells are decreased. Both PPS and DS500 prolong incubation time of prion disease in mice or hamsters, depending on prion strain, inoculation route, and time point of drug administration (Farquhar & Dickinson, 1986; Diringer & Ehlers, 1991; Ladogana et al., 1992). If administered by intraventricular infusion, PPS is slightly effective in mice after intracerebral inoculation even if treatment is initiated upon onset of clinical symptoms (Doh-Ura et al., 2004). Other polyanionic compounds inhibiting PrP^{Sc} formation in cell culture are congo red (CR) (Caughey & Race, 1992), heparan sulfate mimetics (Adjou et al., 2003; Schonberger et al., 2003; Larramendy-Gozalo et al., 2007), or suramin (Ladogana et al., 1992; Gilch et al., 2001). Congo red is a widely used dye for staining of amyloid deposits. Reduction of PrP^{Sc} in chronically infected cells and in *in vitro* conversion assays by CR has been repeatedly reported (Caughey & Race, 1992; Caughey et al., 1993). *In vivo* studies in hamsters revealed a delay in onset of disease in i.p. inoculated animals (Ingrosso et al., 1995; Poli et al., 2004), but the progression of disease was unaltered (Ingrosso et al., 1995). Mechanistically, CR is similar to polysulfated compounds and causes a reduction in cell-surface PrP^{c} (Shyng et al., 1995) and may bind and over-stabilize PrP^{Sc} (Caspi et al., 1998). Heparan sulphate mimetics are dextran polymers chemically modified with sulphate-, carboxymethyl- and benzylamide-groups. The substances HM2602, HM5004 (Adjou et al., 2003; Schonberger et al., 2003) and the more recent CR36 (Larramendy-Gozalo et al., 2007) inhibit PrP^{Sc} formation in cell culture, while only HM2602 decreased incubation time of prion disease *in vivo* (Adjou et al. 2003). The naphthylurea compound suramin, developed for the treatment of trypanosomiasis in humans, binds to PrP^{c} and induces its aggregation in the secretory pathway. PrP^{c} then bypasses the plasma membrane by re-routing to lysosomes, making it inaccessible for prion conversion (Gilch et al., 2001). Prolongation of incubation times in mice and hamsters upon peripheral prion infection was observed (Ladogana et al., 1992; Gilch et al., 2001).

Both PrP^{c} and PrP^{Sc} are localised in lipid rafts. Taraboulos and co-workers demonstrated that localisation of PrP^{c} in lipid rafts is a pre-requisite for propagation of PrP^{Sc}, and inhibitors of cholesterol synthesis like lovastatin (Taraboulos et al., 1995) or squalestatin (Bate et al.,

2004) can impede PrP^{Sc} conversion in ScN2a cells. In case of lovastatin, this is probably due to intracellular retention of PrP^{c} (Gilch et al., 2006), and also squalestatin influences trafficking and neurotoxic properties of a PrP-derived peptide encompassing residues 105-132 (Wilson et al., 2007). Polyene antibiotics with the prototype substance amphotericin B (AmB) can bind to cholesterol and therefore alter the membrane lipid composition. Accordingly, PrP^{Sc} generation in prion infected cell cultures is inhibited by AmB (Mange et al., 2000). AmB has been shown to prolong incubation time of prion disease in hamsters (Pocchiari et al., 1987; McKenzie et al., 1994). Later, the less toxic AmB derivative MS-8209, which allows administration of higher doses, was tested for its efficacy against scrapie in mice and hamsters (Demaimay et al., 1994; Adjou et al., 1995; Adjou et al., 1999). However, within the mouse model of prion disease, effects of AmB and MS-8209 were dependent on the strain used for infection. Whereas both BSE- and scrapie-infected mice exhibited prolonged incubation times, both drugs were more effective in scrapie-infected mice (Adjou et al., 1996).

Tetrapyrrolic compounds provide structural similarities with CR, and their interaction with protein surfaces can induce structural changes in proteins. Initially, they were screened in the ScN2a cell model and in a cell free system for their inhibitory effect on prion propagation (Caughey et al., 1998). The three most potent compounds in decreasing PrP^{Sc} levels, phthalocyanine tetrasulfonate (PcTS), meso-tetra(4-N-methylpyridyl)porphine iron (III) (TMPP-Fe3+) and deuteroporphyrin iX 2,4-bis-(ethylene glycol) iron(III) (DPG2-Fe3+), were then administered to transgenic mice (Priola et al., 2000). The results of the *in vivo* experiments were in good correlation with the *in vitro* data, and with all 3 compounds a significant increase in the mean survival time of intraperitoneally infected mice was monitored when treatment was started at the day of infection. Additionally, PcTS can, when incubated with the inoculum prior to infection of mice, completely inactivate low levels of prion infectivity (Priola et al., 2003). Since none of the substances crosses the blood-brain-barrier, they can be useful only for post-exposure prophylaxis. Similarly, tetracyclines reduce the protease resistance of vCJD and BSE prions and infectivity of 263K hamster prions when incubated with the inoculum (Forloni et al., 2002).

Dendritic polyamines and cationic polyamines, which can be components of lipid transfection reagents, can clear prion-infected cells of both PrP^{Sc} and prion infectivity (Supattapone et al., 1999; Winklhofer & Tatzelt, 2000; Supattapone et al., 2001). Their postulated mode of action is to cause disaggregation of PrP^{Sc} at acidic pH, thereby making it more susceptible to proteolytic digestion (Supattapone et al., 1999). Bioassays were performed with phosphorus containing dendrimers, which are less toxic in combination with an increased bioavailability compared to polyamines (Solassol et al., 2004). A reduction of PrP^{Sc} accumulation in the

spleen of i.p. infected mice was reported, but data on an effect on incubation time are lacking. Assuming that lysosomes may be organelles important for prion conversion, various lysosomotropic agents have been screened in a prion-infected cell model for anti-prion activity (Doh-Ura et al., 2000). Thereby, the anti-malarial drug quinacrine turned out to be a potent inhibitor of PrP^{Sc} propagation in cell culture, however, in bioassays no anti-prion effect was observed (Doh-Ura et al., 2000; 2004). Later, bis-acridines comprising two acridines joined by a linker were found to be even more effective in cell culture (Korth et al., 2001), but it remains to be determined whether these novel compounds are beneficial in animal models.
A novel class of anti-prion compounds, namely inhibitors of signal transduction, is represented by imatinib (STI571, gleevec) (Ertmer et al., 2004). This drug impedes the tyrosine kinase c-abl and can lead to induction of autophagy (Ertmer et al., 2007). In prion-infected cells, imatinib induced the clearance of PrP^{Sc} and prion infectivity. In peripherally infected mice, levels of PrP^{Sc} in spleens were reduced and, upon early treatment after peripheral infection, neuroinvasion was slightly delayed (Yun et al., 2007). Although the drug is pharmacologically well characterised in humans, is widely used in patients suffering from chronic myeloic leukaemia (CML), and was believed to cross the blood-brain-barrier, neither intraperitoneal nor intracerebroventricular administration of imatinib induced clearance of PrP^{Sc} in the CNS (Yun et al., 2007).

2.3.3 Nucleic acids and peptides

Within the class of interfering nucleic acids, one again can distinguish between molecules targeting PrP^{c}, PrP^{c}-PrP^{Sc} interactions, or formation of high molecular weight PrP^{Sc} aggregates. One strategy to achieve knock-down of PrP^{c} is the design of highly specific small interfering RNAs (siRNA) targeting PrP mRNA. Such siRNA has been successfully used to knock down PrP^{c} expression (Tilly et al., 2003; Daude et al., 2003) and to abrogate PrP^{Sc} accumulation in cell culture (Daude et al., 2003). One advantage of this strategy is that anti-prion effects are completely independent of the prion strain used for infection, which may not be the case when using molecules that target PrP^{Sc} or PrP^{c}-PrP^{Sc} interactions. However, in cell culture knock-down approaches for PrP^{c} were only transient, and for transfection of non-dividing cells like neurons methods have to be applied which allow efficient gene transfer. This can be achieved by using lentiviral vectors able to stably integrate into the genome of both dividing and non-dividing cells (Pfeifer 2006). By intracranial injection of lentivral vectors encoding short hairpin RNA (shRNA) targeting PrP^{c} mRNA, PrP^{c} expression was reduced around the site of injection (Pfeifer et al., 2006; White et al., 2008). When chimeric mice expressing variable degrees of PrP-specific shRNA were inoculated with RML prions, a significant prolongation of incubation time was observed, depending on the percentage of transgene expressing neuronal cells (Pfeifer et al., 2006). Of importance, lentiviral delivery of

siRNA to mice already infected with prions prolonged the life span of these animals, reduced spongiform degeneration and prevented neuronal loss (White et al., 2008). Although these siRNA approaches provide proof of principle, the transgene delivery is still highly artificial, and to make it applicable in humans methods for vector transfer more physiological than those described have to be evaluated. This is also the case for other nucleic acid compounds active against PrP^{Sc} and generation of prion infectivity in cell culture. Among those are phosphorothioate oligonucleotides, which inhibit PrP^{Sc} replication in cell culture in a sequence independent manner by an unknown mechanism (Kocisko et al., 2006; Karpuj et al., 2007). Binding to PrP^{c} and incorporation into PrP^{Sc} aggregates, thereby rendering them more susceptible to PK digestion, has been suggested to be the basis of the anti-prion effect of RNA aptamer DP7 in infected cell cultures (Proske et al., 2002). In bioassays, stimulation of innate immunity by post-exposure administration of high doses of CpG-motif containing oligonucleotides significantly prolonged incubation times (Sethi et al., 2002). However, upon similar experimental design heavy re-organisation of spleen architecture was observed, arguing that these side effects were responsible for the anti-prion effects (Heikenwalder et al., 2004).

Peptide inhibitors of prion conversion were screened in cell-free and cell-based assays (Chabry et al., 1999; Horiuchi et al., 2001). The latter employed PrP-derived peptides to interfere with prion conversion, an approach which provides important insights into which PrP sequences are important for conversion and, when using different species, species barrier aspects (Chabry et al., 1999; Horiuchi et al., 2000). Another interesting approach has been presented by Soto and colleagues (Soto et al., 2000). Here, β-sheet breaker peptides, which revert the structural transitions occurring in PrP^{Sc}, were designed. Upon incubation with infected brain homogenates, PrP^{Sc} lost PK resistance and the homogenates were less infectious in bioassays.

Interaction of PrP^{c} with PrP^{Sc} is crucial for the conversion process. Consequently, inhibition of this binding leads to an impaired conversion. This can be achieved by incubation of prion-infected cell cultures with antibodies specific against PrP^{c}. For this purpose, monoclonal antibodies (Peretz et al., 2001; Enari et al., 2001; Pankiewicz et al., 2006; Feraudet et al., 2005; Perrier et al., 2004), mouse polyclonal antibodies elicited by auto-immunisation (Gilch et al., 2003; Oboznaya et al., 2007) targeting PrP^{c}, or antibodies recognising additionally PrP^{Sc} (Beringue et al., 2004) were used. Besides inhibiting PrP^{c}-PrP^{Sc} interactions, increased endocytosis and enhanced degradation of PrP^{c} have been described to mediate anti-prion effects in cell culture. Later on, antibody fragments like single-chain antibodies (scFv) were used for interference in cell culture (Donofrio et al., 2005; Cardinale et al., 2005; Vetrugno et al., 2005). Either paracrine effects in case scFvs were secreted into culture medium

(Donofrio et al., 2005) or intracellular interference by fusion of scFv with an ER retention motif (Cardinale et al., 2005; Vetrugno et al., 2005) were reported.

2.3.5 Vaccination approaches

The knowledge that antibodies can interfere with prion conversion in cell culture elicited tremendous efforts towards establishing active or passive immunisation strategies against prion diseases. Further encouragement was provided by a report published by the group of A. Aguzzi describing that transgenic mice expressing hemizygously the heavy chain of the anti-PrP antibody 6H4 have an increased incubation time upon i.p. prion infection (Heppner et al., 2001). Very promising results were also obtained by passive immunisation (White et al., 2003). Upon repeated peripheral administration of high amounts of monoclonal antibodies in peripherally infected mice, prion infectivity in the spleen was markedly reduced. Upon continued treatment, mice survived more than 300 days longer than untreated control mice.

Since PrP^c is an endogenous protein, active immunisation is severely hampered by self-tolerance. A huge variety of vaccination protocols was tested to overcome this phenomenon. As antigen, peptides (Souan et al., 2001; Schwarz et al., 2003; Arbel et al., 2003; Beringue et al., 2004; Bainbridge et al., 2004; Handisurya et al., 2007), recombinant PrP expressed in *E. coli* (Sigurdsson et al., 2002; Wisniewski et al., 2002; Koller et al., 2002), dimeric recombinant PrP (Gilch et al., 2003; Polymenidou et al., 2004; Kaiser-Schulz et al., 2007), DNA vaccination (Fernandez-Borges et al., 2006), and retroviral (Nikles et al., 2005) or papilloma virus-based (Handisurya et al., 2007) presentation of PrP peptides were employed. Although anti-PrP titers can be elicited with almost all approaches, data on prion challenge after immunisation are either missing or the effects on incubation time after peripheral (Sigurdsson et al., 2002; Polymenidou et al., 2004), intracerebral (Fernandez-Borges et al., 2006), or oral (Schwarz et al., 2003) infection are only moderate. For possibly the most promising study an attenuated *Salmonella* vaccine strain expressing mouse PrP was used (Goni et al., 2005). The authors assumed that for preventing oral prion infection, which is probably the physiological route for acquiring vCJD, combating prion propagation as early as possible by induction of gut mucosal immunity should be beneficial. Indeed, by this strategy ~30% of the immunised animals were alive without symptoms 500 days after oral prion challenge, compared to 185 days median survival time of control mice. In another study ~25% of mice were apparently also completely protected upon active vaccination with recombinant dimeric PrP together with adjuvant and anti-OX40 followed by intraperitoneal prion infection (Polymenidou et al., 2004).

2.3.6 Therapy in humans

In humans, the situation is by far more complicated than in the available animal models, and even in well-controlled animal bioassays no definitely therapeutic substances were identified. In case of acquired and sporadic prion diseases, respectively, the time point of infection or onset of clinical disease is unpredictable. Therefore, treatment can only start as early as the disease is diagnosed, meaning that drugs need to efficiently cross the blood-brain barrier, to diminish also already pre-existing PrP^{Sc}, and to completely inhibit *de novo* prion synthesis. Contrary, in genetic forms of prion disease, early diagnosis and pre-clinical treatment to prolong the incubation time is more realistic. Nevertheless, so far no routinely applicable therapy is available for human prion diseases.

However, a few substances were tested in patients with clinical prion diseases, namely PPS, quinacrine and flupirtine. PPS was applied intraventricularly to patients suffering from vCJD (Todd et al., 2005; Whittle et al., 2006; Parry et al., 2007). In almost all patients, PPS treatment was well tolerated. Whereas progression could not be arrested or reverted by PPS infusion, treatment of at least one patient may have resulted in a prolonged survival time (Todd et al., 2005). Quinacrine, a rather effective substance in cell-based models (Korth et al., 2001), did not influence incubation times in animal bioassays (Doh-Ura et al., 2004; Barret et al., 2003). Nevertheless, due to its promising pharmacokinetics it was applied in clinical trials to human CJD, vCJD or FFI patients. Unfortunately, no beneficial effects were observed (Benito-Leon et al., 2004; Haik et al., 2004), which again indicates that results obtained by *in vitro* and cell culture testing need to be carefully evaluated.

Flupirtine, in contrast, is an inhibitor of the NMDA receptor with proposed neuroprotective effects initially identified to prevent induction of apoptosis by a toxic PrP peptide in primary cortical neurons (Perovic et al., 1995). Recently, a double-blind placebo controlled clinical study including 28 CJD patients was performed. It was found that flupirtine treatment has positive effects on the cognitive functions of patients (Otto et al., 2004).

Given the multiple approaches and efforts described above to combat prion diseases, it is quite disappointing that so far no successful therapy could be established. It indicates that the development of promising therapeutic strategies is still a big challenge in prion research.

2.3 Peptide aptamers

Peptide aptamers comprise a class of molecules consisting of a variable peptide sequence inserted within and presented by a constant scaffold protein. The variable peptide sequence is linked N- and C-terminally to the scaffold (Colas et al., 1996; Hoppe-Seyler et al., 2004). Thereby, its conformational freedom is reduced compared to free peptides or peptides fused

terminally to a carrier protein, leading to a more stable fold, an increased affinity for their target molecules and an increased stability (Ladner 1995). Similar to antibodies, they can be used for diagnostic purposes (Johnson et al., 2008). Due to the small molecule size when compared to antibodies the can recognise pockets at the surfaces of proteins that are not amenable to huge binding partners. This is interesting in particular for the identification of novel drug targets, for example active sites of enzymes.

Originally, the bacterial thioredoxin A (trxA) was the first scaffold protein used for the presentation of peptide aptamers (Colas et al., 1996). Here, the peptide moiety is inserted into the active-site loop of the enzyme, thereby destroying its catalytic activity. In the meantime, several scaffold proteins became available, e. g. green fluorescent protein (GFP; Peelle et al., 2001), the Z domain of staphylococcal protein A (Nord et al., 1997) or the lipocalin fold ("anticalins"; Beste et al., 1999). Peptide aptamers are usually selected by yeast-two hybrid screening, providing the advantage of intracellular screening in contrast to *in vitro* methods like phage display. The binding affinity of a certain peptide sequence, however, depends on the scaffold protein, meaning that transfer of a peptide isolated in a given scaffold to another scaffold protein might alter its affinity (Woodman et al., 2005).

In the first report on peptide aptamers, a trxA-based peptide library has been used to select peptide aptamers targeting cyclin-dependent kinase 2 (Colas et al., 1996). Here, inhibition of the target protein by interaction with the peptide aptamers was demonstrated. Binding affinities of those peptide aptamers could be further improved by random mutagenesis of the DNA encoding the peptide moiety followed by a second round of selection (affinity maturation). To further increase the inhibitory activity of the high-affinity peptide aptamers, targeting and modifying signals were introduced into the peptide aptamers by fusion to a nuclear import signal or to the active part of an ubiquitin ligase, respectively. These manipulations cause transport of the target protein to the nucleus or induce its rapid proteasomal degradation (Colas et al., 2000). In further attempts, functional peptide aptamers have been generated, among others, against the hepatitis B-virus (HBV) core protein (Butz et al., 2001). Interestingly, binding of the peptide aptamers to the HBV core protein or of aptamers interacting with the human papilloma virus E6 protein results in an intracellular re-distribution of the proteins and their sequestration into aggresomes (Tomai et al., 2006). Expression of peptide aptamers targeting the hepatitis C virus (HCV) protease NS3 inhibits HCV RNA replicons by perturbing protease activity (Trahtenherts et al., 2008). In several studies, peptide aptamers against proto-oncogenes, e. g. Ras, were selected in order to inhibit the transforming potential (Pamonsinlapatham et al., 2008; Kunz et al., 2006; Zhao & Hoffmann, 2006).

Furthermore, peptide aptamers can be employed for elucidating the function of proteins. For reverse analysis, peptide aptamers against a specific target protein are selected and subsequently, the effects of intracellular expression of the selected molecules is analysed. Conversely, forward analysis includes the expression of a combinatorial peptide library in an organism and the analysis of the phenotype induced by the peptide aptamers. One advantage of this approach over classical genetic methods is that the genetic information of cellular proteins is not affected (Geyer et al., 1999; 2001). Functional analysis using peptide aptamers also involves the identification of protein-protein interactions (Stevens & Hupp, 2008).

All the studies described above indicate that peptide aptamers are useful tools for diagnostic, therapy and basic research but that there might be a huge array of applications and modifications not investigated so far.

2.4 Objective of the thesis

The conversion of PrP^{c} into PrP^{Sc} requires a direct interaction of the two PrP isoforms. Molecules that interfere with this binding are possible inhibitors of PrP^{Sc} generation. In order to identify compounds that recognise PrP^{c} with high affinity peptide aptamers from a combinatorial peptide library presented by the bacterial trxA protein interacting with PrP23-231 should be isolated in a Y2H approach. The potential of interfering with the prion conversion process was analysed by treatment of prion-infected cell lines with purified peptide aptamers expressed recombinantly in *E. coli*. Since *in vivo* application of purified peptide aptamers might not be feasible, one goal was to establish peptide aptamers expressed in the secretory pathway, an application that has not been demonstrated so far. This necessitated fusion of the cytosolic trxA-scaffold with a N-terminal signal peptide for ER import. The secretory peptide aptamers shall further be manipulated by the addition of intracellular retention and targeting signals at the carboxy-terminus. All modified peptide aptamers shall be expressed in infected and non-infected cell lines for detailed analysis of subcellular localisation, interaction with PrP^{c} and, finally, effects on PrP^{Sc} propagation in cells infected persistently or *de novo* with prions.

3. Materials and Methods

3.1 Materials

3.1.1 Chemicals

Agarose	Invitrogen, Karlsruhe, Germany
Ammonium peroxodisulfate	Roth GmbH & Co, Karlsruhe, Germany
Bacillol Plus	Roth GmbH & Co, Karlsruhe, Germany
Bacto Agar	Becton Dickinson, Heidelberg, Germany
5-Bromo-4-Chloro-3-indolyl α-D-galactopyranoside (α-X-Gal)	Glycosynth, Warrington, UK
Bromphenole blue	Merck, Darmstadt, Germany
Coomassie Brillant Blue G250	Roth GmbH & Co, Karlsruhe, Germany
β-Mercaptoethanol	Sigma-Aldrich Chemie GmbH, Steinheim, Germany
Dimethylsulfoxide (DMSO)	Sigma-Aldrich Chemie GmbH, Steinheim, Germany
Ethanol p. a. 99 %	Roth GmbH & Co, Karlsruhe, Germany
Ethidium bromide solution (10 mg/ml)	Invitrogen, Karlsruhe, Germany
Ethylen diamine tetraacetate, sodium salt (EDTA)	Roth GmbH & Co, Karlsruhe, Germany
Gelatine 40 % solution	Sigma-Aldrich Chemie GmbH, Steinheim, Germany
Glucose	Sigma-Aldrich Chemie GmbH, Steinheim, Germany
Glycerol	Roth GmbH & Co, Karlsruhe, Germany
Glycine	Roth GmbH & Co, Karlsruhe, Germany
HCl 37 % (w/w)	Roth GmbH & Co, Karlsruhe, Germany
Hybond-P PVDF membrane	GE Healthcare, Freiburg, Germany
Isopropanol p. a.	Roth GmbH & Co, Karlsruhe, Germany
Isopropyl-β-D-thiogalactopyranosid (IPTG)	Roth GmbH & Co, Karlsruhe, Germany
Magnesium chloride	Sigma-Aldrich Chemie GmbH, Steinheim, Germany
Magnesium sulfate	Sigma-Aldrich Chemie GmbH, Steinheim, Germany
Methanol p. a.	Roth GmbH & Co, Karlsruhe, Germany

N,N,N',N'-Tetramethylenediamine (TEMED)	Sigma-Aldrich Chemie GmbH, Steinheim, Germany
N-Lauryl-Sarcosine	Sigma-Aldrich Chemie GmbH, Steinheim, Germany
Pefabloc SC	Roche, Mannheim, Germany
Permafluor	Beckmann Coulter, Marseille, France
Phosphate buffered saline (PBS)	Invitrogen, Karlsruhe, Germany
Potassium chloride	Sigma-Aldrich Chemie GmbH, Steinheim, Germany
Pro Bond Resin	Invitorgen, Karlsruhe, Germany
Protein A Sepharose	GE Healthcare, Freiburg, Germany
Protogel Ultra Pure 30 %, Acrylamide : Bisacrylamide 37,5:1	National Diagnostics, Atlanta, USA
Re-blot Plus Strong Solution	Chemicon Int., Carrigtwohill, Ireland
Roti-Histofix	Roth GmbH & Co, Karlsruhe, Germany
Saponin	Roth GmbH & Co, Karlsruhe, Germany
SD Minimal Base	Becton Dickinson, Heidelberg, Germany
Skim milk powder	Merck, Darmstadt, Germany
Sodium chloride	Roth GmbH & Co, Karlsruhe, Germany
Sodium deoxycholate (DOC)	Roth GmbH & Co, Karlsruhe, Germany
Sodium dodecylsulfate (SDS)	Roth GmbH & Co, Karlsruhe, Germany
Sodium hydroxide (NaOH)	Roth GmbH & Co, Karlsruhe, Germany
Soy bean trypsin inhibitor	Sigma-Aldrich Chemie GmbH, Steinheim , Germany
Synthetic dropout (SD) supplements	Becton Dickinson, Heidelberg, Germany
Tris-hydroxy-methyl-aminomethan (Tris)	Roth GmbH & Co, Karlsruhe, Germany
Triton-X 100	Sigma-Aldrich Chemie GmbH, Steinheim , Germany
Tryptone	Becton Dickinson, Heidelberg, Germany
Tween 20	Roth GmbH & Co, Karlsruhe, Germany
X-ray films Kodak Biomax MS	Sigma-Aldrich Chemie GmbH, Steinheim, Germany
Yeast extract	Becton Dickinson, Heidelberg, Germany
7-Amino-Actinomycin D (7-AAD)	Becton Dickinson, Heidelberg, Germany

3.1.2 Enzymes and antibodies

3.1.2.1 Enzymes

Calf intestine alkaline phosphatase (CIP)	Roche, Mannheim, Germany
Klenow Polymerase	Roche, Mannheim, Germany
N-Glycosidase F (PNGase F)	Roche, Mannheim, Germany
Pfu Polymerase	Metabion, Munich, Germany
Phosphatidyl-inositol specific Phospholipase C	Sigma-Aldrich Chemie GmbH, Steinheim, Germany
Proteinase K (PK)	Roth GmbH & Co, Karlsruhe, Germany
Restriction enzymes (all)	Metabion, Munich, Germany
T4 Ligase	Roche, Mannheim, Germany
Trypsin-EDTA (0,25 %/1mM	Invitrogen, Karlsruhe, Germany

3.1.2.2 Antibodies

Table 4. Antibodies used in this thesis

Primary antibody	Source and Reference	Specificity	Application	Dilution
4H11	Mouse monoclonal (Ertmer et al., 2004)	PrP of various species, including mouse and hamster	Immunoblot Indirect immunofluorescence immunoprecipitation	1:1000 1:100 1 :300
A7	Rabbit polyclonal (Gilch et al., 2003)	PrP of various species, including mouse and hamster	FACS analysis Immunoprecipitation	1:100 1:300
3F4	Mouse monoclonal provided by Dr. M. Baier, Robert Koch Institute, Berlin, Germany	3F4-epitope of Syrian hamster and human PrP; amino acids 109-112 (MKHM)	Immunoblot	1:2500
Anti-Flag	Rabbit polyclonal Sigma, Deisenhofen, Germany	Flag-epitope (DYKDDDDK)	Immunoblot Indirect immunofluorescence and FACS analysis	1:5000 1:100

Penta-His	Mouse monoclonal Invitrogen, Karlsruhe, Germany	5 x Histidin-Tag	Immunoblot	1:100
Anti-LAMP	Rat monoclonal BD Biosciences, Heidelberg, Germany	Lysosome-associated membrane protein I	Indirect immunofluorescence	1:100
Anti-Transferrin receptor	Mouse monoclonal Invitrogen, Karlsruhe, Germany	Murine transferrin receptor	Immunoblot	1:2500
Secondary antibody	**Source**	**Specificity**	**Application**	**Dilut**
Horseradish peroxidase-conj. anti-IgG	Sheep GE Healthcare, Freiburg, Germany	Mouse IgG	Immunoblot	1:7500
Cy3-conj. anti-IgG	Donkey Dianova, Hamburg, Germany	Mouse IgG	Indirect Immunofluorescence	1:200
Cy3-conj. anti-IgG	Donkey Dianova, Hamburg Germany	Rabbit IgG	Indirect Immunofluorescence	1:200
Cy2-conj. anti-IgG	Donkey Dianova, Hamburg, Germany	Rabbit IgG	FACS analysis Indirect immunofluorescence	1:400 1:200
Cy2-conj. anti-IgG	Donkey Dianova, Hamburg, Germany	Mouse IgG	Indirect Immunofluorescence	1:200

3.1.3 Bacterial and yeast strains

All plasmids were propagated in *E. coli* XL-1 Blue (*Sup*E44, *hsd*R17, *end*A1, *ec*A1, *gyr*A46, thi-1, *rel*A1, lac$^-$, F'(proABlacI^q, lacZ∆M15, Tn10(ter^R); Stratagene). For expression of recombinant proteins, *E. coli* BL21 were used. Y2H screening was performed in *S. cerevisiae* AH109 (*MATa, trp1-901, leu2-3, 112, ura3-52, his3-200, gal4Δ, gal80Δ, LYS2::GAL1$_{UAS}$-GAL1$_{TATA}$-HIS3, GAL2$_{UAS}$-GAL2$_{TATA}$-ADE2, URA3::MEL1$_{UAS}$-MEL1$_{TATA}$ -lacZ, MEL1).*

3.1.4 Plasmids and constructs

For transient expression of recombinant proteins in mammalian cells genes were cloned into pcDNA3.1/Zeo (Invitrogen, Karlsruhe). For evaluation of transfection efficiencies, pEGFP-C1 (Clontech, Mountain View, CA, USA) was used. For Yeast two hybrid approaches the shuttle vectors pGAD-T7 and pGBK-T7 (Clontech, Mountain View, CA, USA), suitable for propagation both in yeast and bacteria were utilised. The plasmid pQE-30 (Qiagen) encodes 6 histidine residues fused to the amino-terminus of the gene of interest and allows purification of proteins expressed recombinantly in *E. coli*. Maps of all plasmid vectors are depicted in **Fig. 12**, constructs used in this thesis are listed in **Table 5.** The correctness of all subcloned genes was confirmed by DNA sequencing (GATC Biotech; Konstanz).

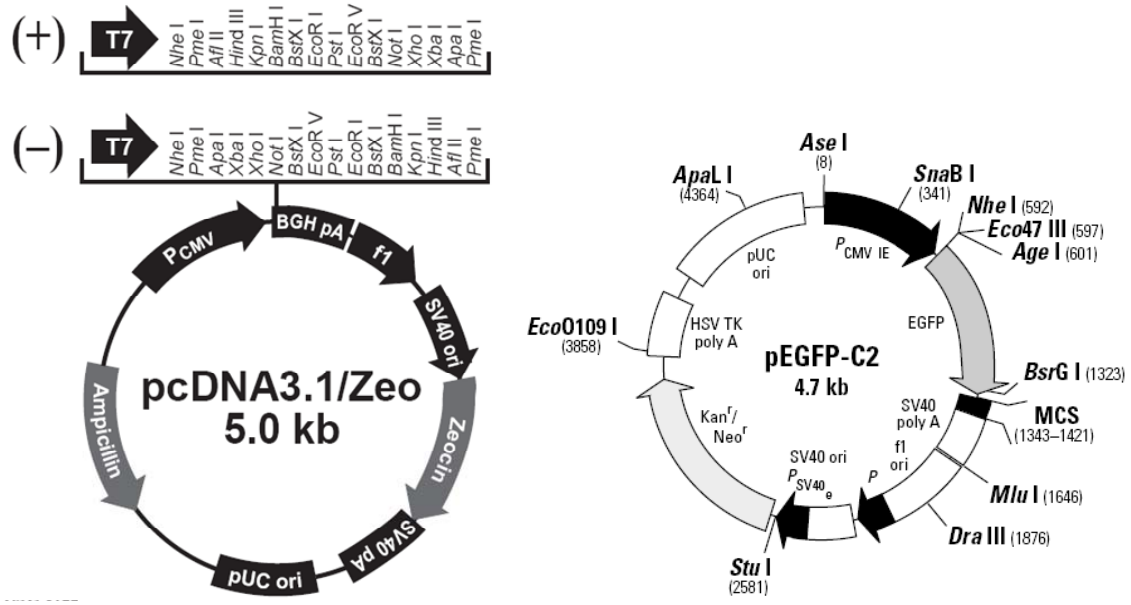

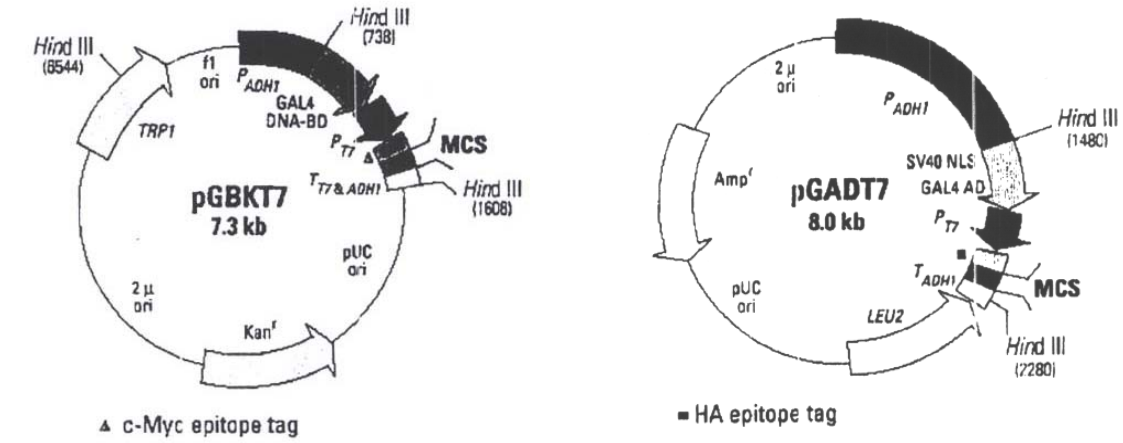

Fig. 12. Plasmid vectors used in this thesis.

Table 5. List of constructs.

Plasmid + Insert	Description	Restriction enzymes used for cloning 5'→3'
pGBK-T7 PrP23-231	Murine PrP aa 23-231	BamHI/EcoRI
pGBK-T7 PrP23-100	Murine PrP aa 23-100	BamHI/EcoRI
pGBK-T7 PrP90-231	Murine PrP aa 90-231	BamHI/EcoRI
pGAD-T7 trxA-BamHI	*E. coli* trxA ; BamHI site introduced by site-directed mutagenesis for subcloning of peptide library	EcoRI/BamHI/XhoI
pGAD-T7 peptide library	Combinatorial peptide library introduced into trxA-BamHI via BamHI restriction site ; PrP-binding peptide aptamers were denoted PA1, 8 and 16	EcoRI/BamHI/XhoI
pGAD-T7 trxA	*E. coli* wild-type trxA	EcorRI/XhoI
pQE30 trxA	N-terminal fusion of *E. coli*	SphI/HindIII

	wild-type trxA to 6 x His residues	
pQE30 PA1	N-terminal fusion of PA1 to 6 x His residues	SphI/HindIII
pQE30 PA8	N-terminal fusion of PA8 to 6 x His residues	SphI/HindIII
pQE30 PA16	N-terminal fusion of PA16 to 6 x His residues	SphI/HindIII
pcDNA3.1 trxA-GPI	N-terminal signal peptide of murine PrP (aa 1-22; SP), Flag-tag, trxA, GPI-signal peptide of murine PrP (aa 231-254; GPI)	HindIII, EcoRI, XhoI, XbaI
pcDNA3.1 1-GPI	SP::Flag::PA1::GPI	HindIII, EcoRI, BamHI, XhoI, XbaI
pcDNA3.1 8-GPI	SP::Flag::PA8::GPI	HindIII, EcoRI, BamHI, XhoI, XbaI
pcDNA3.1 16-GPI	SP::Flag::PA16::GPI	HindIII, EcoRI, BamHI, XhoI, XbaI
pcDNA3.1 trxA-KDEL	SP::Flag::trxA fused to a KDEL ER retention motif	HindIII, EcoRI, XhoI
pcDNA3.1 1-KDEL	SP::Flag::PA1::KDEL	HindIII, EcoRI, BamHI, XhoI
pcDNA3.1 8-KDEL	SP::Flag::PA8::KDEL	HindIII, EcoRI, BamHI, XhoI
pcDNA3.1 16-KDEL	SP::Flag::PA16::KDEL	HindIII, EcoRI, BamHI, XhoI
pcDNA3.1 trxA-LAMP	SP::Flag::trxA::LAMP-1 transmembrane and cytosolic domain (aa 348 - 382; LAMP)	HindIII, EcoRI, XhoI, XbaI
pcDNA3.1 1-LAMP	SP::Flag::PA1::LAMP	HindIII, EcoRI, BamHI, XhoI, XbaI
pcDNA3.1 8-LAMP	SP::Flag::PA8::LAMP	HindIII, EcoRI, BamHI, XhoI, XbaI
pcDNA3.1 16-LAMP	SP::Flag::PA16::LAMP	HindIII, EcoRI, BamHI, XhoI, XbaI

3.1.4 Eucaryotic cell lines

Table 6. Utilized mammalian cell lines

Cell line	Description	Reference
N2a	Murine neuroblastoma cell line	ATCC CCl 131
N2a wt	N2a cells stably transfected with pcDNA3.1/Zeo encoding murine PrP	Established by Elke Maas in our laboratory
Clone 21	3F4 ScN2a cells cured from prion infection by treatment	Diploma thesis Gloria Lutzny

	with pentosan polysulphate	
22LN2a	N2a cells persistently infected with 22L scrapie prions	Infected by myself in our laboratory
3F4-ScN2a	Murine neuroblastoma cells overexpressing 3F4-tagged PrP; persistently infected with RML prions	Gilch et al., 2001
Hpl3-4	Murine hippocampus cell line	Sakudo et al., 2005
Hpl 3F4	Hpl3-4 cells stably overexpressing 3F4 tagged mouse PrP	Established by Elke Maas in our laboratory

3.1.5 Cell culture media and additives

OptiMEM with Glutamax	Invitrogen, Karlsruhe, Germany
Dulbeccos MEM (D-MEM)	Invitrogen, Karsruhe, Germany
Fetal bovine serum (FCS)	Invitrogen, Karlsruhe, Germany
Penicillin/Streptomycin	Invitrogen, Karlsruhe, Germany

3.1.6 Kits

DNA ladder (100 bp and 1 kB)	New England Biolabs, Frankfurt, Germany
ECL Plus	GE Healthcare, Freiburg, Germany
Fugene 6 Transfection Kit	Roche, Mannheim, Germany
GFX Micro Plasmid Prep Kit	GE Healthcare, Freiburg, Germany
GFX PCR DNA and Gel Band Purification Kit	GE Healthcare, Freiburg, Germany
Grow'N'Glow Yeast Plasmid Isolation Kit	MoBiTec GmbH, Göttingen, Germany
High range protein molecular weight marker	GE Healthcare, Freiburg, Germany
Lipofectamine 2000	Invitrogen, Karlsruhe, Germany
Plasmid Maxi Kit	Qiagen, Hilden, Germany
TNT T7 Quick Coupled Transcription/ Translation System	Promega GmbH, Mannheim, Germany

3.1.7 Oligodeoxynucleotides

All oligodeoxynucleotides used as primers for polymerase chain reactions (PCR) or site-directed mutagenesis were obtained from Metabion, Munich, with high purity achieved by high-performance liquid chromatography (HPLC).

3.1.8 Radioactive Compounds

(^{35}S)-Met/Cys (Promix; 1000 Ci/mmol)	GE Healthcare, Freiburg

3.1.9 Instruments

Autoclave V95	Systec, Wettenberg, Germany

Axiovert 40C microscope	Carl Zeiss Jena GmbH, Göttingen, Germany
Fuchs-Rosenthal Hemocytometer	Roth GmbH & Co, Karlsruhe, Germany
CO_2 Incubator	Heraeus GmbH, Hanau, Germany
Centrifuges:	
- Eppendorf 5417C	Eppendorf-Nethaler-Hinz GmbH, Köln, Germany
- Sigma 4K15	Sigma-Aldrich, Schnelldorf, Germany
- Beckmann Avanti	Beckmann Coulter GmbH, Krefeld, Germany
- Beckmann TL-100 ultracentrifuge	Beckmann Coulter GmbH, Krefeld, Germany
Coverslips and slides	Marienfeld, Bad Mergentheim, Germany
Cryotubes	Corning Inc., USA
Eppendorf tubes (1,5 or 2 ml)	Eppendorf-Nethaler-Hinz GmbH, Köln, Germany
FACS-polystyrene tubes	Becton Dickinson, USA
Falcon tubes (15 or 50 ml)	Falcon, Le Pont de Claix, France
Flow cytometer EPICS XL	Beckmann Coulter GmbH, Krefeld, Germany
LSM510 confocal laser microscope	Carl Zeiss Jena GmbH, Göttingen, Germany
Midi protein gel chamber	Peqlab Biotechnologie GmbH, Erlangen, Germany
Optimax X-Ray film processor	PROTEC Medizintechnik GmbH & Co-KG, Oberestenfeld, Germany
Pipets (0,5-10 µl; 10-100 µl; 100-1000 µl)	Eppendorf-Nethaler-Hinz GmbH, Köln, Germany
Pipetus	Hirschmann Laborgeräte, Germany
Power Supplies	GE Healthcare, Freiburg, Germany
Spectrophotometer	GE Healthcare, Freiburg, Germany
Sunrise ELISA Reader	Tecan, Maennedorf, Switzerland
Tissue culture dishes and plates	Falcon, Le Pont de Claix, France
Trans Blot SD Semi-dry Transfer Cell	Biorad Laboratories GmbH, München, Germany
Transfer unit Semi dry (TE77)	GE Healthcare, Freiburg, Germany

Ultracentrifuge Kontron TGA50	Kontron, Germany
Vacuum Drier	Biorad Laboratories GmbH, München, Germany
Waterbath	GFL, Burgwede, Germany

3.2 Methods

3.2.1 Biological safety and radiation protection

Genetical engineering of organism was accomplished according to the *Gentechnikgesetz* (01.01.2004). Biologically contaminated materials and solutions were collected separately and inactivated according to the guidelines and operation procedures for working with prions. In particular, inactivation with 1 M NaOH for 24 hours for solutions and autoclaving for 60 min at 134° C and 3 bar for solid waste is dictated. Workings with radioactive compounds were carried out according to the *Strahlenschutzverordnung* (26.07.2001).

3.2.2 Molecular biological methods

3.2.2.1 Polymerase chain reaction (PCR)

Polymerase chain reaction (PCR) is a highly efficient method to specifically amplify target DNA sequences, e. g. genes for subcloning. Therefore, the target DNA (template) is mixed with 5' and 3' complementary oligonucleotides (primers), deoxynucleotide triphosphates (dNTPs) and a heat-stable DNA polymerase, for example *Pfu* polymerase. *Pfu* polymerase has, in contrast to *Taq* polymerase which was the first heat-stable polymerase to be used in PCR reactions, proof-reading activity which minimizes the probability of mutations during DNA amplification. The reaction mix is subjected to repeated cycles of **denaturation** of DNA (usually at 94° C), primer **annealing** during which the oligonucleotides hybridise with their complementary sequences and then prime the **elongation** (at 72° C) of the target DNA. Repeating this cycle enables an exponential amplification of target DNA. The energy necessary for the DNA polymerase reaction is provided by the scission of the two energy-rich phosphate bonds of the dNTPs, which are incorporated as deoxynucleotide monophosphates into the newly synthesised DNA strand. To avoid unspecific hybridisation of the primers with non-target sequences the annealing temperature, which is related to the dissociation temperature T_D of the primers is a critical parameter. T_D can be calculated according to the following formula:

T_D[°C] = 2 x (A + T) + 4 x (C+G)

(A, C, G, T = number of respective nucleotides)

PCR reaction mix:		Thermal cycling:	
A. dest	37,5 µl		
10 x Pfu buffer	5 µl	94° C – 5 min	
dNTP (5 mM)	2 µl	94° C – 1 min	} 40 cycles
Primer 5' (10 µM)	2 µl	55° C – 1 min	
Primer 3' (10 µM)	2 µl	72° C – 2 min	
DNA	1 µl	72° C – 5 min	
Pfu Pol (5 U/µl)	0,5 µl		

PCR products were separated by agarose gel electrophoresis (**3.2.2.3**) and processed further for the desired application.

3.2.2.2 Site-directed mutagenesis

This method was used for introducing missense mutations into existing plasmid constructs, including insertion of single nucleotides in order to create recognition sites for a restriction enzyme or nucleotide exchange. Therefore, forward and reverse primers targeting a complementary sequence were designed where the desired mutation was flanked by 15 sequence specific nucleotides both at the 5' and 3' end resulting in complementary primers with about 30 nucleotides in length which were subjected to HPLC purification after synthesis (Metabion, Munich). Mutagenesis was achieved during a PCR reaction using plasmid DNA containing the respective insert to be mutated. During denaturation, the double stranded plasmid is dehybridised, then primers bind to their complementary sequences. For elongation, 2 min/1000 basepairs (bp) are calculated and within this time, the entire plasmid sequence is complementary synthesized. After 14 – 18 cycles, the sample is digested with 10 Units (U) of the restriction enzyme DpnI which selectively cleaves methylated DNA. Since DNA synthesized during the PCR reaction is in contrast to plasmid DNA amplified in *E. coli* XL1 not methylated, only template DNA is degraded. Then an aliquot of the sample is transformed into *E. coli* XL1 (**3.2.2.10**) and cultivated on LB agar plates containing an appropriate antibiotic. Plasmid DNA was isolated from single clones and the insert was sequenced (GATC Biotech, Konstanz) to confirm successful mutagenesis.

PCR reaction mix: Thermal cycling:

A. dest	38 µl		
10 x Pfu buffer	5 µl	94° C – 5 min	
dNTP (5 mM)	2 µl	94° C – 1 min	18 cycles
Primer 5' (10 µM)	2 µl	55° C – 1 min	
Primer 3' (10 µM)	2 µl	68° C – 14 min	
DNA (200 ng/µl)	1 µl	72° C – 5 min	
Pfu Pol (5 U/µl)	1 µl		

3.2.2.3 Agarose gel electrophoresis

During agarose gel electrophoresis nucleic acids can be separated in an electrical field according to their length and conformation (linear, circular or superhelical). Due to their negative charge nucleic acids migrate towards the anode. To visualize the DNA ethidium bromide, a DNA intercalating agent, is added to the gel. Upon exposure to UV light ethidium bromide exhibits a bright fluorescence that enables detection of DNA and comparison to length standard markers.

0,5 – 2 % agarose depending on the size of DNA fragments to be separated were solubilized in TAE buffer by heating. The solution was chilled to ~ 55° C, then 1,5 µl of ethidium bromide (10 mg/ml) were added. After polymerization the gel was placed into a electrophoresis unit and submerged in TAE buffer. DNA samples were mixed with ¼ volume of 5 x loading buffer. Samples were applied to the gel and separated for 30 min at a constant voltage of 110 V. The result was photographically documented by visualizing the DNA on an UV transilluminator system.

TAE buffer	Tris/ Acetat	40 mM
	EDTA	1 mM
5 x loading buffer	Glycerole in TAE buffer	50%
	Bromphenole blue	0,05%

3.2.2.4 Purification of DNA from agarose gels

DNA separated by agarose gel electrophoresis was visualized on a UV transilluminator system. Bands of interest were excised with a scalpel and DNA was recovered using the GFX PCR DNA and Gel Band Purification Kit according to the manufacturer's instructions.

Briefly, 3 volumes of capture buffer were added to the exised agarose gel for solubilisation for 10 min at 55° C. The solution was added to a spin column and centrifuged for 1 min (14000 rpm; Eppendorf 5417C). Flow-through fraction was discarded and the DNA bound to the column was washed once with 400 µl of washing buffer by repeating the centrifugation step. Finally DNA was eluted from the column with 30 µl sterile A. dest.

3.2.2.5 Enzymatic treatment of DNA

Digestion of DNA with restriction enzymes was performed according to the recommendations of the manufacturer (Metabion, Munich). Usually 5 µg of plasmid DNA or 30 µl PCR product purified after agarose gel electrophoresis (**3.2.2.3**) were incubated with 10 U of each enzyme and the appropriate reaction buffer for 4 hours at 37° C in a total volume of 30 µl. Cleaved DNA fragments were again separated by agarose gel electrophoresis and purified as described (**3.2.2.4**). If only one restriction enzyme was used for subcloning, the linearised plasmid was subjected to dephosphorylation prior to ligation in order to reduce the probability of plasmid re-ligation. Therefore, 10 U calf intestine alkaline phosphatase (CIP) and the recommended buffer were added to the linearised plasmid and incubated for 1 hour at 37° C followed by agarose gel electrophoresis (**3.2.2.3**) and purification (**3.2.2.4**).

3.2.2.6 Ligation of DNA fragments

Linearised plasmid DNA and the DNA fragment to be inserted were mixed in a molar ration of 1:5 and were incubated with T4 ligase and the appropriate buffer provided by the manufacturer in a total volume of 15 µl for 16 hours at 14° C in a waterbath. Then the entire sample was transformed into *E. coli* XL1 blue (**3.2.2.10**). For construction of the combinatorial peptide aptamer library (**3.2.2.7**) 200 ng of linearised and dephosphorylated plasmid was applied.

3.2.2.7 Construction of peptide aptamer library

The peptide aptamer library was prepared by cloning a DNA fragment consisting of 48 nucleotides flanked by BamHI recognition sites encoding 16 random amino acids. To generate this fragment, one oligonucleotide with the sequence $(NNK)_{16}$ (N = A, G, C, T; K = T or G) flanked by BamHI sites (Apta1) was synthesized and annealed to a short oligonucleotide (Apta2) complementary to the constant 3'-end of Apta1. Then the DNA strand complementary to the random sequences of Apta1 was synthesised using Klenow polymerase. As recipient construct, trxA used as a scaffold protein for the peptide moieties was subcloned into the Yeast-two-hybrid (Y2H) prey vector pGAD-T7 and between position

102 and 103 one nucleotide was introduced by site directed mutagenesis (**3.2.2.2**) to create a BamHI recognition site necessary for ligation.

3.2.2.7.1 Second strand synthesis and purification of double stranded DNA

In an 1,5 ml reaction tube, the components listed below were mixed and incubated for 2 hours at 37° C. Then the reaction was stopped by heating the sample for 10 min at 75° C. DNA was purified by phenol-chloroform extraction and precipitated with 2,5 volumes of ethanol 100 % overnight at –20° C. DNA was recovered by centrifugation for 20 min at 4° C and 14000 rpm (Eppendorf 5417C centrifuge). The resulting precipitate was resolved in A. dest. and subjected to restriction enzyme digestion (**3.2.2.5**).

Tris pH 7,5 (1 M)	2,5 µl (= 50 mM)
$MgCl_2$ (25 mM)	12,5 µl (= 6,5 mM)
DTT (10 mM)	5 µl (= 1 mM)
Apta1 (10 µM)	5 µl = 0,5 nmol
Apta2 (10 µM)	10 µl = 1 nmol
dNTP (5 mM)	4 µl (= 400 µM)
H_2O	9 µl
Klenow polymerase	2 µl (= 20 U)

3.2.2.7.2 Separation of DNA by polyacrylamide gel electrophoresis

Since pores of polyacrylamid gels are smaller than that of agarose gels a higher resolution is achieved when separating small DNA fragments. The entire DNA sample after restriction enzyme digestion was mixed with 5 x loading buffer (**3.2.2.3**) and loaded on a vertical polyacrylamide gel. Electrophoresis was performed in TBE buffer for 2 hours at a constant voltage of 110 V. DNA was visualised by ethidium bromide staining on a UV transilluminator and bands of interest were exised with a scalpel and purified as described below (**3.2.2.7.3**).

Polyacrylamide gel 20 %	acrylamide (30 %)	20 ml
	(acrylamide:bis-acrylamide 19:1)	
	TBE 10 x	5 ml
	A. dest	25 ml
	APS (10 %)	500 µl
	TEMED	50 µl
	Ethidium bromide (10 mg/ml)	2 µl

TBE 1x	Tris pH8,3	89 mM
	Boric acid	89 mM
	EDTA	2 mM

3.2.2.7.3 Purification of DNA from polyacrylamide gels

DNA fragments excised from polyacrylamide gels were incubated for 2 hours with constant shaking at 37° C in 1 ml of elution buffer. Subsequently, pieces of the gel were separated by centrifugation and the DNA contained in the supernatant was precipitated over night at –20° C using 2,5 volumes ethanol and was recovered as described in **3.2.2.7.1**.

Elution buffer	NH_4Ac	0,5 M	
	EDTA	1 mM	in A. dest

3.2.2.7.4 Titration and amplification of peptide library

The peptide aptamer library ligation approaches were transformed into *E. coli* XL2 blue ultracompetent cells (see **3.2.2.10**) which results in a guaranteed transfection efficiency of 10^9 clones/µg DNA. One hundreth of the transformed bacteria was streaked on LB agar containing ampicillin. The next day, the number of clones was determined. For an optimal complexity of the library confluent growth of bacterial clones should occur which corresponds to a complexity of ~10^6 individual clones contained in the library. If this was almost achieved the residual volume of transformed XL2 was streaked on 50 LB plates (+ ampicillin) and incubated over night at 37° C. All clones were scraped into 1 l of LB medium (+ ampicillin) and incubated for further 3 hours at 37° C with constant shaking (200 rpm) for amplification of the library. Then plasmid DNA was isolated as described in section **3.2.2.11**.

3.2.2.8 Yeast-2-hybrid (Y2H) screen

The Y2H system is a convenient method to detect protein-protein interactions in a eukaryotic cell environment which allows in contrast to bacteria posttranslational modifications and is therefore closer to the situation in mammalian cells. The principle of the system is based on the fact that some yeast transcription factors can be separated into two inactive domains which are re-activated if they are in close proximity to each other. This proximity can be mediated by two interacting proteins that are expressed as fusion proteins each with one of the transcription factor domains. For this thesis, the Matchmaker 3 system (BD Biosciences, Heidelberg, Germany) was used which is based on the GAL4 transcription factor. The bait protein PrP23-231 was ligated in frame with the GAL4-DNA binding domain (BD) in the plasmid pGBK-T7, the peptide aptamer library was encoded in pGAD-T7 fused to the GAL4

activation domain (AD). Screening was performed by sequential co-transformation into *S. cerevisiae* AH109. This reporter organism is characterized by auxotrophy for adenine and the amino acids Trp, Leu and His. Trp and Leu auxotrophy is complemented by the plasmid vectors pGAD-T7 and pGBK-T7 (see **Fig. 12**) and serves as a selection markers for transformed yeast cells. Adenine and His synthesis are activated by GAL4 in case of positive protein-protein interactions. As an additional reporter gene product, α-galactosidase is expressed. To analyse successful transformation and reporter gene activation, yeast cells are plated on synthetic quadruple dropout (QDO) agar plates lacking adenine, His, Trp and Leu. Additionally, α-X-Gal is streaked on the plates for testing for α-galactosidase expression, by which the substance is converted into a blue dye. In summary, positive interactions are characterized by blue yeast colonies growing on QDO medium. As positive controls, pCL1 encoding the entire GAL4 transcription factor and pVA3 co-transformed with pTD1 encoding SV40 large T-antigen and its known interactor p53, respectively, were employed. Positive clones from the library screen were segregated twice on QDO+α-X-Gal and were then subjected to plasmid isolation (**3.2.2.8.3**) and sequencing of the insert. Auto-activation of the prey vector constructs and interaction of PrP23-231 with trxA or GAL4-AD was excluded by co-transformation of pGBK-T7 PrP23-231 and pGAD-T7 and pGAD-T7 trxA, respectively.

3.2.2.8.1 Preparation of competent yeast cells

Yeast cells competent for transformation were prepared using the LiAc-method. Several colonies of AH109 cells were inoculated into 50 ml YPDA medium or if pre-transformed with pGBK-T7 PrP23-231 for the library screen into 150 ml SD-Trp medium. Cultures were incubated over night at 30° C with constant shaking (250 rpm) to the stationary phase (OD_{600} > 1,5). Overnight culture was transferred to 300 ml YPDA (small scale) or 1000 ml SD-Trp (library scale) to produce an OD_{600} of 0,2 – 0,3 and further cultivated for 3 h with constant shaking (250 rpm) at 30° C to an OD_{600} of 0,5. Cells were harvested by centrifugation for 5 min at 1000 rpm (Sigma 4K15) and 20° C. The supernatant was discarded and the cell pellet was resuspended in 50 ml (small scale) or 500 ml (library scale) sterile A. dest and centrifuged again as described above. After discarding the supernatant, the cell pellets were resuspended in 1,5 ml (small scale) or 8 ml (library scale) freshly prepared, sterile 1 x TE/LiAc. To achieve highest transformation efficiencies, competent yeast cells were either used immediately or within one hour after preparation.

YPDA	Bacto Peptone	20 g/l
	Bacto Hefeextrakt	10 g/l

	Adeninhemisulfat	0,003%
	Glucose	2%
TE/LiAc	Tris/HCl pH 7,5	0,01M
	EDTA	1 mM
	LiAc	1mM

3.2.2.8.2 Transformation of yeast cells with plasmid DNA

200 ng of DNA-BD vector construct (bait; pGBK-T7 PrP23-231) were mixed with 100 ng of AD vector construct (prey; in pGAD-T7) and 100 µg herring testes carrier DNA for small scale simultaneous co-transformation. For library screening, 250 µg pGAD-T7 peptide aptamer library were added to 20 mg herring testes carrier DNA. The carrier DNA was denatured by heating to 95° C for 5 min and chilled on ice for 2 min prior to use. For small scale transformation, 100 µl of competent cells and 600 µl sterile PEG/LiAc solution were added, for library scale 8 ml of competent yeast cells pre-transformed with pGBK-T7 PrP23-231 and 60 ml PEG/LiAc. The components were mixed by vortexing at high speed and incubated at 30° C for 30 min with shaking (200 rpm). Then 70 µl (small scale) or 7 ml (library scale) of DMSO were added, samples were mixed by gentle inversion and heat-shocked for 15 min in a 42° C water bath. Subsequently, cells were chilled on ice for 2 min and harvested by centrifugation for 1 min (14000 rpm; Eppendorf 5417C; small scale) or 5 min (1000 rpm; Sigma 4K15; library scale). Supernatants were discarded and cells were resuspended in 500 µl (small scale) or 10 ml (library scale) of sterile 1 x TE. For library screen the entire volume was plated on 50 QDO + α-X-Gal plates (200 µl each). One hundred µl of the small scale samples were plated on QDO + α-X-Gal, SD-Trp and SD-Leu. Colonies were incubated for 5 – 7 days at 30° C.

PEG/LiAc	Tris/HCl pH 7,5	0,01M
	EDTA	1mM
	LiAc	1mM
	PEG 3350	40 %
QDO	SD Minimal Base	26,7 g/l
	DO Supplement –Ade/-His/-Leu/-Trp	0,60 g/l
	(Bacto agar	2 %)

SD/-Trp	SD Minimal Base	26,7 g/l
	DO Supplement -Trp	0,73 g/l
	(Bacto agar	2 %)
SD/-Leu	SD Minimal Base	26,7 g/l
	DO Supplement -Leu	0,69 g/l
	(Bacto agar	2 %)
α-X-Gal	250 µg/ml in di-methylformamide (DMF)	

3.2.2.8.3 Purification of plasmid DNA from yeast cells

Single yeast colonies were inoculated into 5 ml of the respective dropout medium and incubated over night at 30° C with constant shaking. Thereof, 1,5 ml were centrifuged for 30 sec at 14000 rpm (Eppendorf 5417C). Plasmid isolation from the cell pellets was performed with the Grow'n'Glow Yeast Plasmid isolation Kit according to the recommended protocol. In contrast to bacterial cells mechanical disruption of the yeast cell walls is necessary in addition to alkaline lysis. Since the yield of plasmid is to low for sequencing, plasmids isolated from yeast were transformed into bacteria (**3.2.2.10**) for sequencing or further applications. Alternatively, inserts of interest were amplified by PCR (**3.2.2.1**) and purified PCR products were subjected to sequencing.

3.2.2.9 Preparation of chemically competent *E. coli*

One colony of *E. coli* XL1-blue was inoculated into 5 ml LB medium without antibiotics and incubated over night at 37° C with constant shaking (180 rpm). One ml of this culture was transferred to 100 ml LB medium. This culture was further cultivated at 37° C and 180 rpm until an optical density measured at λ = 600 nm (OD_{600}) of 0,6 – 0,8 was reached. Cells were chilled on ice for 10 min and subsequently sedimented by centrifugation at 3500 rpm (Sigma 4K15 centrifuge) and 4° C. Bacteria were resuspended in 50 ml ice-cold sterile $MgCl_2$ solution (100 mM) and were after incubation for 30 min on ice again centrifuged as described above. The supernatant was discarded and cells were resuspended in ice-cold sterile 100 mM $CaCl_2$ solution, incubated for 30 min on ice and sedimented. Then the cell pellet was resuspended in 2 ml ice-cold sterile 100 mM $CaCl_2$ solution and stored for 24 hours on ice. After addition of 2,5 ml sterile ice-cold $CaCl_2$ solution (100 mM) and 0,5 ml glycerol, 100 µl aliquots were prepared and the tubes were immediately transferred to –70° C for storage.

LB (Luria-Bertani-) medium:	Bacto Tryptone	10 g/l

	Bacto Yeast extract	5 g/l
	NaCl	10 g/l in A. dest

3.2.2.10 Transformation of *E. coli* with plasmid DNA

An aliquot (100 µl) of chemically competent *E. coli* XL1 blue was thawed on ice for 10 min. One µl of plasmid DNA was added to 100 µl bacteria. The mixture was gently stirred with the pipet tip and incubated for 30 min on ice. After a heat shock of 90 sec at 42° C in a water bath bacteria were chilled on ice for 2 min. Then 400 µl of SOC medium was added and the transformation mixture was incubated at 37° C with constant shaking (200 rpm) for 45 min. The entire volume was plated on LB agar plates containing the appropriate antibiotics (ampicillin 100 µg/ml or kanamycin 40 µg/ml), depending on the plasmid, for selection of transformed bacterial clones. Plates were incubated for 16 hours at 37° C.

SOC medium:	Bacto Tryptone	2 %
	Bacto Yeast extract	0,5 %
	NaCl	10 mM
	KCl	2,5 mM
	$MgCl_2$	10 mM
	$MgSO_4$	10 mM
	Glucose	20 mM in A. dest

LB (Luria-Bertani-) agar:	Bacto Tryptone	10 g/l
	Bacto Yeast extract	5 g/l
	NaCl	10 g/l
	Bacto Agar	15 g/l in A. dest

3.2.2.11 Isolation of plasmid DNA

A single transformed bacterial clone was inoculated into 5 ml of LB medium with antibiotic and incubated over night at 37° C with constant shaking (180 rpm). 100 µl of this culture were transferred to 100 ml LB medium with antibiotic and incubated for 24 hours at 37° C with constant shaking (180 rpm). Bacterial cells were sedimented by centrifugation for 30 min at 12000 rpm (rotor JA25.50; Beckmann Avanti centrifuge). Plasmid DNA thereof was prepared using the Maxi Plasmid Kit based on alkaline lysis according to the protocol given by the manufacturer. After lysis, bacterial components were separated by centrifugation (12000 rpm; Beckmann Avanti; JA25.50; 30 min). Supernatant was transferred to a column that binds plasmid DNA. After several washing steps plasmid DNA was eluted and precipitated with isopropanol. DNA pellets after centrifugation (12000 rpm; Beckmann Avanti;

JA25.50; 30 min) were resuspended in A. dest and the concentration was determined. Plasmid isolation in an analytical scale (miniprep) was performed by subjecting 1 ml of a 5 ml culture inoculated with a single clone and incubated overnight at 37° C with constant shaking to alkaline lysis and purification according to the instructions provided with the GFX Micro plasmid prep kit (GE Healthcare, Freiburg). DNA was eluted using 100 µl A. dest.

3.2.2.12 Quantification of nucleic acids

Concentration of DNA preparations was determined by measuring the absorbance at a wave length of λ = 260 nm (A_{260}). Here, an absorbance of 1 corresponds to 50 µg DNA/ml, if diluted in A. dest. Therefore, DNA samples were diluted at a ratio of 1:10 in A. dest for measurements. In addition to the absorbance at 260 nm, values at 280 nm were determined. At 280 nm, aromatic amino acids, especially tryptophane, have their absorption maximum, and therefore this value provides information about the protein content of the nucleic acid sample. The ratio between the absorbance at 260 nm and 280 nm gives an estimation about the purity of the samples. For DNA a value of 1,8 ensures high quality preparations.

Concentrations were calculated as following:

DNA: A_{260} x 50 µg/ml x dilution factor = x µg/ml

3.2.3 Protein biochemical methods

3.2.3.1 Expression of recombinant proteins in *E. coli* and purification

TrxA and peptide aptamer constructs were subcloned into pQE30 (Qiagen, Hilden) in frame with 6 aminoterminal histidine residues (His-tag). Fusion to this His-tag enables purification of proteins overexpressed in *E. coli* by immobilized metal affinity chromatography (IMAC). Therefore, the bacterial lysate is incubated with a resin containing Ni^{2+} ions (Pro Bond Resin) that form chelate complexes with the histidines. After several washing steps under stringent conditions the target protein is eluted with high concentrations of imidazole that displaces the complexed histidines by competitive binding to the Ni^{2+} ions.

Plasmid constructs were transformed into the protease deficient *E.coli* strain BL21 and streaked on LB agar plates containing ampicillin. After incubation over night at 37° C, one single clone was inoculated into 50 ml LB medium with ampicillin and bacteria were grown over night at 37° C with shaking (200 rpm). The entire volume was then transferred to 1 l of LB medium (+ amp) and incubated at 37° C with constant shaking (200 rpm) to an OD_{600} =

0,6 – 0,8. Expression of target proteins was induced by adding 1 mM of Isopropyl-β-D thiogalactopyranosid (IPTG) to the cultures which were then grown for further two hours under the described conditions. Genes for expression are under the control of the *lac*-promoter and IPTG displaces the repressor by competitive binding which enables the polymerase to start transcription. Subsequently, bacteria were harvested by centrifugation at 4500 rpm for 15 min at 4° C (Beckmann Avanti; rotor JA10). The resulting pellet was stored over night at –20° C. The next day, bacteria were thawn on ice, resuspended in 10 ml lysis buffer and lysed under rotation for 30 min at 4° C. Lysates were centrifuged for 20 min at 6000 x g (Beckmann Avanti; rotor JA25.50) and the supernatant was rotated for 30 min with the resin packed as a column that was equilibrated by washing twice with A. dest and three times with binding buffer. Resin was resuspended twice in 10 ml binding buffer and centrifuged (2 min; 900 rpm; Sigma 4K15; 4° C). Washing was continued with washing buffer until the OD_{280} of the flow-through fraction was below 0,6. Proteins bound to the column were eluted by addition of 8 ml of elution buffer. Fractions of 0,5 ml were collected, protein concentration of each fraction was determined (**3.2.3.12**) and fractions containing > 0,5 mg/ml of protein were pooled. These samples were dialysed in size exclusion dialysis units (Pierce; excluded molecular weight < 10 kDa) over night at 4° C against dialysis buffer to remove urea and enable re-folding of the proteins. Re-folded proteins were further concentrated by size exclusion chromatography using spin columns (Vivaspin; Pierce; excluded molecular weight < 10 kDa). Finally the protein concentration was adjusted to 5 mg/ml in dialysis buffer. Purity was confirmed by SDS-PAGE (**3.2.3.9**) followed by Coomassie Blue staining (**3.2.3.11**).

Lysis buffer pH = 7,8	Guanidine HCl	6M
	Na-phosphate	20 mM
	NaCl	500 mM
Binding buffer pH = 7,8	Urea	8 M
	Na-phosphate	20 mM
	NaCl	500 mM
Washing buffer pH = 6,3	Urea	8 M
	Na-phosphate	20 mM
	NaCl	500 mM
	Imidazole	80 mM

Elution buffer pH = 6,3	Urea	8 M
	Na-phosphate	20 mM
	NaCl	500 mM
	Imidazole	500 mM
Dialysis buffer pH 3,5	Na-acetate	10 mM

3.2.3.2 *In vitro* trancription/translation

For cell-free expression of proteins, the TNT T7 Quick Coupled Transcription/Translation system (Promega) was used. This kit contains rabbit reticulocyte lysate and all factors necessary for protein transcription and translation including T7 polymerase. It was used to confirm positive interactions between peptide aptamers and PrP23-231 identified in the Y2H screen. Both plasmids, pGBK-T7 and pGAD-T7 harbour a T7 promotor to initiate transcription of the GAL4 fusion proteins. For best yields of protein, sequences covering the T7 promotor and PrP23-231 or peptide aptamers were amplified by PCR. Purified PCR products were used for *in vitro* transcription/translation. In addition, the expressed proteins are differentially tagged with either a myc-tag (pGBK-T7 PrP23-231) or HA-tag (peptide aptamers) for immunoprecipitation. The following optimised approach was used:

TNT-Quick Master-Mix	20 µl
^{35}S-Cys/Met Promix	1 µl
PCR product	20 µl
A. dest	ad 50 µl

Samples were incubated for 90 min at 30° C, then the reaction was terminated by the addition of puromycin (1 µg/ml). Samples containing PrP23-231 were mixed with either of the peptide aptamers, subjected to co-immunoprecipitation (**3.2.3.8**) using anti-HA antibody and separated by SDS-PAGE (**3.2.3.9**). Gels were dried using a vacuum drier (Biorad, Munich) and then were exposed to an X-ray film for 1, 3 or 7 days.

3.2.3.3 Preparation of postnuclear lysates

Cells were washed twice with 5 ml of cold PBS. Then 1 ml lysis buffer was added and incubated for 10 min. The lysates were transferred to a 1,5 ml Eppendorf cup and centrifuged for 1 min at 14000 rpm in an Eppendorf 5417C centrifuge to remove membranes and nuclei. The supernatant was either subjected to Proteinase K digestion (**3.2.3.4**) or detergent

solubility assay (**3.2.3.5**) for detection of PrP^{Sc}. For detection of PrP^{c}, supernatants were transferred to a 15 ml Falcon tube. For precipitation of proteins, 5 ml (5fold volume) of methanol was added and the samples were incubated over night at – 20° C. Precipitated proteins were then sedimented by centrifugation for 25 min at 3500 rpm (Sigma 4K15) and 4° C. Methanol was discarded, the protein pellet was air-dried for 15 min at room temperature and resuspended in 50 – 100 µl TNE buffer. Until analysis in Western Blot (**3.2.3.10**) samples were stored at –20° C.

Lysis buffer	NaCl	100 mM
	Tris-HCl pH7,5	10 mM
	EDTA	10 mM
	Triton X-100	0,5 % (w/v)
	DOC	0,5 % (w/v) in A. dest
TNE buffer	Tris-HCl pH 7,5	50 mM
	EDTA	5 mM
	NaCl	150 mM in A. dest

3.2.3.4 Proteinase K (PK) digestion of postnuclear lysates

Aliquots of postnuclear lysates (**3.2.3.3**) were incubated for 30 min at 37° C with 20 µg/ml of PK. Digestion was stopped by addition of 0,02 % Pefabloc SC proteinase inhibitor. Samples were either subjected to detergent solubility assay (**3.2.3.5**) or precipitated with 5 volumes of methanol over night at –20° C. Precipitated proteins were sedimented as described in **3.2.3.3**, resuspended in 20 – 50 µl TNE buffer and stored at –20° C until further analysis.

Proteinase K (PK)	10 mg/ml stock solution in A. dest
Pefabloc SC	10 mg/ml stock solution in A. dest

3.2.3.5 Detergent solubility assay

By this assay, PrP^{Sc} can be separated from PrP^{c} due to its insolubility in non-ionic detergents. It enables the specific detection of PrP^{Sc} without PK digestion and concentration of low PrP^{Sc} amounts.

Postnuclear lysates (**3.2.3.3**) with or without PK digestion (**3.2.3.4**) were supplied with 1 % N-lauryl-sarcosine and 0,02 % Pefabloc SC in an ultracentrifuge tube (Beckmann). Samples were ultracentrifuged for 1 hour at 4° C and 40000 rpm (Beckmann TL 100 ultracentrifuge;

rotor TLA-45). Supernatants were precipitated with 5 volumes of methanol over night at –20° C, then proteins were sedimented as described in **3.2.3.3**, resuspended in TNE buffer and stored at –20° C until further analysis. Pellet fractions containing PrP^{Sc} were resuspended in 20 µl of TNE buffer and also stored at –20° C until further analysis.

N-lauryl-sarcosine	10 % (w/v) stock solution in A. dest

3.2.3.6 Immunoprecipitation of PrP^{Sc}

Immunoprecipitation is a protein biochemical method to purify a certain protein present in solution by utilizing specific antisera. During incubation of the protein solution with antibodies, they recognise their respective epitopes and antigen-antibody complexes are formed. Since these immunocomplexes only precipitate if equimolar amounts of antibody and antigen are available, protein-A sepharose is added to the sample. Protein A is a bacterial protein that binds F_c-portions of antibodies and the conjugation to sepharose enables to sediment the bound immunocomplexes. By heating in buffer containing detergents and reducing agents, immunocomplexes are then destroyed, the immunoprecipitated protein is released and can be further analysed.

Metabolically labelled cells (**3.2.4.10**) were washed twice with cold PBS on ice, were covered with 1 ml lysis buffer (**3.2.3.3**) and incubated for 10 min on ice. Cell lysates were transferred to 1,5 ml Eppendorf tubes and centrifuged for 1 min at 14000 rpm (Eppendorf 5417C centrifuge) and 4° C to remove cell debris. Supernatants were digested with PK (**3.2.3.4**) and subsequently subjected to detergent solubility assay (**3.2.3.5**). Supernatants thereof were discarded and pellet fractions were resuspended in 100 µl RIPA buffer and denatured for 10 min at 95° C. The samples were chilled on ice for 2 min, then 900 µl sarcosyl buffer, 20 µl Pefabloc SC 1 % and anti-prion antibody A7 (1:300; **Table 1**) were added, followed by incubation at 4° C under constant rotation on a head-over-tail shaker for 24 hours. Protein-A sepharose (100 µl) was added to bind the antibody-PrP immunocomplexes during another 1 hour incubation on the head-over-tail shaker at 4° C. Immunocomplexes bound to protein-A sepharose were sedimented by centrifugation at 14000 rpm and 4° C (Eppendorf 5417C centrifuge) for 2 min. Supernatants were discarded and protein-A sepharose pellets were washed 5 times by repeated resuspension in 400 µl RIPA buffer and centrifugation for 2 min at 14000 rpm and 4° C (Eppendorf 5417C centrifuge). After the last washing step, supernatants were completely removed. To dissociate the immunocomplexes from the protein-A sepharose, pellets were resuspended in 20 µl N-Glycosidase F buffer and heated for 10 min at 95° C. Samples were cooled for 2 min on ice and centrifuged for 2 min at 14000 rpm (Eppendorf 5417C centrifuge) and 4° C. Supernatants were carefully transferred to a

fresh 1,5 ml tube and subjected to deglycosylation with N-Glycosidase F (**3.2.3.7**) followed by separation by SDS-PAGE (**3.2.3.9**). The gels were dried on a gel dryer and exposed to an X-ray film for 1, 3 and 7 days.

RIPA buffer	DOC	0,5 % (w/v)
	Triton-X 100	0,5 % (w/v)
	SDS	1 % (w/v) in PBS
Sarcosyl buffer	NaCl	100 mM
	Tris-HCl pH7,5	10 mM
	EDTA	10 mM
	Triton X-100	0,5 % (w/v)
	DOC	0,5 % (w/v)
	N-lauryl-sarcosine	1% (w/v) in A. dest
Protein-A sepharose	50 % (w/v) in A. dest	
N-Glycosidase F buffer	2-Mercaptoethanol	0,1 M
	SDS	0,5 % (w/v) in PBS

3.2.3.7 Deglycosylation of proteins with N-Glycosidase F

The prion protein contains two N-linked carbohydrate moieties which lead to the appearance of the typical three-banding pattern, consisting of di-, mono-, and unglycosylated PrP. To increase the sensitivity of PrP^{Sc} detection after immunoprecipitation, samples were deglycosylated to concentrate the entire PrP^{Sc} in one band.

Supernatants eluted from protein-A sepharose after immunoprecipitation (**3.2.3.6**) were mixed with 15 µl lysis buffer (**3.2.3.3**), 2,5 µl Pefabloc SC and 0,25 Units N-Glycosidase F. Samples were incubated for 24 hours at 37° C followed by separation by SDS-PAGE (**3.2.3.9**).

3.2.3.8 Co-immunoprecipitation

Cells were grown to confluency, rinsed twice with cold PBS and lysed for 10 min on ice in 1 ml Co-IP buffer. Using a cell scraper cells were detached from the culture dish and the lysate was transferred to a reaction tube. Lysates were centrifuged for 10 min at 14000 rpm and 4° C (Eppendorf 5417C) to remove nuclei and membranes and 80 µl Pefabloc proteinase

inhibitor (1 %) and antibody (4H11 or anti-HA) at a 1:100 dilution were added to the supernatants. Samples were incubated for 3 h on a head-over-tail shaker in the cold room. Subsequently, 100 µl protein A-Sepharose and again 80 µl of Pefabloc (1 %) were added, followed by incubation for 90 min on a head-over-tail shaker in the cold room. After centrifugation for 2 min at 14000 rpm and 4° C (Eppendorf 5417C) the protein A-Sepharose pellet with the bound immune complexes was washed four times with Co-IP wash buffer by resuspending the sepharose with 500 µl of buffer followed by centrifugation. Immune complexes were released by boiling the sepharose pellet for 5 min at 95° C in 30 µl 3 x SDS sample buffer (see **3.2.3.9**). After a further centrifugation step, supernatants were subjected to SDS-PAGE (**3.2.3.9**) and immunoblot (**3.2.3.10**). Samples from the *in vitro* transcription/translation approaches (**3.2.3.2**) were mixed with 1 ml Co-IP lysis buffer and processed further as described above.

Co-IP lysis buffer	Tris-HCl pH 7,5	50 mM
	NaCl	150 mM
	EDTA	0,5 mM
	NaF	1 mM
	Triton-X 100	0,5 %
	Tween-20	1 %
Co-IP wash buffer	Tris-HCl pH 7,5	100 mM
	NaCl	200 mM
	EDTA	0,5 mM
	NaF	1 mM
	Triton-X 100	1 %
	Tween-20	2 %

3.2.3.9 Sodium dodecyl sulfate-polyacrylamide gel electrophoresis (SDS-PAGE)

All protein samples were separated by denaturing SDS-PAGE in a two phase gel for analysis. Thereby, proteins are separated according to their molecular weight. To achieve this, they are denatured by the addition of SDS, an anionic detergent that linearizes and binds to proteins and saturates them with negative charges. In addition, a reducing agent like 2-mercaptoethanol or di-thiothreitol can be used to reduce inter- and intramolecular disulfide bonds. The linearized and reduced proteins are then loaded on a SDS-polyacrylamide gel for

separation. Depending on the concentration of acrylamide and the ratio between acrylamide:bis-acrylamide, pores are formed upon polymerisation of acrylamide, which is started by the addition of TEMED and ammonium peroxodisulfate (APS). Proteins with a low molecular weight can pass the pores faster than proteins with a higher molecular weight, leading to the separation. The vertical gels consist of two phases: a stacking gel with lower acrylamide concentration (5 – 6 % acrylamide) to focus all proteins in a single sharp band, and a resolving gel with with a higher acrylamide content (between 8 – 20 % acrylamide) in which proteins are separated according to their molecular weight during electrophoresis. For tracking the proteins during electrophoresis, a dye, e. g. bromphenol blue, is contained in the sample buffer.

For this thesis, separation of proteins was carried out on denaturing SDS gels containing 12,5 % acrylamide. Glass plates were rinsed with ethanol and spacers were placed on both edges of the plates. Then plates were wrapped into a plastic bag and placed into the casting chamber. The mixture for the resolving gel (lower gel) was poured between the glass plates and overlaid with isopropanol. After the resolving gel was polymerised, isopropanol was completely removed, the resolving gel was overlaid with the mixture for the stacking gel (upper gel) and immediately the combs were inserted. When polymerisation was finished, the combs were removed and the glass plates containing the gel were vertically placed into an electrophoresis chamber and covered with electrophoresis buffer. Samples (between 10 and 30 µl) and molecular weight marker (5 µl) were loaded and electrophoresis was started. To avoid precipitation of proteins during entering the stacking gel or during the transfer from the stacking gel into the resolving gel, low power (30 mA) was applied until the proteins entered the resolving gel. Then electrophoresis was accomplished under constant power (45 mA) until the tracking dye had reached the bottom of the resolving gel.

4 x Lower gel solution	Tris-HCl pH 8,8	1,5 M
	SDS	0,4 % (w/v) in A. dest
4 x Upper gel solution	Tris-HCl pH 6,8	0,5 M
	SDS	0,4 % (w/v) in A. dest
APS	10 % (w/v) stock solution in A. dest	
3 x SDS sample buffer	Tris-HCl pH 6,8	83 mM
	SDS	6,7 % (w/v)
	Glycerol	33 % (v/v)

	2-mercaptoethanol	16,6 % (v/v)
	bromphenole blue	in A. dest
10 x SDS electrophoresis buffer	Tris	250 mM
	Glycine	2,5 M
	SDS	1 % (w/v) in A. dest
Resolving gel mixture	A. dest	20,4 ml
(12,5 % acrylamide)	Lower gel solution	15,4 ml
	Protogel	25,9 ml
	APS 10 %	192 µl
	TEMED	90 µl
Stacking gel mixture	A. dest	9,9 ml
(5 % acrylamide)	Upper gel solution	4,2 ml
	Protogel	2,8 ml
	APS 10 %	168 µl
	TEMED	30 µl

3.2.3.10 Immunoblot (Western Blot)

This technique allows the detection by specific antisera of proteins separated by SDS-PAGE. By applying constant voltage, negatively charged proteins are transferred out of the gel onto a nitrocellulose or polyvinyl difluoride (PVDF) membrane. The membrane is saturated with protein by incubation with skim milk or albumine solution to avoid non-specific binding of antibodies to the membrane. Then it is incubated with an antibody specifically recognising the protein of interest, followed by incubation with a secondary antibody directed against immunoglobulins of the species in which the first antibody was produced (e. g. recognising mouse IgG). The secondary antibody is conjugated with horseradish peroxidase or other enzymes that catalyse the conversion of for example chemiluminescent substrates. The resulting chemiluminescence can be detected by exposure of the PVDF membrane to a X-ray film.

Six blotting papers and one PVDF membrane were cut to the size of the acrylamide gel. Blotting papers were soaked in blotting buffer, the PVDF membrane was rinsed with methanol and then with A. dest. On the anode of a semidry blotting chamber, 3 blotting papers were overlaid with the membrane. The gel was placed on the membrane and covered with further 3 blotting papers. The chamber was closed with the cathode and electric power

(18 V) was applied for 30 min. The membrane was then soaked in blocking buffer for 30 min at room temperature. The primary antibody (**Table 4**) was added at the appropriate dilution (prepared in TBST) and incubated on a horizontal shaker over night at 4° C. After five washing steps with TBST for 5 min each the secondary antibody (**Table 4**) diluted in TBST was added for 60 min at room temperature, followed again by five washing steps in TBST for 5 min each. For detection, the membrane was briefly dried between two blotting papers and covered with the chemiluminescence substrate (ECL Plus), prepared according to the manufacturers instructions, for 3 min in the dark. Then the membrane was exposed to X-ray films for 1 min, 5 min and 3 hours.

Blotting buffer	Tris	3 g
	Glycine	14.4 g
	Methanol	20 % (v/v)
	A. dest	ad 1000 ml
10 x TBST	Tris-HCl pH 8,0	100 mM
	NaCl	100 mM
	Tween-20	0,5 % (v/v) in A. dest
Blocking buffer	Skim milk powder	5 % in 1x TBST
ECL Plus Detection Kit		

3.2.3.11 Coomassie Blue staining of SDS-polyacrylamide (SDS-PA) gels

SDS-PA gels were submerged in Coomassie solution and stained for 30 min with gently rocking at room temperature. Coomassie solution was removed and the gels were discolored by washing with discoloring buffer until protein bands of interest were clearly visible and no Coomassie blue background staining was present.

Coomassie solution	Coomassie Brillant blue G-250	1,5 g
	Methanol	455 ml
	Acetic acid 99 %	80 ml
	A. dest	ad 1000 ml
Discoloring buffer	Methanol	45 %

Acetic acid 99 %	10 % in A. dest

3.2.3.12 Determination of protein concentration by Bradford assay

Five µl of protein solution diluted 1:20 in A. dest or protein standard dilutions were mixed with 250 µl Coomassie Brilliant Blue reagent in a 96well plate and incubated for 5 min at room temperature. By binding to proteins the absorption maximum of Coomassie Blue is shifted from a wave length of 465 nm to 595 nm. Absorption of protein samples was measured at a wave length of λ = 595 nm in an ELISA reader. Since protein concentrations are in linear relation to the extinction measured, a standard curve using the extinction of the protein standard dilutions was created that allowed to determine the protein concentration of the samples.

3.2.4 Cell biological methods

All works with mammalian cell cultures were accomplished in a biosafety level 2 laminar flow. Gloves and disposable plastic pipets were used to avoid microbial contamination. For handling of liquid nitrogen, appropriate safety protection shields and suitable gloves were worn.

3.2.4.1 Thawing of cells

Cells preserved for long-term storage in liquid nitrogen were thawed at 37° C. The cell suspension was then transferred to a 15 ml Falcon tube, 10 ml culture medium were added and the sample was centrifuged for 10 min at 800 rpm (Sigma 4K15 centrifuge) at 20° C. Thereby, agents added for cryoconservation that might be toxic for the cells (e. g. DMSO) are washed out. The supernatant was discarded and the cell pellet was resuspended in 10 ml culture medium containing fetal calf serum (FCS) and all additives and plated on a cell culture dish.

3.2.4.2 Cultivation and passaging of mammalian cells

Cells were cultivated on cell culture dishes at 37° C in a humidified atmosphere containing 5 % CO_2. The different cell lines were kept in culture medium as listed below:

N2a	OptiMEM + GlutaMAX + 10 % FCS + Pen/Strep

N2a wt	OptiMEM + GlutaMAX + 10 % FCS + Pen/Strep
Clone 21	OptiMEM + GlutaMAX + 10 % FCS + Pen/Strep
22LN2a	OptiMEM + GlutaMAX + 10 % FCS + Pen/Strep
3F4-ScN2a	OptiMEM + GlutaMAX + 10 % FCS + Pen/Strep
Hpl3-4	D-MEM + GlutaMAX + 10 % FCS + Pen/Strep
Hpl-3F4	D-MEM + GlutaMAX + 10 % FCS + Pen/Strep

Culture medium was changed every other day. When confluency was reached, cells were rinsed once with 5 ml PBS and detached from the culture dish by digestion with 1 ml Trypsin/EDTA solution. Nine ml of culture medium were used to suspend the detached cells, the appropriate volume of cell suspension was transferred to a fresh cell culture dish and 10 ml culture medium were added for further cultivation.

3.2.4.3 Cryoconservation of cells

Cells were detached from the culture dish (**3.2.4.2**) at 80 % confluency and centrifuged at 1000 rpm (Sigma 4K15 centrifuge) for 5 min at 20° C. The cell pellet was resuspended in freshly prepared freezing medium. Aliquots of 1 ml each were pipeted into cryoconservation tubes. The tubes were immediately placed at – 80° C over night and were then transferred to a liquid nitrogen tank for long-term storage.

Freezing medium	Culture medium (containing all additives)
	+ 10 % FCS
	+ 10 % DMSO

3.2.4.4 Determination of cell number

Cells were detached from the culture dish (**3.2.4.2**) and suspended in 10 ml culture medium. An aliquot was diluted 1:10 in PBS and filled into a Fuchs-Rosenthal hemocytometer. The cell number in four diagonally lying squares consisting of 16 small squares was counted. One square has an area of 1 mm^2 and a depth of 0,2 mm, giving a volume of 0,2 mm^3. Multiplying the cell number/square with 5000 results in the cell number/ml, which was assessed according to the following equation:

Cell number/ml = counted cells : no. of counted squares x dil. Factor x 5000

3.2.4.5 Transfection of cells

In order to achieve a high transfection efficiency, different transfection reagents were tested for each cell line to find the best combination. The efficiency of the DNA transfer is influenced by cell density, DNA concentration and ratio between DNA and transfection reagent. Initially, different cell numbers (2,5 x 10^5, 5 x 10^5, 1 x 10^6) per 6 cm dish were plated. The day after seeding, transfection was done with different reagents (Fugene 6, Lipofectamine 2000) according to the manufacturers instructions. To enable evaluation of transfection efficiency, the plasmid pEGFP-C1 encoding an enhanced green fluorescent protein (EGFP) was transfected. Two days after transfection, the percentage of cells showing autofluorescence of EGFP was determined by fluorescence microscopy. The combination with the highest percentage was used for further experiments.

These are in particular:

1 x 10^6 of Hpl3-4 or Hpl-3F4 cells were seeded in a 6 cm culture dish. The day after, they were transfected using Lipofectamine 2000 transfection reagent, a cationic amine and lipid reagent that complexes DNA due to electrostatic interaction for transferred to eukaryotic cells. Four µg of plasmid DNA were diluted in 250 µl OptiMEM without supplements. Ten µl of Lipofectamine 2000 reagent was mixed with 250 µl of OptiMEM without supplements and incubated for 5 min at room temperature. The two samples were then combined and incubated for further 20 min at room temperature. Subsequently, the mixture was added to the cell cultures which were prepared by changing the culture medium. Six hours after transfection, the culture medium was changed to avoid toxic effects of the Lipofectamine 2000 reagent.

All other cell lines were transfected with Fugene 6 reagent, a mixture of different lipid components. 2,5 x 10^5 cells were seeded in a 6 cm dish the day before transfection. Six µl of Fugene 6 reagent were added to 100 µl medium without FCS and antibiotics and mixed carefully with 2 µg of plasmid DNA. The sample was incubated for 15 min at room temperature and added dropwise to the cell cultures. Media was changed before the transfection mixture was added. Due to low toxicity of Fugene 6 culture medium was again changed the day after transfection. For subsequent double transfection experiments, cells were trypsinised three days post transfection and seeded at a density of 2,5 x 10^5 cells/6 cm dish and transfected the next day as described.

3.2.4.6 Treatment of 3F4-ScN2a cells with peptide aptamers or suramin

Treatment of cells was started the day after seeding. Purified recombinantly expressed proteins adjusted to a protein concentration of 350 µM were added to the culture medium at

concentrations as indicated. Medium was changed and fresh protein was added every other day. Treatment was performed for 5 days. As a control for inhibition of *de novo* synthesis cells were treated with suramin (200 µg/ml) for 16 hours in parallel to the metabolic labeling.

3.2.4.7 Trypsin digestion

At a confluence of 80 % cells were washed twice with cold PBS and incubated with trypsin/EDTA solution for 10 min on ice. Then soybean trypsin inhibitor (10 mg/ml) was added, cells were detached from the culture dish by rinsing with culture medium and harvested by centrifugation for 5 min at 4° C and 1000 rpm (Sigma 4K15). The cell pellet was resuspended in 5 ml PBS supplemented with trypsin inhibitor. After repeating the centrifugation step, the cell pellet was lysed in 1 ml lysis buffer as described in section **3.2.3.3**.

3.2.4.8 Release of GPI-anchored proteins by phosphatidyl-inositol specific Phospholipase C (PIPLC)

Subconfluent cells grown on 6 cm dishes were washed twice with PBS. Then 2 ml of culture medium without supplements and FCS and 200 mU of PIPLC were added. The culture was incubated for 4 hours at 37° C under cell culture conditions. Media were collected and centrifuged first for 5 min at 1000 rpm (4° C; Sigma 4K15). The supernatant was again centrifuged for 5 min at 3500 rpm (4° C; Sigma 4K15). Supernatants thereof were precipitated with 5 volumes of methanol. Cells were lysed as described in section **3.2.3.3**.

3.2.4.9 Preparation of prion-infected brain homogenates

The mouse-adapted scrapie strains 22L and RML were propagated in C57/Bl6 and CD1 mice, respectively. 22L and RML infected mouse brains were kindly provided by Prof. Dr. M. Groschup, Friedrich-Löffler-Institut, Bundesforschungsinstitut für Tiergesundheit, Isle of Riems. The brains were weighed and a 10 % (w/v) homogenate in PBS was prepared using a glass douncer. The homogenate was aliquoted into cryoconservation tubes and stored at –80° C.

3.2.4.10 Infection of cells with prions

Cells (2,5 x 10^5) were seeded in 12-well plates for infection. One day after seeding, culture media were removed and 270 µl of fresh culture medium was added. Brain homogenates were thawn at room temperature and 30 µl were added to the cells, giving a final concentration of 1 % brain homogenate. The brain homogenate was incubated for 24 hours and was then removed. Cultures were washed 3 – 4 times with PBS to remove residual brain homogenate. Fresh culture medium was added and cells were cultivated until further analysis. In transiently transfected cells, infection was performed one day after transfection.

3.2.4.11 Metabolic labelling

Metabolic labelling enables to monitor the biosynthesis, modification and degradation of proteins. To achieve this, cells are cultivated for a given time frame in the presence of certain radioactively labelled amino acids (pulse), usually cysteine and methionine containing a sulfur isotope (^{35}S). During protein translation, these labelled amino acids are incorporated into all newly synthesised proteins. During the pulse, non-radioactive cysteine and methionine are omitted from the culture medium and only low amounts of FCS are added in order to avoid competition with non-labelled amino acids and obtain best possible labelling. Cell cultures may either by lysed directly after the pulse or may be cultivated further for different time periods (chase) to follow up the metabolism of the protein of interest. This protein is upon lysis of cell cultures isolated by immunoprecipitation and subjected to SDS-PAGE and autoradiography.

At a confluency of 70 – 80 %, cells were rinsed once with PBS pre-warmed to 37° C. One ml/6 cm dish of culture medium without cysteine/methionine supplied with 1 % FCS and penicillin/streptomycin was added and cells were incubated for 1 hour at 37° C. Then 10 MBq of (^{35}S)-cys/met were added. Since PrP^{Sc} cannot be detected earlier than 8 hours after pulse (Taraboulos et al., 1994), cultures were incubated for 16 hours with (^{35}S)-cys/met for metabolic labelling of PrP^{Sc}. This long labelling period should increase the sensitivity of detection. Afterwards, cells were processed as described for immunoprecipitation (**3.2.3.6**).

3.2.4.12 Fluorescence-activated cell sorting (FACS)

Cell surface staining

Cells were detached from the culture dish as described (**3.2.4.2**). 1 x 10^6 cells were transferred to FACS tubes and sedimented by centrifugation for 3 min at 1200 rpm (Sigma 4K15 centrifuge) and 4° C. The cell pellet was resuspended in 500 µl FACS buffer and

incubated on ice for 10 min for blocking. Then the cell suspension was again centrifuged (1200 rpm; 3 min; 4° C; Sigma 4K15). Next, cells were incubated for 30 min on ice with the primary antibody (**Table 4**) diluted in FACS buffer. Then, three washing steps followed, which were carried out by repeated sedimentation of cells (1200 rpm; 3 min; 4° C; Sigma 4K15) and resuspension in 500 µl FACS buffer. Staining was accomplished by addition of Cy2-conjugated secondary antibodies (**Table 4**) diluted in FACS buffer for 30 min on ice. Excessive secondary antibody was removed by again 3 washing steps with FACS buffer. In order to exclude permeabilised cells from the analysis, 7-AAD diluted in FACS buffer was added to the cells prior to the measurement and incubated for 5 min on ice. If cells are stained by this dye it is assumed that antibodies could also enter the interior of the cell, which is undesired if selective cell surface protein staining is performed. As controls, cells without staining for gating the cell population and cells without primary antibody for background substraction were employed. Samples were measured in a Coulter EPICS XL apparatus.

FACS buffer:	FCS	2,5 %
	NaN_3	0,05 % in PBS

Staining of intracellular proteins

Cells were detached from the culture dish, resuspended in FACS buffer and 1 x 10^6 cells were transferred to FACS tubes. After centrifugation (3 min – 1200 rpm – Sigma 4K15 centrifuge) the sedimented cells were resuspended in Roti-Histofix and incubated for 10 min at room temperature for fixation. Subsequently, cells were washed twice in Saponin-buffer and were incubated for further 10 min in quenching solution. After 2 further washing steps antibody incubation was performed as described for cell surface staining. However, for antibody dilutions and washing steps saponin buffer was used instead of FACS buffer. Saponin is a detergent mediating permeabilisation of cellular membranes to enable the antibodies to enter the cell interior. In addition, no 7-AAD was added since all cells were expected to be permeabilised. As controls, cells without staining to gate the cell population and cells stained without primary antibody for background substraction were used.

Saponin buffer	FACS buffer + saponin 0,5 %	
Quenching solution	NH_4Cl	50 mM
	Glycine	20 mM in PBS

3.2.4.13 Indirect immunofluorescence assay and confocal microscopy

Cells were seeded on glass cover slips and cultivated until they were 60 – 70 % confluent. Then, cover slips were transferred to 12well culture plates and cells were fixed for 30 min at room temperature with 500 µl Roti-Histofix. The fixation solution was removed, the samples were rinsed 3 times with PBS and quenched with NH_4Cl/glycine solution for 10 min at room temperature. Thereby, free aldehyde groups of the fixation solution are saturated to avoid unspecific cross-linking of primary antibodies. Samples were rinsed again 3 times, then a permeabilisation step, done by a 10 min treatment of the samples with Triton-X 100 (0,3 %) followed. Thereby, the plasma membrane and all internal membranes are permeabilised. After further 3 washes, cover slips were submerged in blocking solution for 10 min at room temperature. Then the primary antibodies (**Table 4**) diluted in PBS were incubated for 45 min at room temperature in a humid chamber. Cells were rinsed 3 times with PBS before addition of the Cy2- and Cy3-conjugated secondary antibodies (**Table 4**) diluted in PBS for 45 min at room temperature in the dark. Finally, samples were rinsed again 3 times with PBS and mounted in anti-fading solution Permafluor for storage at 4° C in the dark. Analysis was done using an LSM510 confocal laser microscope.

Quenching solution	NH_4Cl	50 mM
	Glycine	20 mM in PBS

Triton-X100 0,3 % in PBS; freshly prepared

Blocking solution	Gelatine	0,2 % in PBS

3.2.4.14 Isolation of detergent-resistant microdomains (DRM; lipid rafts)

For the isolation of detergent resistant microdomains (DRM) or lipid rafts, 3 x 10^7 cells were solubilized in 400 µl TX100 buffer and incubated on ice in the cold room for 30 min. The cell lysates were mixed with Nycodenz 70 % in TNE to a final concentration for Nycodenz of 35 % and loaded into an ultracentrifuge tube. This fraction was overlaid by a discontinuous Nycodenz gradient formed by 200 µl fractions of Nycodenz solutions with concentrations of 25, 22.5, 20, 18, 15, 12, and 8 %. After ultracentrifugation (200.000 g, 4 h, 4° C, Beckmann TLS55 rotor), 200 µl fractions were collected from the top to the bottom of the gradient and precipitated with 5 volumes of methanol. After centrifugation for 30 min at 3500 rpm the pellets were resuspended in TNE and an aliquot of each fraction was analysed in immunoblot.

TX100 buffer	NaCl	150 mM
	Tris-HCl pH 7,5	25 mM
	EDTA	5 mM
	TX100	1 %
TNE	NaCl	150 mM
	Tris-HCl pH 7,5	25 mM
	EDTA	5 mM
Nycodenz solutions	indicated % (w/v) in TNE	

4. Results

The possibilities to interfere with prion propagation *in vivo* are very limited, although numerous substances were identified during the last decades that effectively inhibit PrP^{Sc} formation in *in vitro* assays as well as in cell culture models. Therefore, the development of innovative strategies in cell culture models that can successfully be transferred to the *in vivo* situation is still a major challenge in prion research. Peptide aptamers targeting PrP^{c} might be one class of compounds that fulfils these requirements.

4.1 Identification of PrP-binding peptide aptamers

4.1.1 Construction of a combinatorial peptide aptamer library

In previous studies, peptide aptamers interacting for example with cyclin-dependent kinase 2 (Colas et al., 1996) were identified by Y2H-screening of a peptide library based on the yeast transcription factor Lex A. Since in our laboratory a GAL4-based system was well established (Spielhaupter & Schätzl, 2001) it was decided to prepare a novel library. As a scaffold protein, the most frequently used *E. coli* thioredoxin A (trxA) was used. Here, the peptide library can be inserted into the active-site loop which is comprised by two Cys residues at amino acid positions 33 and 36. **Fig. 13** depicts the secondary structure model of trxA with the indicated site of peptide library insertion.

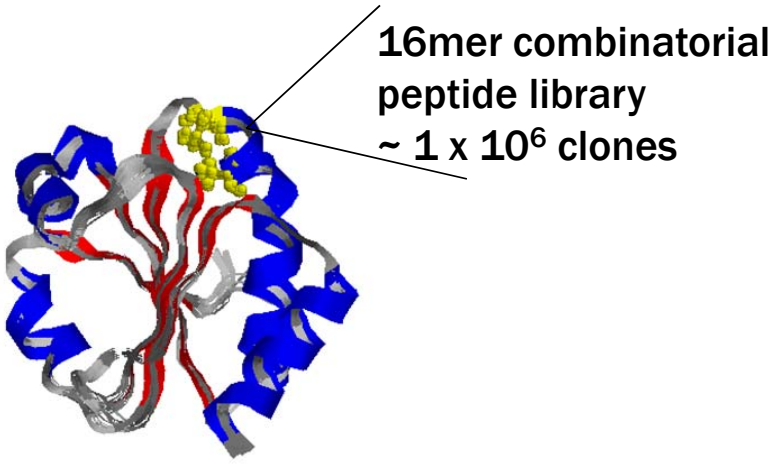

Fig. 13. Design of the peptide aptamer library. Ribbon model of trxA secondary structure (Protein Data Base Accession no. 1XOA). α-helices are given in blue, β-sheets in red. The yellow residues are the Cys residues constituting the active site. The peptide library is inserted into the loop between the two cysteines.

For cloning purposes, one nucleotide (A) was introduced between nucleotide position 102 and 103 by site-directed mutagenesis to create a BamHI restriction site. The coding sequences for a 16mer random peptide library was generated as described in section **3.2.2.7** and the double-stranded oligonucleotides were ligated into linearised pGAD-T7 trxA-BamHI. Complete digestion of the oligonucleotides using BamHI was confirmed by subjecting an aliquot to polyacrylamide gel electrophoresis together with the single stranded oligonucleotides and a double stranded DNA fragment of 48 nucleotides for comparison of the respective migration properties (**Fig. 14**).

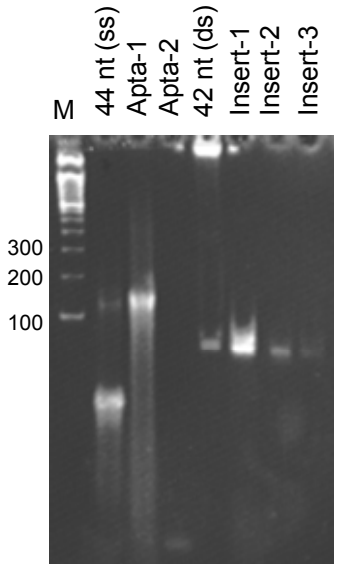

Fig. 14. Second-strand synthesis of random sequence by Klenow polymerase. Single-stranded DNA (44 nucleotides; nt; lane 1), the oligonucleotides Apta-1 and -2 (lanes 2 and 3), a 42-nucleotide double-stranded DNA fragment (lane 4) and three double-stranded aptamer encoding random sequences produced by Klenow reaction and BamHI digestion (lanes 5 – 7) were separated by polyacrylamide gel electrophoresis. M indicates the length standard, number of basepairs are given on the left.

Finally, a peptide library encompassing ~ 10^6 individual clones was obtained. In order to assure successful ligation of the oligonucleotides, 10 clones were analysed for the occurrence of inserts by preparation of plasmid DNA in an analytical scale followed by analysis using digestion with the restriction enzymes EcoRI and XhoI that were used for insertion of trxA into pGAD-T7 (**Fig. 15**). Compared to trxA (320 bp) the inserts of clones containing peptide encoding sequences migrate slower, and comparison to the length standard marker revealed that the shift corresponded to ~ 50 – 100 basepairs.

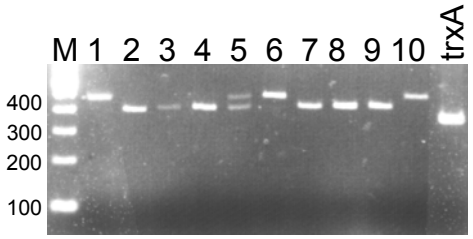

Fig. 15. Restriction enzyme analysis of peptide aptamer library clones. Plasmid DNA for analytical purposes was isolated from 10 clones of the peptide aptamer library. Restriction enzyme analysis using EcoRI/XhoI was performed and DNA was separated by agarose gel (2 %) electrophoresis. TrxA served as a control for comparison of insert length. M indicates the length standard, number of basepairs are given on the left.

In summary, a combinatorial peptide aptamer library using trxA as a scaffold protein was newly created. A complexity of 10^6 individual clones was achieved, as assessed by counting bacterial clones after ligation of the random sequences.

4.1.2 Three peptide aptamers reproducibly interact with PrP23-231

In order to identify peptide aptamers interacting with PrP a Y2H screen was performed. As a bait, murine PrP23-231 fused to the GAL4 DNA-BD (in pGBK-T7) was employed. This sequence does not contain the N- and C-terminal signal peptides, respectively, since they are co- and post-translationally cleaved off and are no constituents of the mature form of PrP. As a prey, the peptide aptamer library as fusion to the GAL4-AD (in pGAD-T7) was used. By interaction of bait and prey the activity of the transcription factor GAL4 is reconstituted due to spatial proximity induced by interaction of the fused proteins, resulting in the activation of reporter gene expression. Thereby, using the *S. cerevisiae* AH109 strain colonies can grow on histidine and adenine deficient media. In addition, the reporter gene MEL1 encoding α-galacosidase is activated which can convert α-X-Gal into a blue dye. These high stringency conditions implicating three individual reporter genes minimize the possibility of false positive interactors.

Initially, 222 clones were found to be positive for reporter gene activation. All clones were re-streaked twice for segregation. After this procedure, 63 clones were still positive under high stringency conditions. However, sequencing revealed that most inserts contained either stop codons within the trxA scaffold or frame shift events occured. The reason for these frame shifts was the insertion of not only one peptide encoding sequence but several of the 48-nucleotide units. This was due to the use of only one restriction enzyme (BamHI), which led to ligation of inserts.

Finally, 6 clones were found to be reproducibly positive. One sequence (PA1) was identified four times and, of importance, in two independent screens. Therefore, three different peptide aptamers, designated PA1, PA8 and PA16 were used for further investigations. The primary

structures are listed in **Table 7**. Of note, PA1 harbours a duplicated insert, resulting in a length of 35 amino acids.

Table 7. Primary structures of PrP-binding peptide aptamers. Residues depicted in red indicate putative β-strands.

Peptide 1	RFGSLFDWVSVFFAAAGGSYFSSVQARLPSWGLGL
Peptide 8	ARFEYLRDGYWVWRFT
Peptide 16	CGRWAIRTVHIWLACG

To further reduce the probability of false positive interactions, binding of PA1, PA8 and PA16 was confirmed in several independent simultaneous co-transformation approaches with PrP23-231 in yeast. Furthermore, auto-activation of GAL4 by these peptide aptamers which could be the result of an interaction with the GAL4-DNA-BD was excluded by co-transformation with empty pGBK-T7 plasmid.

However, it was necessary to confirm positive interactions with a second assay. An elegant approach is offered by coupled *in vitro* transcription/translation systems. Here, the controlled expression of proteins is enabled by incubating rabbit reticulocyte lysates that contain all components necessary for protein expression of DNA sequences harbouring the T7 promoter and T7 polymerase. Both pGAD-T7 and pGBK-T7 encode the T7-promoter enabling *in vitro* transcription/translation of the bait- and prey- proteins. In addition, the fusion proteins are then differentially tagged with the myc- and the HA-epitope for bait and prey proteins, respectively, for co-immunoprecipitation. In order to test the interaction of PrP23-231 with PA1, PA8 and PA16, PCR fragments were generated and purified that covered the T7 promoter, epitope tags and target proteins. The PCR products were applied for *in vitro* transcription/translation using the TNT Quick Coupled *in vitro* transcription/translation kit (Promega) which contains all necessary components. For metabolic labeling of newly synthesized proteins, (^{35})S-Cys/Met was added. To confirm expression of the peptide aptamers, immunoprecipitation with anti-HA antibody was performed. For co-immunoprecipitation, samples containing PrP23-231 or peptide aptamers were combined and immunoprecipitated using an anti-myc antibody specific for myc-PrP23-231. Then samples were subjected to SDS-PAGE, gels were dried and exposed to an X-ray film (**Fig. 16; lanes 5 - 10**). Grb-2, a known interactor of PrP^{c} (Spielhaupter & Schätzl, 2001), served as a positive control (lane 9). As a negative control a sample containing Grb-2 but no PrP was used (lane 5). In further approaches it was confirmed that the myc-antibody does not precipitate any of the peptide aptamers (data not shown).

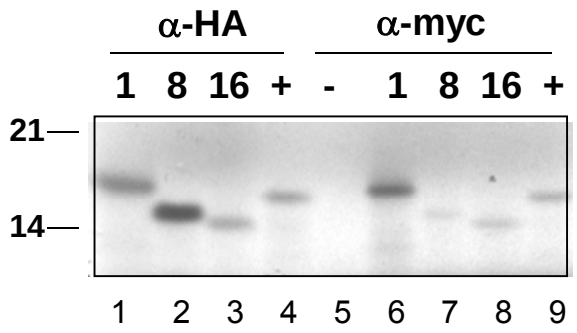

Fig. 16. Co-immunoprecipitation of peptide aptamers and PrP23-231 upon *in vitro* transcription/translation. DNA fragments encoding peptide aptamers 1, 8 or 16, the positive control grb-2 or PrP23-231 were generated by PCR. DNA was subjected to coupled in vitro transcription/translation approach by T7-polymerase in the presence of $^{(35)}$S-Cys/Met. Bait and prey proteins were mixed and co-immunoprecipitation was performed using anti-myc antibody which recognized PrP (lanes 5 – 9). As a control, prey proteins were precipitated with anti-HA antibody (lanes 1 – 4). Samples were separated by SDS-PAGE (12,5 %) and exposed to a X-ray film.

By this assay, interactions of PrP with PA1, PA8 and PA16 could be confirmed, as indicated by the bands precipitated with anti-myc which must be due to binding of the respective proteins to PrP23-231 (lanes 6 – 9). PA1 has a slightly higher molecular weight than PA8 and PA16 due to the duplication of inserts. Immunoprecipitation of prey proteins with anti-HA antibody confirmed the correct molecular weight and successful *in vitro* protein synthesis (lanes 1 - 4).

To sum up, Y2H screening of a combinatorial peptide aptamer library for peptides interacting with PrP23-231 resulted in the identification of three aptamers that reproducibly interacted with PrP23-231 in yeast. In addition, the interactions could be confirmed by co-immunoprecipitation of PA1, PA8 and PA16 with PrP23-231 upon *in vitro* transcription/translation of the proteins.

4.1.3 Mapping of peptide aptamer binding sites by Y2H

Having found that PA1, PA8 and PA16 bind reproducibly to PrP23-231, the next issue was to determine which domain of PrP they recognize. Therefore, mapping studies by Y2H were performed. PrP23-231 was roughly divided into an N-terminal (aa 23 - 100) and a C-terminal (aa 90 - 231) part. The amino-terminus comprises a highly flexible (Riek et al., 1996) but evolutionary well conserved (Schätzl et al., 1995; Wopfner et al., 1999) region of PrP, whereas aa 90 - 231 represent the globular domain which becomes PK resistant upon conversion into PrP^{Sc}. Grb-2 was again used as a positive control, trxA served as a negative control (**Fig. 17**).

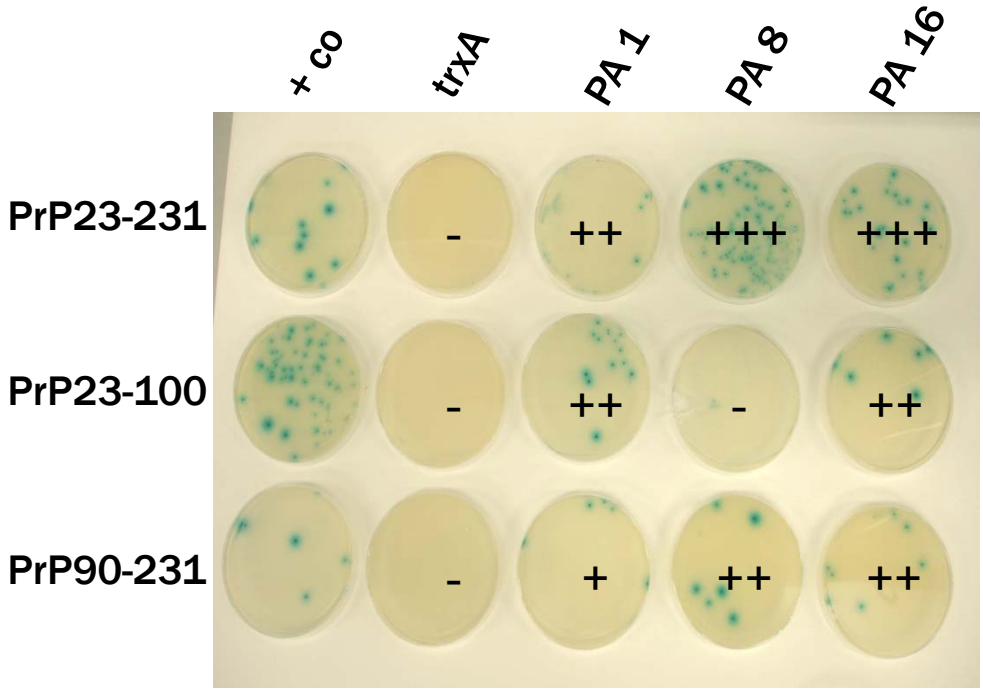

Fig. 17. Mapping of peptide aptamer binding sites to PrP by Y2H. Bait constructs are given on the left, prey constructs on top of the image. Grb-2 served as a positive control. Blue yeast colonies indicate positive interactions.

AH109 yeast cells co-transformed with pGBK-T7-PrP23-231, -PrP23-100 and -PrP90-231 and pGAD-T7-PA1, -PA8, -PA16, -Grb-2 and –trxA were streaked on QDO plates (+ α-X-Gal). Blue colonies indicated positive interactions (**Fig 17**). As expected, trxA did not interact with any of the PrP constructs, whereas Grb-2 (+ co) bound to both amino- and carboxy-terminal PrP. This was also observed for PA1 and PA16. In contrast, PA8 only exhibited a positive interaction with PrP90-231. **Table 8** summarizes the results of the mapping of the binding sites.

Table 8. Binding sites of peptide aptamers.

	trxA	#1	#8	#16
PrP 23-231	-	++	+++	+++
PrP 23-100	-	++	-	++
PrP 90-231	-	+	++	++

In this thesis, it was shown that PA1 and PA16 bound to PrP23-100 and PrP90-231, whereas the binding site of PA8 is located within PrP90-231. Further studies revealed that PA1 and PA16 do not bind to the overlapping region of the two constructs (aa 90 - 100) but indeed have two binding sites (Bachelors thesis H. Anders; 2008). One is located between aa 23 - 90, the second between aa 120 - 150. These more detailed mapping studies further revealed that PA8 binds to PrP 90 - 120.

4.2 Peptide aptamers expressed in E. coli interfere with PrP^{Sc} formation in prion-infected cell cultures

4.2.1 Expression and purification of peptide aptamers in *E. coli*

The goal of the project was to identify peptide aptamers that interfere with PrP^{Sc} formation in prion-infected cell cultures. Having selected peptide aptamers binding to PrP23-231, the next question was whether they might be able to interfere with the formation of PrP^{Sc} in neuroblastoma cells persistently infected with prion strain RML (3F4-ScN2a). Consequently, peptide aptamers and trxA were subcloned into pQE30 plasmid that enables inducible overexpression of proteins in *E. coli* under the control of the *lac*-promoter. Furthermore, proteins of interest are fused to 6 N-terminal His residues which allow purification of fusion proteins by IMAC. Peptide aptamers and trxA were expressed upon induction with IPTG and purified from inclusion bodies under denaturing conditions using urea and guanidinium chloride. Proteins were re-folded by dialysis, further concentrated by size exclusion chromatography and adjusted to an equal concentration of 350 µM. Purity of the preparations was confirmed by SDS-PAGE followed by Coomassie blue staining (**Fig 18**).

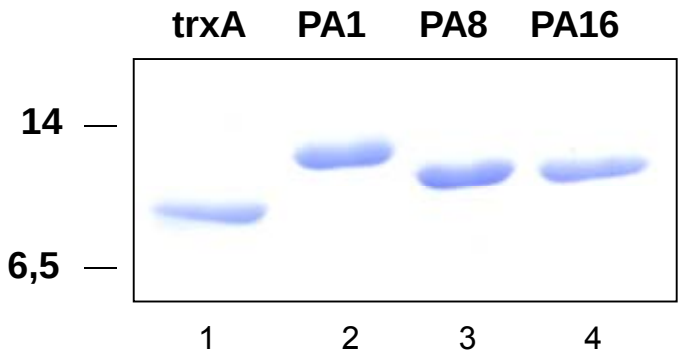

Fig. 18. Analysis of recombinantly expressed and purified peptide aptamers. Peptide aptamers were expressed recombinantly in *E. coli* and purified under denaturing conditions. Upon dialysis and concentration by size exclusion chromatography, 2 µg of protein was separated by SDS-PAGE (20 %) and stained with Coomassie Brilliant Blue.

In all protein solutions only one band specific for trxA or the peptide aptamers was visible.

4.2.2 Treatment of prion-infected 3F4-ScN2a cells with peptide aptamers

To assess the anti-prion effect of the purified peptide aptamers, 3F4-ScN2a were treated for 5 days with rising concentrations (0,07, 0,35, 0,7 and 1,8 µM) of peptide aptamers and trxA. Then the cells were lysed and half of the lysates were subjected to PK digestion. All protein samples (-/+ PK) were subjected to SDS-PAGE and immunoblot analysis using anti-PrP mAb 4H11 (**Fig. 19**). PrP^{Sc} appears in immunoblot typically with three bands, namely the un-, mono- and di-glycosylated forms. The molecular weight is about 7 kDa lower than that of PrP^{c} due to trimming of the flexible N-terminal part (aa 23 – 90) by PK digestion.

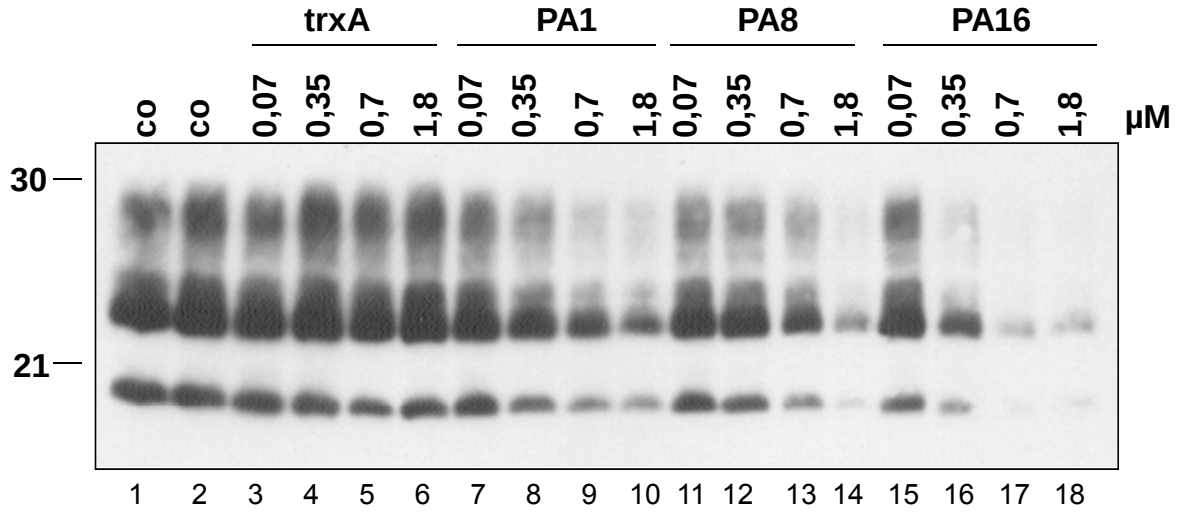

Fig. 19. Treatment of 3F4-ScN2a cells with peptide aptamers. Rising concentrations (as indicated) of purified peptide aptamers were added to the culture medium of 3F4-ScN2a cells for 5 days. Aliquots of PK-digested cell lysates were analysed in immunoblot using anti-PrP antibody 4H11. Treatment with trxA served as a negative control, as an additional control untreated cells were employed.

First, it has to be noted that treatment with peptide aptamers did not influence the amount of PrP^{c} in 3F4-ScN2a cells (data not shown). In contrast, treatment with PA1, PA8 or PA16 (**Fig. 19;** lanes 7 – 18) led to a dose-dependent reduction of PrP^{Sc} when compared to the untreated controls (lanes 1 and 2) or to cells treated with trxA (lanes 3 – 6). PA16 had the most pronounced effect with a strong PrP^{Sc} reduction already at a concentration of 0,35 µM. Similar effects of PA1 and PA8 are exhibited at doses of about 0,7 µM.

These results indicate that PA1, PA8 and PA16, recombinantly expressed in *E. coli* and purified, can inhibit PrP^{Sc} propagation in a dose-dependent manner when added to the culture medium of 3F4-ScN2a cells.

4.2.3 Uptake and solubility of peptide aptamers in infected and non-infected cells

Peptide aptamers described here were selected for binding to PrP23-231, the folding of which is expected to correspond to mature PrP^{c} lacking glycosylation. To assess whether the aptamers might in addition interact with PrP^{Sc} the solubility of purified peptide aptamers in 3F4-ScN2a cells and N2awt cells overexpressing murine PrP^{c} was analysed. The solubility assay is a further biochemical criterion that allows discrimination between PrP^{c} and PrP^{Sc}. Upon addition of non-ionic detergents and ultracentrifugation of cell lysates, PrP^{c} is rendered soluble and is contained in the supernatant whereas PrP^{Sc} aggregates are sedimented and can be detected in the pellet fraction. The assumption was that upon binding to PrP^{Sc} peptide aptamers might participate to the pellet fraction whereas in non-infected cells they might be found in the supernatant. To analyse this, N2awt and 3F4-ScN2a cells were treated for 24 hours with 25 µg/ml of the purified peptide aptamers or trxA or were left untreated. Subsequently, cells were lysed, lysates were subjected to solubility assay and both pellet and supernatants thereof were analyzed in immunoblot either with an anti-His antibody that recognizes the N-terminal His-tag of the peptide aptamers (**Fig. 20A**) or with 4H11 specific for PrP (**Fig. 20B**). As a control, lysates of untreated cells were used.

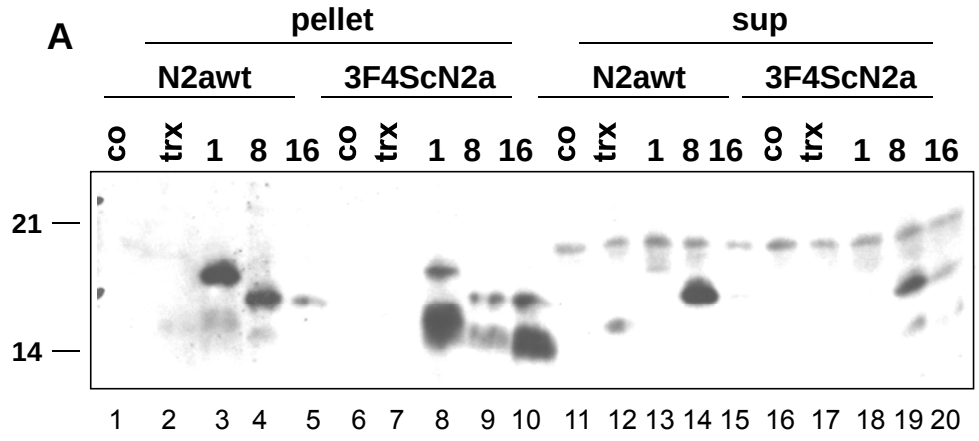

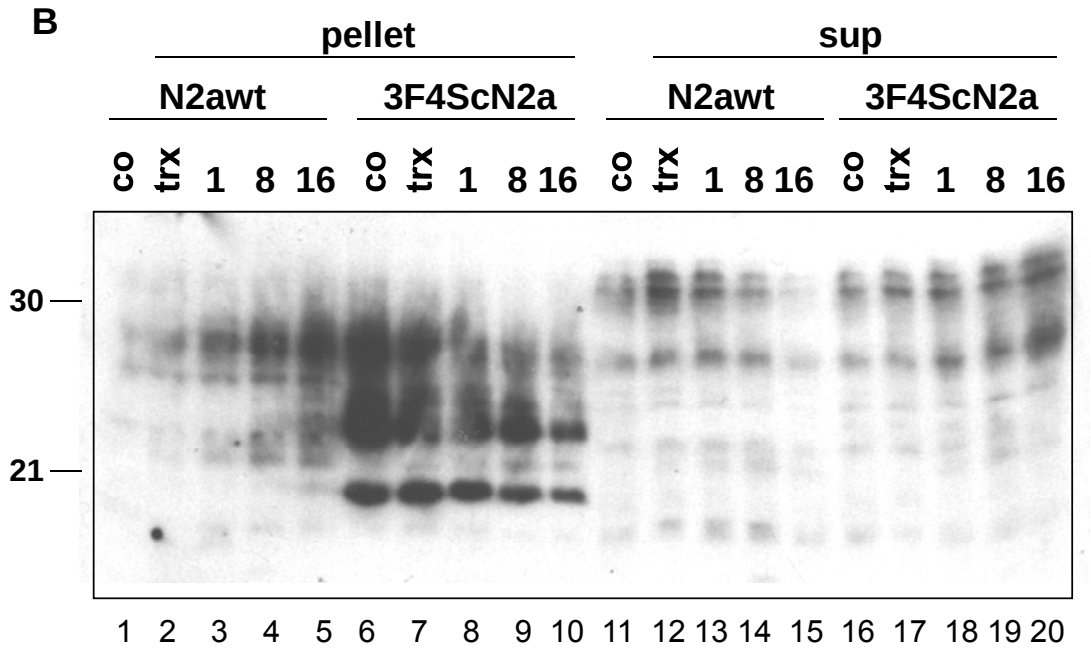

Fig. 20. Solubility of peptide aptamers in N2awt and 3F4-ScN2a cells. N2awt or 3F4-ScN2a cells were treated for 24 hours with purified peptide aptamers (25 µg/ml). Cells were lysed and solubility assay was performed. Supernatant and pellet fraction were subjected to immunoblot using anti-Flag antibody for detection of peptide aptamers (**A**) or 4H11 for PrP (**B**).

All peptide aptamers were detectable in the cell lysates, in contrast to trxA which only was weakly present in the supernatant (sup) of N2awt cells (**Fig. 20A;** lane 12). However, peptide aptamers participated predominantly in the pellet fractions of 3F4-ScN2a as well as in N2awt (**Fig. 20A;** lanes 1-10) indicating that insolubility of the peptide aptamers is independent of binding to PrP^{Sc}. PA8 and, in 3F4-ScN2a also PA16, were in addition present in the soluble supernatant fraction. This might be a hint that these aptamers interact more tightly with PrP^{c} than PA1. Regarding PrP signals the distribution between soluble and insoluble fraction was as expected (**Fig. 20B**). PrP^{c} was mainly soluble with a slight background signal in the pellet fraction of N2awt (lanes 1 – 5). PrP^{Sc} was present in the pellet fractions of 3F4-ScN2a cells. Of note, already after the short treatment for only 24 hours, the PrP^{Sc} signal appeared to be reduced compared to the control of cells treated with trxA (lanes 6 – 10).

From these data it was concluded that PA1, PA8 and PA16 are more effectively internalized by N2awt and 3F4-ScN2a cells than trxA. However, no difference in the solubility behaviour between infected and non-infected cells could be found.

4.3 TrxA-based peptide aptamers can be targeted to the secretory pathway and retain binding properties

The results described in section **4.2** provide proof-of-principle evidence that the peptide aptamers identified by Y2H that bind to PrP^{c} can inhibit PrP^{Sc} propagation in prion infected

cultured cells. However, purified proteins might be hardly applicable in an *in vivo* situation, for example due to immune reactions that might be induced by the foreign proteins. This drawback might be circumvented by gene transfer using lentiviral delivery of peptide aptamer sequences into the brain. For this intracellular expression approach it was necessary to target the peptide aptamers to the secretory pathway which is the subcellular locale harbouring PrP^c. This required fusion of the peptide aptamers to a N-terminal signal peptide that mediates co-translational ER entry and it was decided to use the PrP signal peptide (aa 1 – 22). At the C-terminus, the PrP signal peptide necessary for the attachment of a GPI-anchor was added to avoid secretion and to have the highest probability of co-localisation of the peptide aptamers with PrP^c. Of note, GPI-anchoring leads to association of proteins with lipid rafts, which are cholesterol-rich plasma membrane domains that are suspected to be the compartments of prion conversion (Caughey & Raymond, 1991; Taraboulos et al., 1995; Vey et al., 1996) A scheme of the expression constructs for mammalian cells subcloned into pcDNA3.1/Zeo is depicted in **Fig 21.** For selective detection, a Flag-tag was incorporated between amino-terminal signal peptide and trxA scaffold.

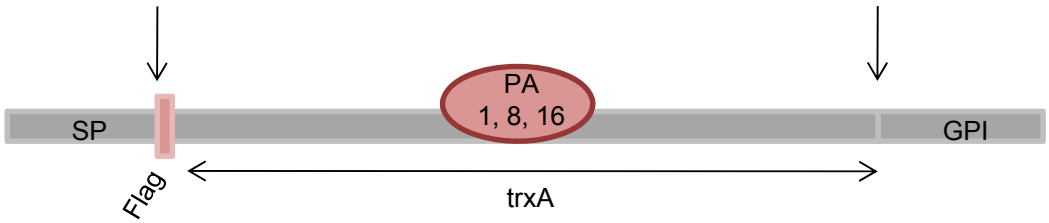

Fig. 21. Scheme of GPI-peptide aptamer constructs. The peptide aptamers (peptide embedded in trxA scaffold) were fused N-terminally to a signal peptide for ER entry followed by a Flag-tag. C-terminally a signal for attachment of a GPI-anchor was added. Vertical arrows indicate cleavage of signal peptides by signal peptide peptidases.

4.3.1 Expression and subcellular localization of GPI-peptide aptamers

To verify cell surface localization, the constructs (1-, 8-, 16- and trxA-GPI) were transiently transfected into N2a cells. Two days post transfection, expression of the aptamers was analysed by fluorescent cell surface staining using anti-Flag antibody and a Cy2-conjugated secondary antibody followed by FACS analysis (**Fig. 22**).

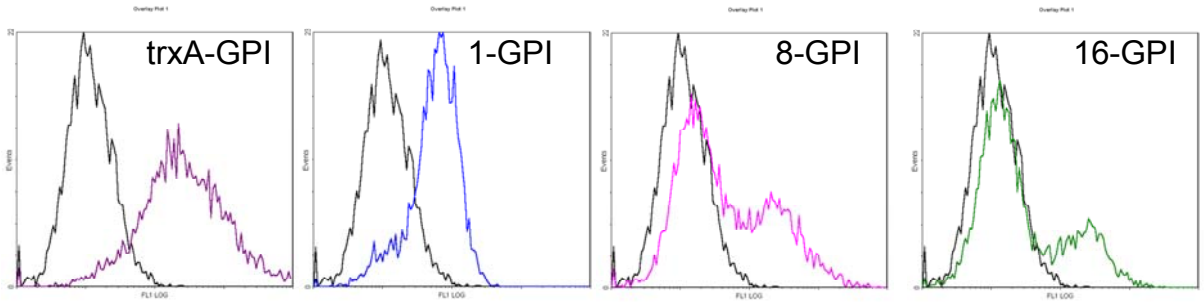

Fig. 22. Surface FACS analysis of N2a cells expressing GPI-peptide aptamers. N2a cells were transiently transfected with the GPI-peptide aptamers and trxA. Surface FACS-analysis with non-permeabilized cells was performed using anti-Flag antibody for detection of surface expression. For excluding dead cells from the analysis, 7-AAD was added. The black line represents the negative control, where the first antibody was omitted. The x-axes depict fluorescence intensity in a logarithmic scale, the y-axes the cell count.

Thereby, it was clearly shown that all aptamer constructs were transported to the outer leaflet of the plasma membrane indicated by the shift of the peak to the right end of the x-axes (coloured lines). The black peak represents the negative control where the first antibody was omitted. Cells were not permeabilized and dead cells were excluded from the analysis. 8-GPI (pink) and 16-GPI (green) had double peaks probably representing two cell populations.

These results had to be confirmed biochemically. For this purpose trypsin digestion of transiently transfected N2a cells was performed. Trypsin digests all cell surface proteins resulting in a net lack of those proteins in the cell lysate. If amounts of target protein contained in the cell lysate are compared between samples with and without trypsin digestion, a reduction of the protein is indicative for its localisation at the plasma membrane. Two days post transfection, N2a cells were subjected to trypsin digestion or not and were lysed. Subsequently, samples were analysed in immunoblot which was incubated with anti-Flag antibody for detection of peptide aptamers and trxA. Analysis of the samples using 4H11 for detection of PrP^c served as a control to confirm the successful digestion of cell surface proteins (**Fig 23**).

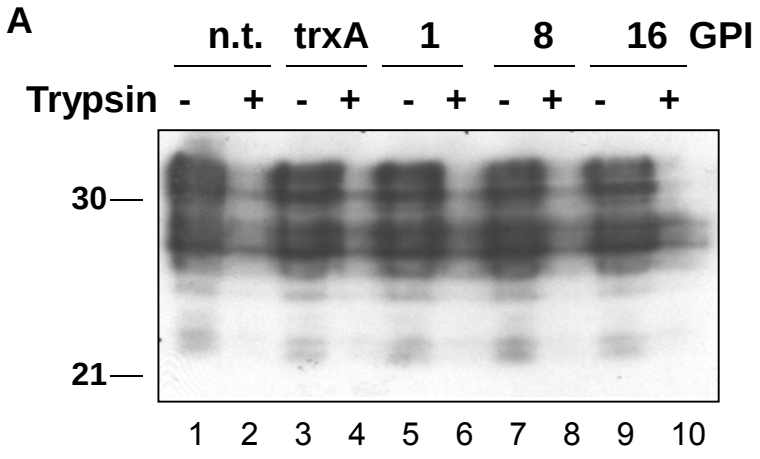

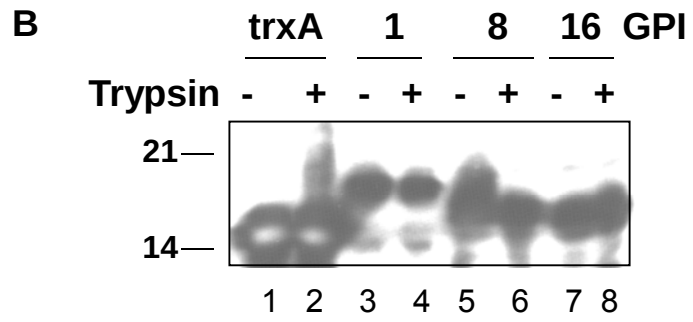

Fig. 23. Trypsin digestion of N2a cells expressing GPI-peptide aptamers. Transient transfection of N2a cells with GPI-peptide aptamers and trypsin digestion 2 days post transfection were performed. Aliquots of lysates derived from cells with or without trypsin treatment were analysed in SDS-PAGE and immunoblot using 4H11 (**A**) or anti-Flag antibody (**B**).

When examining PrP^c (**Fig. 23A**), in all samples trypsin digestion of cells resulted in a reduction of PrP^c in the cell lysates (compare lanes – and + trypsin) independent of transfection with trxA-GPI or GPI-anchored peptide aptamers. Non-transfected cells (n.t.; lanes 1 and 2) were included as a further control. However, when transfected samples were analysed with anti-Flag to visualize peptide aptamers (**Fig. 23B**) there was no significant reduction of the GPI-anchored peptide aptamers or trxA-GPI induced by the trypsin treatment. Only for 8-GPI a slight effect was observed.

However, N2a cells endogenously express PrP^c and it was argued that PrP^c expression might influence the cell surface localisation of the peptide aptamers. Therefore, the trypsin assay was repeated using Hpl3-4, a hippocampal cell line derived from a $PrP^{0/0}$ mouse line (Sakudo et al., 2005), and Hpl3F4 which is the counterpart of Hpl3-4 that stably overexpress 3F4-PrP. These two cell lines were transiently transfected with 1-, 8-, 16- and trxA-GPI and two days post transfection trypsin digestion was performed. Lysates of cells with or without trypsin treatment were subjected to immunoblot and band intensities detected with anti-Flag antibody were compared (**Fig 24**). It was observed that in general the signals in Hpl3F4 cells were weaker, which might be due to a lower transfection efficiency. Only in Hpl3-4, the 1-GPI signal (lanes 3 and 4) was again slightly diminished by trypsin. All other GPI-peptide aptamers and also trxA-GPI were not affected by the treatment. Therefore, it was confirmed that the inaccessibility to trypsin digestion was not due to PrP^c expression.

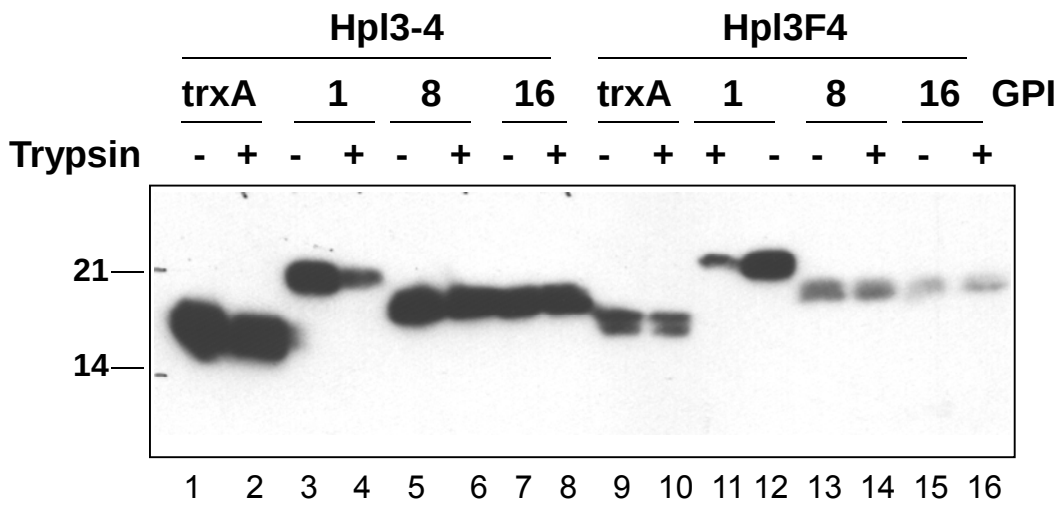

Fig. 24. Trypsin digestion of GPI-peptide aptamer expressing Hpl3-4 and Hpl3F4 cells. Hpl3-4 or Hpl3F4 cells were transiently transfected with GPI-peptide aptamer constructs. Two days post transfection, trypsin digestion was performed, all cells were lysed and aliquots thereof were subjected to immunoblot analysis using anti-Flag antibody.

Since results concerning cell surface localisation of GPI-peptide aptamers were still conflicting, an indirect immunofluorescence assay was performed to visualize the localization of the proteins by confocal microscopy. N2a cells were transiently transfected with the GPI-peptide aptamer constructs and trxA-GPI. Two days post transfection, cells were fixed and one sample was permeabilized with Triton-X 100 (TX100) prior to antibody incubation, whereas the second was not. TX100 permeabilizes the plasma membrane and also internal membranes of ER and Golgi complex which enables staining of extracellular and intracellular proteins. In non-permeabilized cells the antibody has no access to the interior of the cell and can only react with proteins at the extracellular side of the plasma membrane. As a primary antibody, anti-Flag was used, followed by incubation with Cy3-conjugated anti-rabbit IgG (**Fig. 25**).

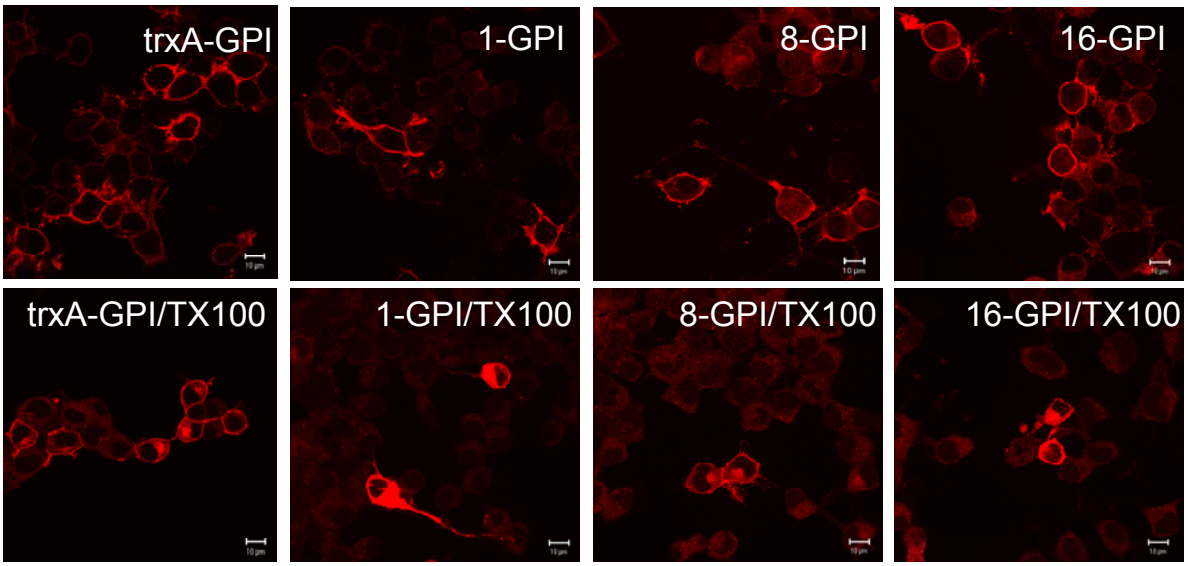

Fig. 25. Immunofluorescence analysis of the localisation of GPI-peptide aptamers. N2a cells transiently transfected with the indicated constructs were permeabilized (TX100) or not and stained with anti-Flag antibody and Cy3-conjugated secondary antibody. Analysis was performed using a Zeiss LSM510 confocal microscope.

The upper panel (**Fig. 25**) depicts non-permeabilized cells. Here, the bright staining surrounding the cells confirmed the results obtained by FACS analysis showing that all GPI-constructs were located at the cell surface. For 1-GPI the percentage of cells exhibiting cell surface staining appeared to be lower than that of the other proteins. This might be due to an overall lower transfection efficiency or to a reduced transport to the cell surface. In TX100-treated cells (lower panel), trxA-GPI and 8-GPI were found at the cell surface and in a distinct intracellular compartment most probably corresponding to the Golgi complex. 8-GPI and 1-GPI were also found at the cell surface but to a much more pronounced extent intracellularly. Here, it was difficult to discriminate between cytosolic and compartmentalized staining, especially for 1-GPI, and it was assumed that at least part of the protein is not properly imported into the ER or retro-translocated to the cytosol for degradation.

In summary, it was demonstrated for the first time that peptide aptamers based on the trxA scaffold protein can be targeted to the secretory pathway. The efficiency of ER import might be different for the various constructs.

4.3.2 Interaction of GPI-peptide aptamers with PrP^c

Although the GPI-peptide aptamers can be targeted to the secretory pathway and the plasma membrane, the most critical question was whether they still bind to PrP^c under these altered conditions. For example, in yeast, interaction occurs in the cytosol where reducing conditions are present whereas in the lumen of ER and Golgi of mammalian cells the conditions are non-reducing. To address this question, co-immunoprecipitation experiments were

conducted. N2awt cells which overexpress murine PrP^c were transiently transfected with the GPI-peptide aptamers and trxA-GPI. Two days post transfection cells were lysed under non-denaturing conditions in order to conserve protein complexes. For precipitation of PrP^c-peptide aptamer complexes anti-PrP antibody 4H11 was used. As negative controls, trxA-GPI was used since trxA reproducibly did not interact with PrP23-231 in yeast. Furthermore, non-transfected control cells were employed and binding of peptide aptamer constructs to protein-A sepharose was excluded by omitting the primary antibody (data not shown). The complexes precipitated with 4H11 were separated by SDS-PAGE and subjected to immunoblot. The membrane was incubated with anti-Flag antibody which only should recognize the peptide aptamers upon complex formation with PrP^c (**Fig 26**).

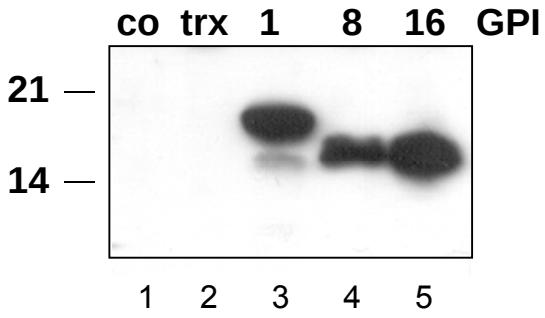

Fig. 26. Co-immunoprecipitation of GPI-peptide aptamers with PrP^c. N2awt cells were transiently transfected with trx-GPI, 1-GPI, 8-GPI, 16-GPI or left non-transfected as a control (co). After two days, cells were lysed under mild conditions and co-immunoprecipitation was performed using the anti-PrP antibody 4H11 for precipitation of potential complexes. An aliquot of the samples was analysed in immunoblot with anti-Flag antibody for detection of trxA or peptide aptamers. Molecular weight marker is given on the left.

In controls (lanes 1 and 2) no bands were detected with anti-Flag antibody, confirming that the antibody did not react unspecifically with components of untransfected N2awt cell lysates (lane 1) and that trxA-GPI did not bind to PrP^c (lane 2). Lanes 3 – 5 nicely depict that 1-, 8- and 16-GPI were co-precipitated with 4H11 antibody, providing convincing evidence that GPI-peptide aptamers interact with PrP^c.

In a further approach, the results obtained by Y2H concerning binding of the peptide aptamers to the C-terminal domain of PrP should be confirmed in mammalian cells using a N-terminally (aa 23 – 90) truncated PrP construct (ΔN-PrP). Therefore, Hpl3-4 $PrP^{0/0}$ cells were co-transfected with GPI-peptide aptamers or trxA-GPI and either ΔN-PrP or wild-type (wt)-PrP. Two days post transfection co-immunoprecipitation experiments were performed. Again, 4H11 antibody that recognizes both PrP constructs was used for precipitation of protein complexes. Samples were subjected to SDS-PAGE and immunoblot with anti-Flag antibody for detection of the binding partners of PrP (**Fig. 27**). As a control, cells transfected only with wt-PrP were employed, and here no signal was visible in the immunoblot (lane 1).

TrxA-GPI did not bind to ΔN-PrP (lane 2) or wt-PrP (lane 6). However, GPI-peptide aptamers were detected in both ΔN-PrP (lanes 3 – 5) and wt-PrP (lanes 7 – 9) transfected Hpl3-4 cells.

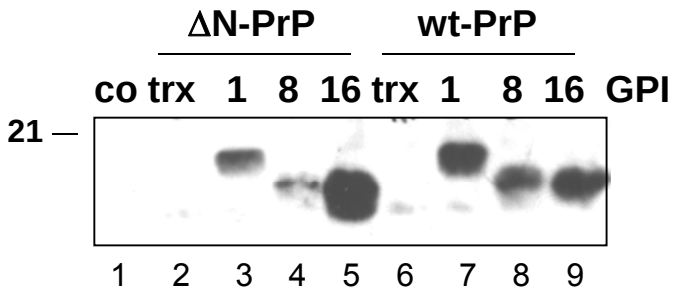

Fig. 27. Co-immunoprecipitation of GPI-peptide aptamers with wtPrP or N-terminally truncated PrP. Hpl3-4 cells transiently co-transfected with ΔN-PrP or wt-PrP and with GPI-peptide aptamers were subjected to co-immunoprecipitation using 4H11 two days post transfection. Samples were analysed in immunoblot using anti-Flag antibody for detection of peptide aptamers.

Therefore, it was concluded that despite altered conditions GPI-peptide aptamers interact with PrP^c in N2a and Hpl3-4 cells, in the latter upon co-transfection of peptide aptamers with PrP. In addition, the interaction with the carboxy-terminal domain of PrP (aa 90 – 231) as observed in Y2H could be confirmed.

4.3.3 Effects of GPI-peptide aptamers on PrP^{Sc} propagation in 3F4-ScN2a cells

The finding that GPI-peptide aptamers interact with PrP^c in N2a cell cultures is the most important requirement for a possible inhibition of PrP^{Sc} generation by expression of GPI-peptide aptamers in prion-infected cultured cells.

To analyze the effect on PrP^{Sc} propagation, 3F4-ScN2a cells were transiently transfected with GPI-peptide aptamers or empty plasmid as a control. Since in transiently transfected cells the expression levels drop at day 3 post transfection, it is difficult to assess effects on PrP^{Sc} within this time frame if only the *de novo* synthesis is inhibited. PrP^{Sc} has a half life of more than 24 hours in 3F4-ScN2a cells (Ertmer et al., 2004) which has to be at least partly degraded before effects on the entire PrP^{Sc} load can be observed. Thus, 3F4-ScN2a cells were trypsinized 3 days post transfection and seeded again in triplicate for a second transfection which was performed the following day. This enabled expression of the GPI-peptide aptamer constructs for about 6 consecutive days. Cells were finally lysed 3 days after the second transfection. Cell lysates were divided and one half was digested with PK whereas the second half was immediately precipitated with methanol. All samples were

subjected to SDS-PAGE followed by immunoblot analysis using 4H11 antibody (**Fig 28A**). Comparing the PrP signals of samples without PK digestion (- PK) of GPI-peptide aptamer transfected to mock transfected cells, no differences could be observed. PK-treated lysates of control cells (lane 2) contained high amounts of PrP^{Sc} represented by un-, mono- and di-glycosylated forms.

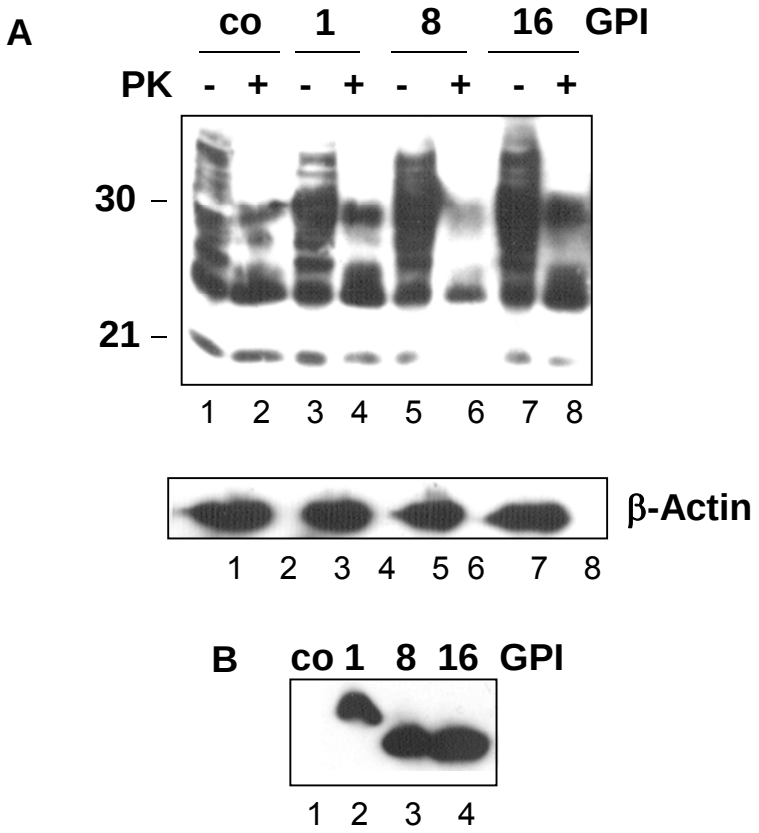

Fig. 28. Effects of GPI-peptide aptamers on PrP^{Sc} levels in 3F4-ScN2a cells. (A) GPI-peptide aptamers were expressed for 6 days in 3F4-ScN2a. Lysates of cells were treated with PK or left untreated and analysed by SDS-PAGE and immunoblot using 4H11. The membrane was de-hybridized and incubated with an antibody against β-Actin which served as a loading control. **(B)** Lysates without PK digestion were analysed in immunoblot with anti-Flag antibody to monitor the expression of GPI-peptide aptamers.

The intensity of this signal was not affected by expression of 1-GPI (lane 4) and 16-GPI (lane 8). Only 8-GPI expression led to a reduction of the amount of PrP^{Sc} (lane 6). As a loading control, the PVDF membrane was de-hybridized and incubated with an anti-β-Actin antibody which served as a loading control (**Fig 28A;** lower panel). Here, no significant differences were discovered indicating equal loading. Furthermore, samples without PK digestion were analysed by anti-Flag antibody to visualize the expression of GPI-peptide aptamers, which were all present in high amounts in the lysates (**Fig 28B**).

Data described above showed that despite binding of the GPI-peptide aptamers to PrP^{c} and expression at high levels, only 8-GPI exerted an effect on the PrP^{Sc} content of transiently transfected 3F4-ScN2a cells.

4.3.4 Localisation of GPI-peptide aptamers in lipid rafts

Lipid rafts are cholesterol- and sphingolipid-rich microdomains that are assembled in the trans-Golgi network (TGN) and transported to the cell surface. Both PrP^{c} and PrP^{Sc} are located in these domains, and this appears to be crucial for prion conversion in persistently infected cells (Caugey & Raymond, 1991; Taraboulos et al., 1995; Vey et al., 1996). GPI-peptide aptamers harboured the signal peptide responsible for GPI-anchoring of PrP^{c} and therefore it was assumed that during transport to the cell surface they are sorted into lipid rafts. However, the weak effects only of 8-GPI on PrP^{Sc} propagation in 3F4-ScN2a posed the question whether this was indeed the case. In order to analyze the raft association of proteins, lysis of cells in cold detergents like TX100 followed by centrifugation on a density gradient was performed. Rafts are not disassembled by the TX100 treatment and therefore can be found in low density fractions of the gradient.

N2a cells were transiently transfected with GPI-peptide aptamers and trxA-GPI. Two days post transfection the floatation assay was performed. After ultracentrifugation, 10 fractions were collected from the top to the bottom of the tube and precipitated with methanol. Protein precipitates were subjected to SDS-PAGE and immunoblot analysis using 4H11, anti-Flag and, as a marker for non-raft compartments, anti-Transferrin receptor (TfR) antibody (**Fig 29**). TfR is a transmembrane protein which is not associated with lipid rafts. In **Fig 29A** the distribution of PrP^{c} in transfected N2a cells is depicted.

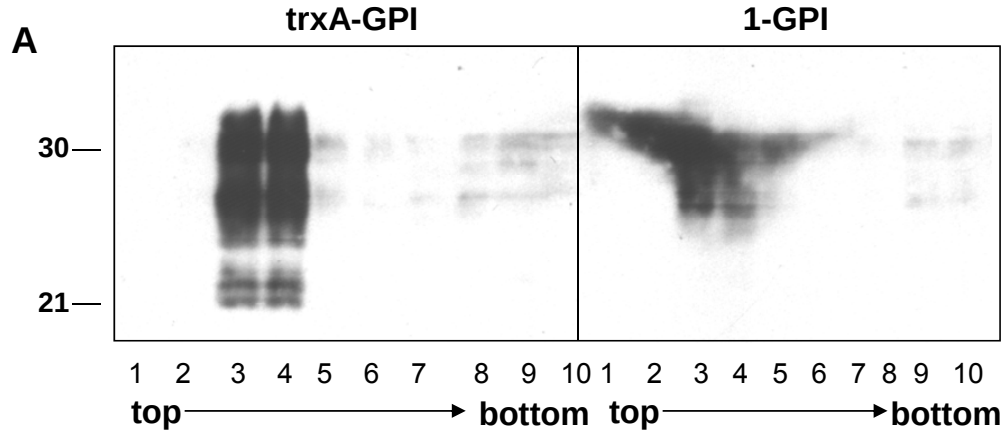

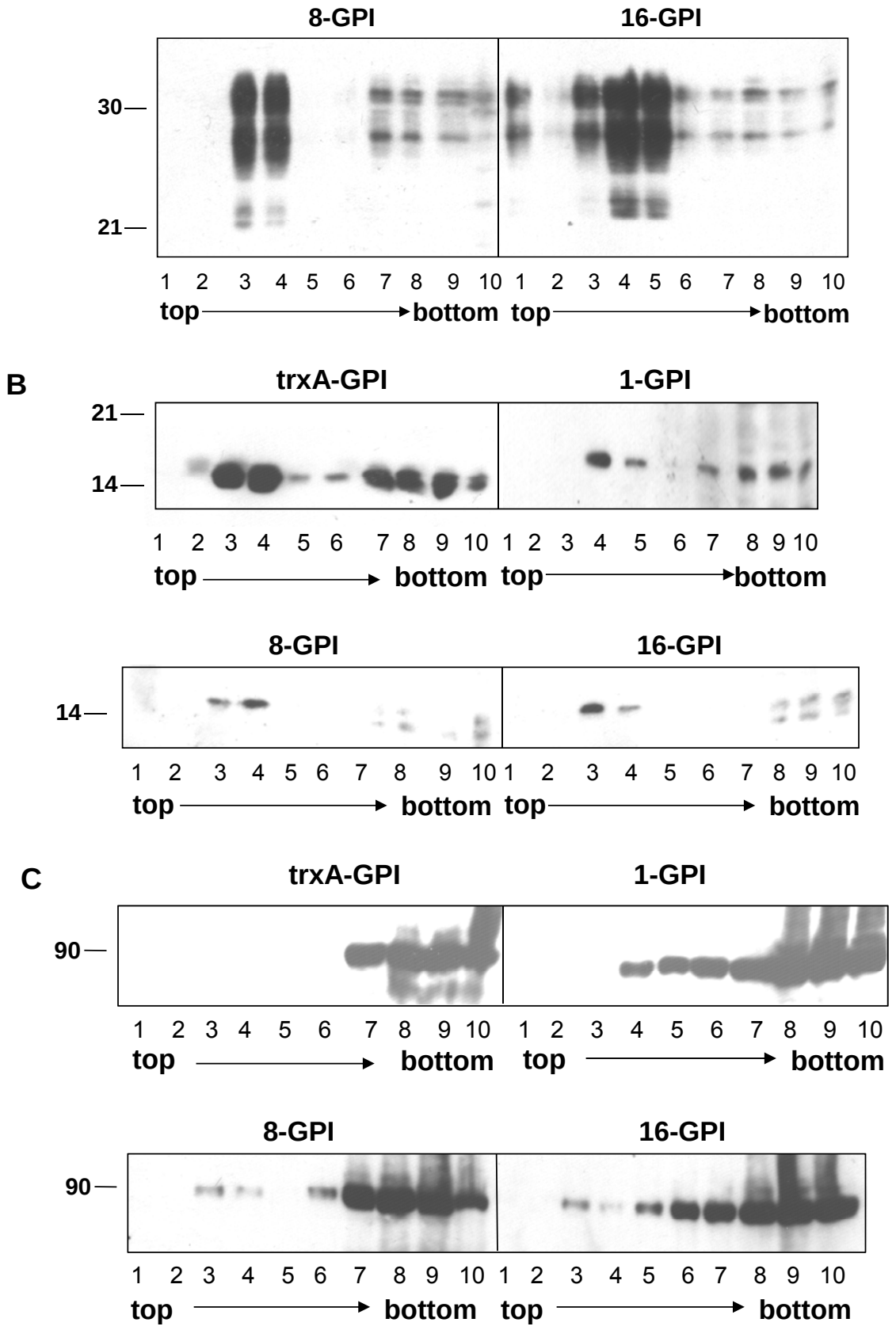

Fig. 29. Raft localisation of GPI-peptide aptamers. N2a cells transiently transfected with GPI-peptide aptamers were subjected to isolation of lipid rafts by floatation assay. Fractions were separated by SDS-PAGE and immunoblot using (**A**) 4H11, (**B**) anti-Flag antibody or (**C**) an antibody directed against the Transferrin receptor.

As expected, peak levels of PrP^c were found in fractions 3 and 4 or 3 – 5 in 16-GPI transfected cells. All other fractions harboured only low levels of PrP^c. Analysis of the samples with anti-Flag revealed a similar pattern for the GPI-peptide aptamers (**Fig 29B**). 8-GPI and 16-GPI were almost exclusively detected in fraction 3 and 4, whereas 1-GPI and trxA-GPI were also present in fractions 7 – 10. Determination of TfR verified the successful preparation of the cell lysates (**Fig 29C**). In contrast to the GPI-anchored proteins, TfR was mainly found in fractions 7 – 10 corresponding to non-raft localization.
These results did not support the hypothesis that the weak effects of GPI-peptide aptamers on PrP^{Sc} propagation are due to an absence of lipid raft association.

4.4 Fusion of intracellular retention or re-routing signals improve anti-prion effects of peptide aptamers

Unfortunately, although the binding properties to PrP^c were retained when targeting the PrP-binding peptide aptamers to the secretory pathway and to lipid rafts, their anti-prion effects did not meet our expectations. Thus, it was necessary to introduce further manipulations in order to improve this activity. It is well established that the intracellular trafficking and the localization of PrP^c are critical for prion conversion in cell cultures (Gilch et al., 2001). In particular, our group was able to establish a novel anti-prion strategy by inducing intracellular aggregation and subsequent re-routing of PrP^c from the TGN to lysosomes by applying the compound suramin to prion-infected cells. This strategy also significantly prolonged incubation times of prion disease when evaluated in mouse bioassays (Gilch et al., 2001). On the protein level, such re-routing can be achieved by fusion to certain sorting signals. Here, two different strategies were chosen: first, C-terminal fusion of peptide aptamers to a KDEL ER retention motif, and second, C-terminal addition of the transmembrane and cytosolic domain of lysosome-associated membrane protein (LAMP)-I. KDEL is a sorting signal of soluble ER resident proteins, e.g. the chaperone BiP, and interacts preferentially in the *cis*-Golgi compartment with the membrane-bound KDEL receptor. The cytosolic domain of this transmembrane protein is recognized by COPI coat proteins that mediate retrieval of KDEL receptor cargo (Lewis et al., 1992; Orci et al., 1997). Similarly, the LAMP-I cytosolic domain contains a tyrosine-based sorting signal (YxxΦ) serving as a ligand of the AP-3 complex that induces transport from the TGN to lysosomes thereby by-passing the plasma membrane (Le Borgne et al., 1998). These signal sequences were used to replace the GPI-signal peptide (see scheme; **Fig. 30**) and the intention was to retain PrP^c in the ER or to mediate a by-pass of the plasma membrane by the interaction with KDEL- and LAMP-peptide aptamers, respectively.

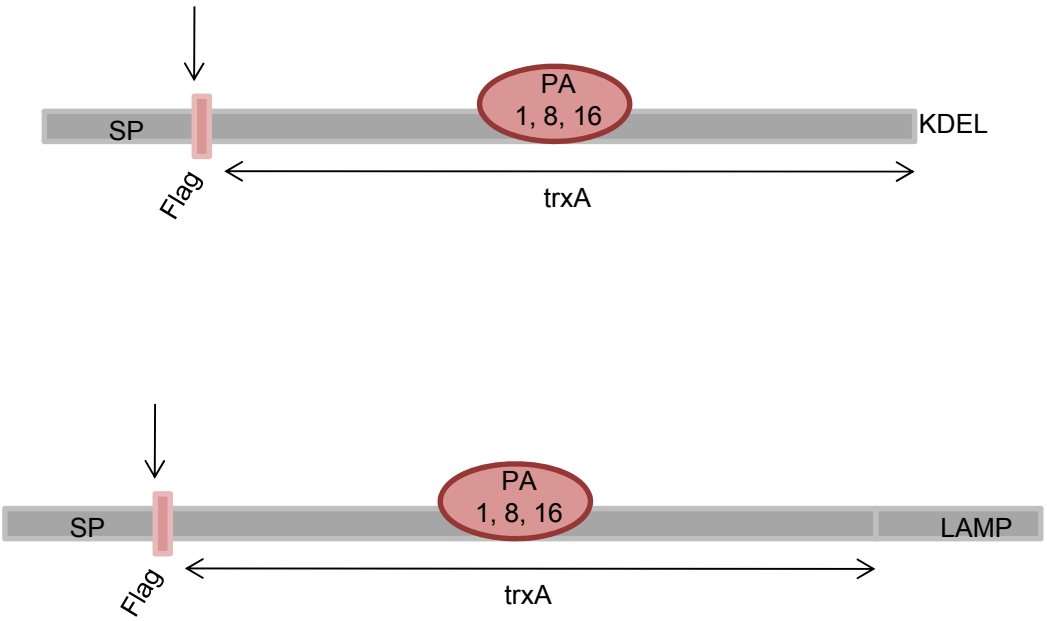

Fig. 30. Schematic depiction of KDEL- and LAMP peptide aptamers. Excluding the C-terminal modifications, constructs are identical to the GPI-peptide aptamers.

4.4.1 Co-localization of KDEL- and LAMP-peptide aptamers and interaction with PrP^c

First of all, the subcellular localization of the KDEL- and LAMP-peptide aptamers and co-localization with PrP^c was analyzed by indirect immunofluorescence assay and confocal microscopy. N2awt cells were transiently transfected with 1-, 8- and 16-KDEL or –LAMP constructs. Two days post transfection, cells were fixed and permeabilized with TX100. As primary antibodies, anti-Flag (rabbit polyclonal) and 4H11 (mouse monoclonal) were used, followed by incubation with Cy-2 conjugated anti-rabbit IgG and Cy3-conjugated anti-mouse IgG. Merged images obtained by confocal microscopy are shown in **Fig. 31**.

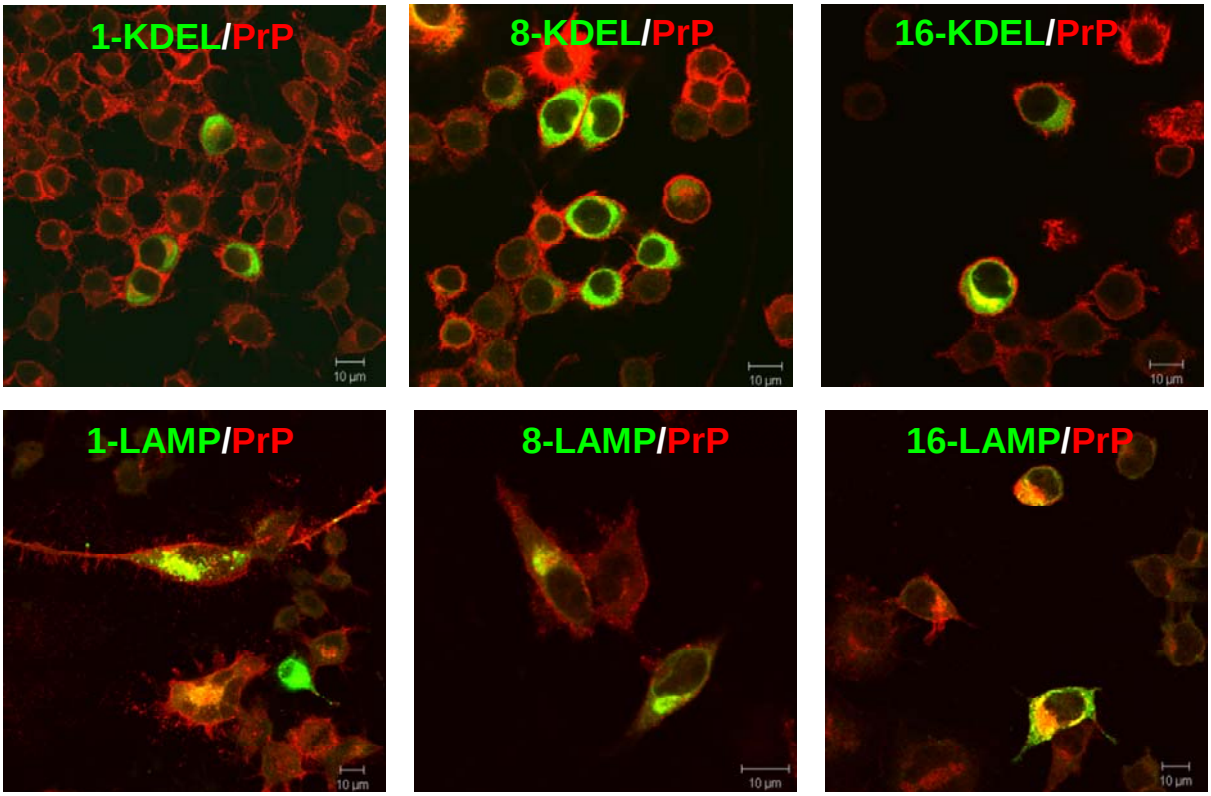

Fig. 31. Co-localization of KDEL- and LAMP-peptide aptamers with PrP^c. N2awt cells transiently transfected with KDEL- or LAMP-peptide aptamers were stained with anti-PrP antibody 4H11 and anti-Flag antibody. Staining was accomplished by incubation with Cy2-conjugated anti-rabbit IgG and Cy3-conjugated anti-mouse IgG. Images were obtained by confocal microscopy using a Zeiss LSM510 confocal microscope.

Peptide aptamers are depicted in green, PrP in red, the yellowish staining indicates co-localisation. KDEL-peptide aptamers (upper panel) were expressed perinuclearly and were not transported to the cell surface. In 8- or 16-KDEL transfected cells, ~ 50 % of peptide aptamer expressing cells exhibited co-localization with PrP^c. In cells transfected with 1-KDEL, this percentage appeared to be significantly lower, with one out of four cells that showed only slight co-localization. LAMP-peptide aptamers (lower panel) were distributed perinuclearly and in addition staining displayed a vesicular localization. Regarding co-localization, all LAMP-peptide aptamers partially co-localized with PrP^c.

Furthermore, the localization of LAMP-peptide aptamers was further analysed by co-staining with an anti-LAMP-I antibody to assure that the vesicles which were stained by anti-Flag indeed correspond to lysosomes. Thus, N2awt cells transfected with 1-, 8- and 16-LAMP were stained 2 days post transfection with anti-LAMP-1 (rat monoclonal) and anti-Flag (rabbit polyclonal) followed by Cy3-conjugated anti-rat IgG and Cy2-conjugated anti-rabbit IgG. The images obtained by confocal microscopy are depicted in **Fig. 32**.

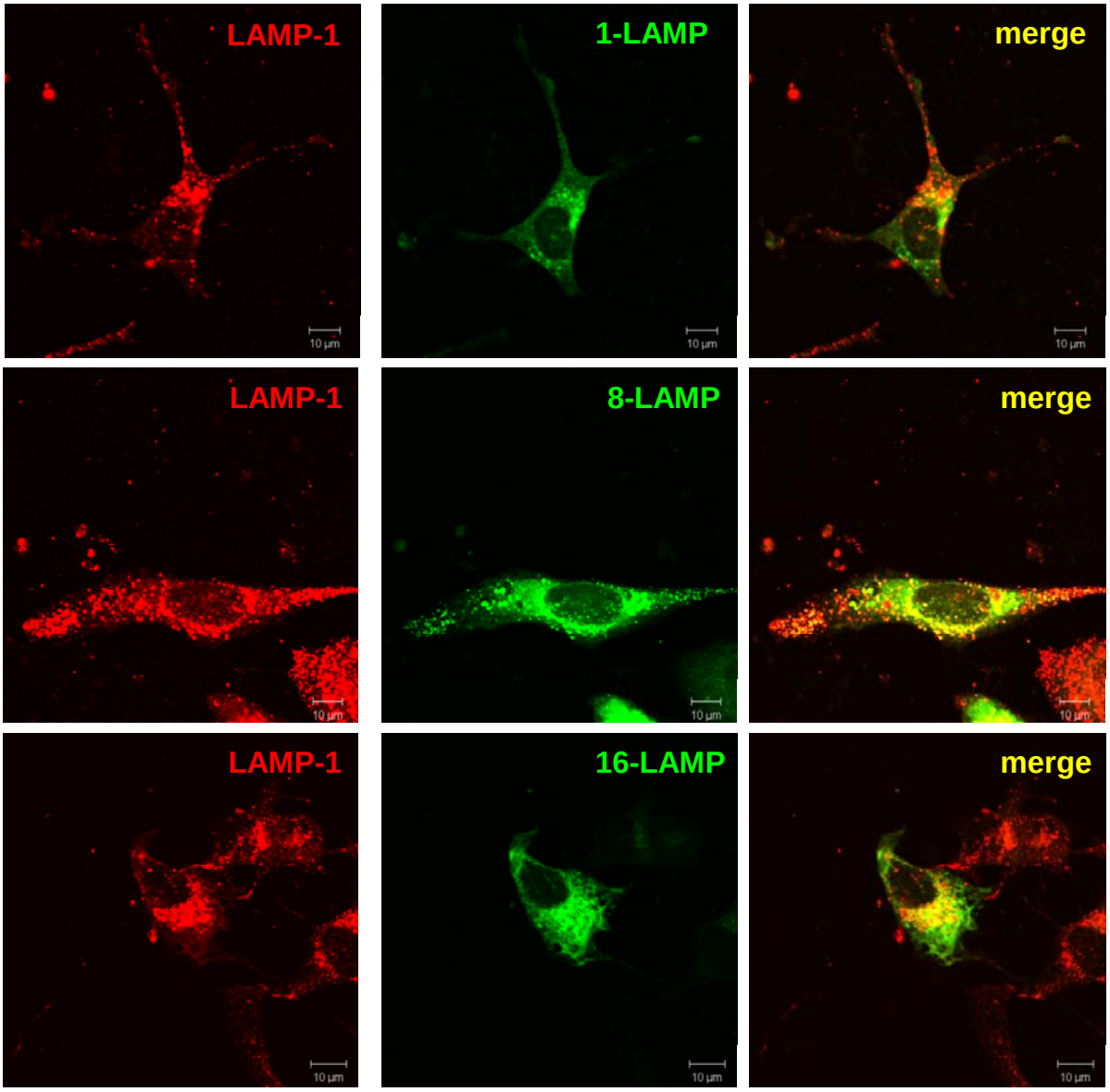

Fig. 32. Localisation of LAMP-peptide aptamers in lysosomes. N2awt cells transiently transfected with LAMP-peptide aptamer constructs were incubated with anti-Flag and anti-LAMP-1 antibodies. Cy2-conjugated anti-rabbit antibodies and Cy3-conjugated anti-rat antibodies were used to visualize the proteins. Images were obtained by confocal microscopy using a Zeiss LSM510.

LAMP-1 antibody (left images) revealed a vesicular staining with a consistent distribution of the lysosomes in the cytoplasm. 1-LAMP (upper panel) was identified in vesicles which partially co-localize with lysosomes and in addition a fraction of the protein was distributed perinuclearly and did not correspond to lysosomes. For 8-LAMP (middle panel) and 16-LAMP (lower panel) the vesicular staining and co-localization with LAMP-1 was more pronounced although also these peptide aptamers were additionally detected in compartments not corresponding to lysosomes which were assumed to be organelles of the secretory pathway, e.g. ER.

However, co-localization only provides a hint that interaction between two proteins is possible but does not prove this interaction. Thus, co-immunoprectipitation experiments of

KDEL- and LAMP-peptide aptamers with PrP^c were performed. N2awt cells were transiently transfected with either of the constructs or with empty pcDNA3.1 vector as a negative control. Two days post transfection cells were lysed under non-denaturing conditions and immunoprecipitation with anti-PrP antibody 4H11 was conducted. Samples were subjected to SDS-PAGE and immunoblot using anti-Flag antibody for the detection of co-immunoprecipitated KDEL- or LAMP-peptide aptamers (**Fig 33**).

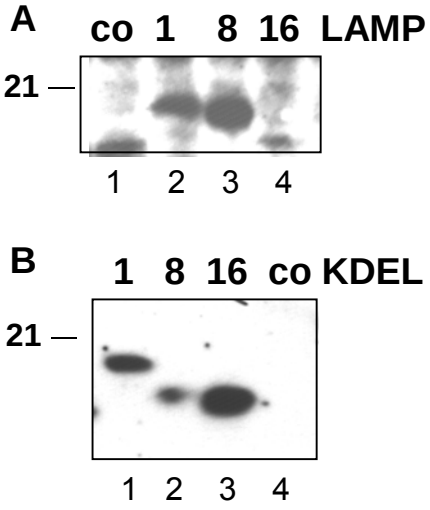

Fig. 33. Co-immunoprecipitation of KDEL- and LAMP-peptide aptamers with PrP^c. N2awt cells transiently transfected with KDEL- or LAMP-peptide aptamer constructs were lysed under mild conditions two days post transfection. Co-immunoprecipitation was performed using 4H11 antibody. Samples were separated by SDS-PAGE and peptide aptamer-specific signals were visualised in immunoblot with anti-Flag antibody.

In mock-transfected control cells no specifc signal could be detected (**Fig. 33A** lane 1 and **Fig. 33B** lane 4). 1-LAMP and 8-LAMP (**Fig. 33A**; lanes 2 and 3) both could be co-precipitated with PrP whereas for 16-LAMP only a very weak signal was visible. In contrast, all KDEL-peptide aptamers (**Fig. 33B**) exhibited a pronounced signal indicative for strong binding to PrP^c.

In summary, KDEL- and LAMP-peptide aptamers are retained intracellularly and co-localize at least partially with PrP^c. LAMP-peptides were found to be contained in lysosomes. Thus, intracellular retention mutants of the PrP-binding peptide aptamers still interact with PrP^c, although for 16-LAMP only a weak signal was detected upon co-immunoprecipitation.

4.4.2 Effects of KDEL- and LAMP-peptide aptamers on PrP^c cell surface expression

The next question was whether expression of KDEL- and LAMP-peptide aptamers can influence the cell surface expression of PrP^c. This was addressed by treatment of KDEL- and

LAMP-peptide aptamer expressing cells with phosphatidyl-inositol specific Phospholipase C (PIPLC), an enzyme that specifically releases GPI-anchored proteins from the cell surface. As a consequence, the amounts of these proteins contained in the cell lysates are reduced when compared to untreated cells. N2a cells were transiently transfected with KDEL- or LAMP-peptide aptamers. Two days after transfection, one half of the cells was treated with PIPLC (+ PIPLC) whereas the other half was not (- PIPLC). All cells were lysed and analysed in immunoblot using anti-PrP antibody 4H11. Cells transfected with empty vector (pcDNA3.1) served as a control (**Fig 34**).

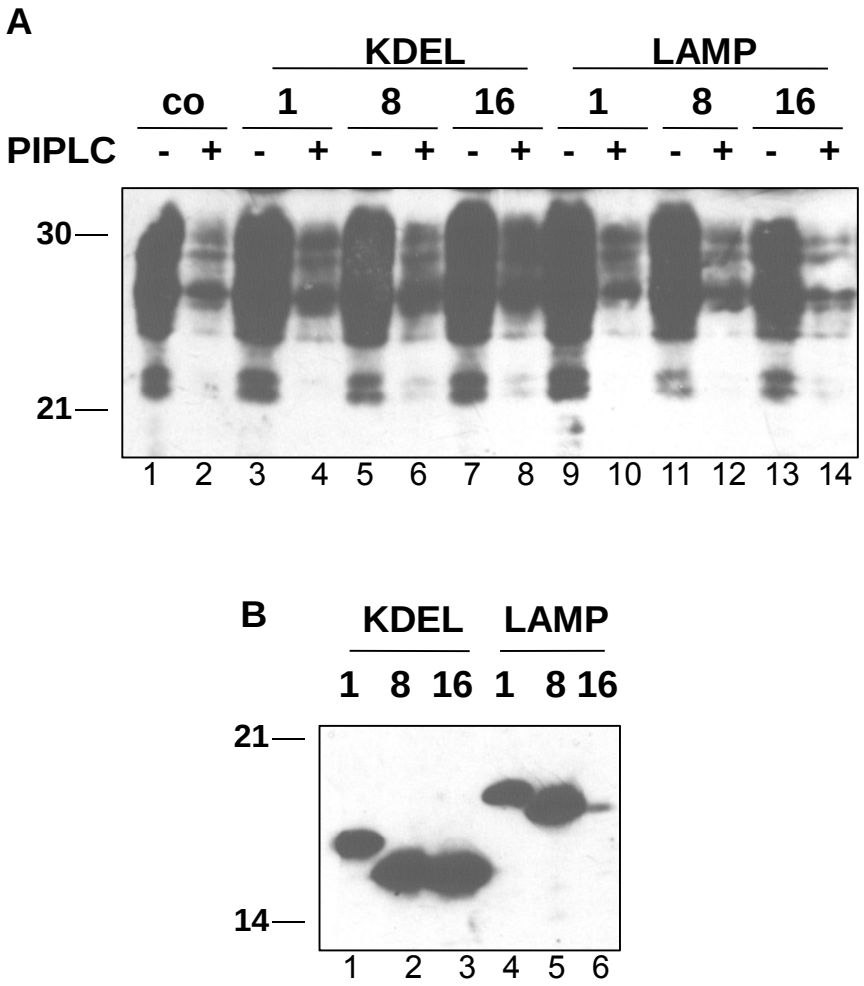

Fig. 34. Effects of KDEL- and LAMP-peptide aptamer expression on surface localization of PrP^c. (A) N2a cells were transiently transfected with KDEL- or LAMP-peptide aptamer constructs. Two days post transfection PIPLC digestion was performed followed by lysis of the cells. Aliquots of all lysates (-/+ PIPLC) were separated by SDS-PAGE and analysed in immunoblot using 4H11. **(B)** Samples without PIPLC digestion were analysed in immunoblot for peptide aptamer expression using anti-Flag antibody.

In control cells, a strong PrP^c signal was detected without PIPLC digestion (lane 1) which was almost undetectable after treatment with the enzyme (lane 2). In cells transfected with the KDEL- and LAMP-peptide aptamers, a huge portion of PrP^c was released by PIPLC treatment. However, in cells transfected with the KDEL-peptide aptamers or 1- and 8-LAMP,

the amount of PrP^c located intracellularly, as indicated by the signals in lysates of PIPLC-digested cells, was higher when compared to the control cells. This provides a hint that a fraction of PrP^c is retained intracellularly. When analysing lysates without PIPLC digestion with anti-Flag antibody to confirm expression of the peptide aptamers, 16-LAMP was almost not detectable whereas all other peptide aptamers were expressed at high levels.
This indicates that certain KDEL- or LAMP-peptide aptamers might lead to a reduction of PrP^c levels at the cell surface. 16-LAMP appeared to be expressed only at very low levels.

4.3.3 Anti-prion activities of KDEL- or LAMP-peptide aptamers

The pivotal experiment, however, was to express KDEL- or LAMP-peptide aptamers in prion-infected cell cultures and to monitor whether thereby PrP^{Sc} is reduced. For this purpose, 3F4-ScN2a cells were transfected with the different constructs or, as a negative control, with pcDNA3.1. Three days after transfection, cells were seeded and transfected in triplicate again the following day. Six days after the first transfection, cell cultures were lysed and half of the lysates were treated with PK. All samples (- and + PK) were loaded on SDS-PAGE and subjected to immunoblot which was incubated with 4H11. Due to the high specificity of this antibody, anti-β-Actin could be added in parallel. **Fig. 35** depicts the result of one representative experiment. The signals for β-actin confirmed equal loading and are indicated by an arrow (**Fig. 35A**).

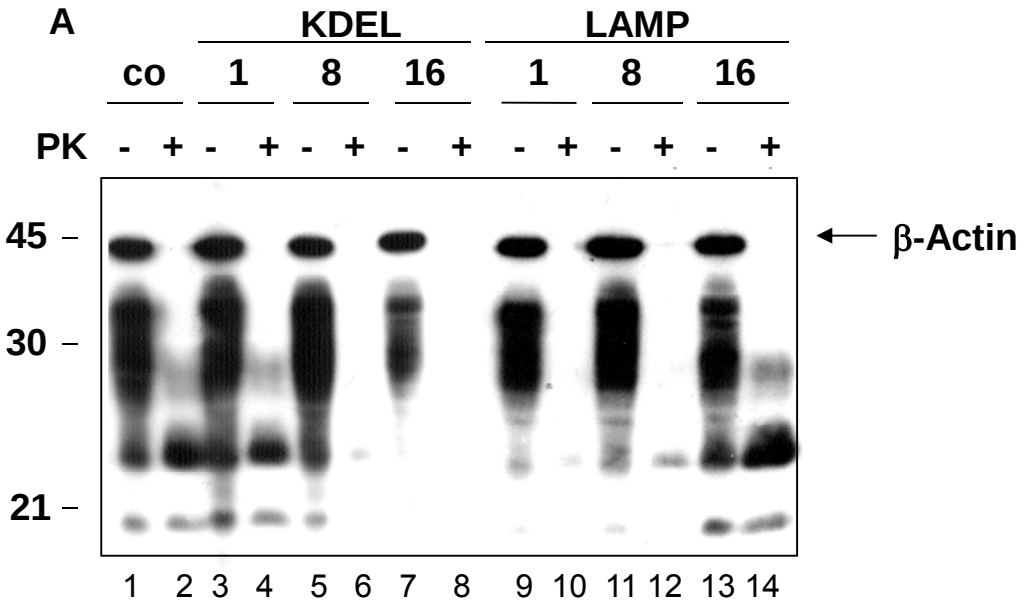

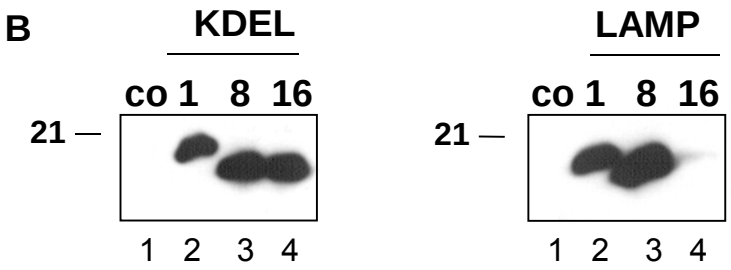

Fig. 35. Effects of KDEL- and LAMP-peptide aptamers on PrP^{Sc} levels in 3F4-ScN2a cells. (A) 3F4-ScN2a cells were transiently transfected twice with KDEL- or LAMP-peptide aptamers. Cells transfected with pcDNA3.1 served as negative control. Three days after the second transfection, cells were lysed and subjected to PK digestion (+PK) or left untreated (-PK). All samples were analysed in immunoblot using 4H11 for detection of PrP specific bands in parallel to anti-β-Actin as a loading control. Molecular weight marker is given on the left. **(B)** Expression of peptide aptamers in 3F4-ScN2a was confirmed by immunoblot using anti-Flag antibody as primary antibody.

As expected, control cells harboured high amounts of both PrP^{c} (lane 1) and PrP^{Sc} (lane 2). Expression of 1-KDEL did not influence PrP^{Sc} signals (lane 4). However, 8-KDEL (lane 6), 16-KDEL (lane 8) and 1-LAMP (lane 10) expression abrogated PrP^{Sc} to levels below the detection limit of the immunoblot. 8-LAMP significantly reduced the amounts of PrP^{Sc} and here, only a slight band of mono-glycosylated PrP^{Sc} was visible (lane 12). 16-LAMP did not influence PrP^{Sc} amounts in this experiment. When analysing samples without PK digestion with anti-Flag antibody in immunoblot, all peptide aptamers except 16-KDEL were shown to be overexpressed at high levels (**Fig. 35B**).

In order to test whether in a short time frame a reduction of *de novo* synthesis of PrP^{Sc} in persistently infected cells can be revealed metabolic labelling and immunoprecipitation experiments of PrP^{Sc} were performed. 3F4-ScN2a cells were transiently transfected with KDEL- and LAMP-peptide aptamers or with empty vector as a control. Cells treated with suramin which is known to completely abrogate PrP^{Sc} *de novo* synthesis (Gilch et al., 2004) were used as a further control. The day after transfection metabolic labelling was performed by the addition of (^{35})S-Cys/Met in the absence of FCS and in medium without Cys/Met for 16 hours. This long labelling period is necessary to detect *de novo* generated PrP^{Sc}. Then cells were lysed and lysates were treated with PK. PrP^{Sc} was separated by solubility assay. Immunoprecipitation of PrP^{Sc} from the pellet fraction was performed with the polyclonal anti-PrP antibody A7. This was followed by de-glycosylation of samples with PNGase F in order to increase the sensitivity of detection (**Fig. 36**).

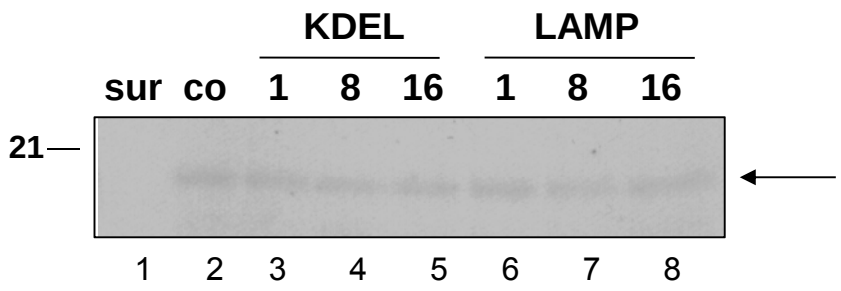

Fig. 36. Analysis of PrP^{Sc} *de novo* synthesis in KDEL- and LAMP-peptide aptamer expressing 3F4-ScN2a cells. One day after transient transfection of 3F4-ScN2a cells with KDEL- or LAMP-peptide aptamer constructs or empty vector (co), metabolic labelling using (^{35})S-Cys/Met was performed for 16 hours. Suramin (200 µg/ml) was added during the labelling period (lane 1). Cells were lysed, lysates were digested with PK and subjected to solubility assay. PrP^{Sc} was immunoprecipitated from the pellet fraction using polyclonal anti-PrP antibody A7. To increase the sensitivity, precipitated proteins were deglycosylated with PNGase F. Samples were separated by SDS-PAGE, the gel was dried and exposed to an X-ray film. The arrow indicates the band specific for unglycosylated PrP^{Sc}.

In control cells (lane 2) a clear band of ~ 19 kDa corresponding to un-glyosylated PrP^{Sc} was visible which was absent in suramin-treated cells (sur; lane 1). Unfortunately, none of the peptide aptamers exhibited a significant inhibition of PrP^{Sc} *de novo* synthesis under the used experimental conditions.

In addtion to therapeutic approaches, prophylactic effects of anti-prion compounds can be assessed in cell culture experiments. To mimick such a scenario, cells susceptible to prion infection can be used for *de novo* infection in presence or absence of putative anti-prion compounds. In this thesis, clone 21 was used which was produced by curing 3F4-ScN2a cells by treatment with pentosan polysulfate for several passages. Cells negative for PrP^{Sc} were then subcloned and re-infected with brain homogenates of terminally sick mice after infection with prions. Here, clone 21 proved to be highly susceptible for infection (G. Lutzny, diploma thesis). One huge advantage of these cells is that they express 3F4-tagged PrP^{c} which enables selective detection of newly produced PrP^{Sc} by application of the monoclonal antibody 3F4. This antibody does not react with PrP^{Sc} derived from the mouse brain homogenates since mouse PrP does not contain the 3F4-epitope.

Clone 21 was transiently transfected with 1-, 8- or 16-KDEL and with empty vector. One day post transfection, brain homogenate (1 %) of mice infected with scrapie strain RML was added and incubated for 24 hours with the cells. Homogenates were removed and cultures were passaged twice after reaching confluence. Then cultures were lysed, lysates were treated with PK and solubility assay was performed to precipitate PrP^{Sc}. Pellet fractions thereof were analysed in immunoblot using mAb 3F4 (**Fig. 37**). In mock transfected control cells and cells transfected with 1-KDEL a distinct PrP^{Sc} signal appeared. Upon overexpression of 8-KDEL and 16-KDEL only slight PrP^{Sc} signals became apparent.

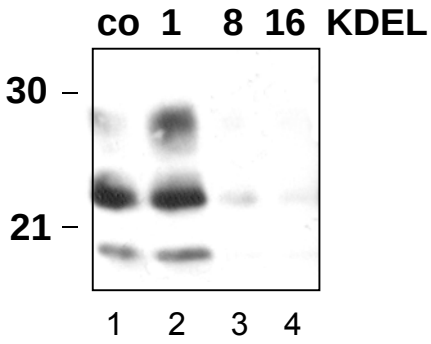

Fig. 37. Inhibition of *de novo* prion infection by expression of KDEL-peptide aptamers. Clone 21 cells were transfected transiently with KDEL-peptide aptamers or empty pcDNA3.1 (co). The following day, RML infected brain homogenate (1 %) was added for 24 hours. Brain homogenate was removed and cells were passaged twice. Then cultures were lysed, lysates were digested with PK and solubility assay was performed. Pellet fractions were separated by SDS-PAGE and immunoblot was analysed using anti-PrP antibody 3F4 which selectively detects *de novo* generated PrP^{Sc}.

In conclusion, anti-prion effects in 3F4-ScN2a cells were demonstrated for 8- and 16-KDEL and 1- and 8-LAMP. These results were reproducible in several independent experiments. In line with this, overexpression of 8-KDEL and 16-KDEL significantly reduced the efficiency of *de novo* infection of susceptible cells with scrapie strain RML.

4.3.4 Analysis of post-translational modification of peptide aptamers

It was conspicuous that in several experiments 16-LAMP was not or only at very low levels detectable in immunoblot upon transient transfection. However, in indirect immunofluorescence assays cells were found that harboured the protein even at the expected locale, namely in lysosomes. Also in co-immunoprecipitation a slight signal indicating binding to PrP^{c} was visible. Analysis of the primary structure of PA16 revealed that it contains two additional Cys residues (**Table 7**). This in turn might form a disulfide bond which might lead to an increased degradation of 16-LAMP if not properly folded. The assessment whether a protein harbours a disulfide bond is possible by applying the samples to SDS-PAGE under non-reducing conditions which are achieved by omitting the reducing agent, i. e. 2-mercapto-ethanol from the sample buffer. Upon retaining a disulfide bridge the respective protein is more compactly folded than its reduced counterpart. Therefore, it migrates faster in SDS-PAGE than its reduced counterpart.

To analyse this, lysates of N2a cells transiently transfected with trxA-, 1-, 8- or 16-KDEL and the LAMP-versions of all constructs were applied to SDS-PAGE either with (+ 2-ME; lanes 1 – 8) or without (- 2-ME; lanes 9 – 16) reducing agent. Immunoblot was developed using anti-Flag antibody (**Fig. 38**).

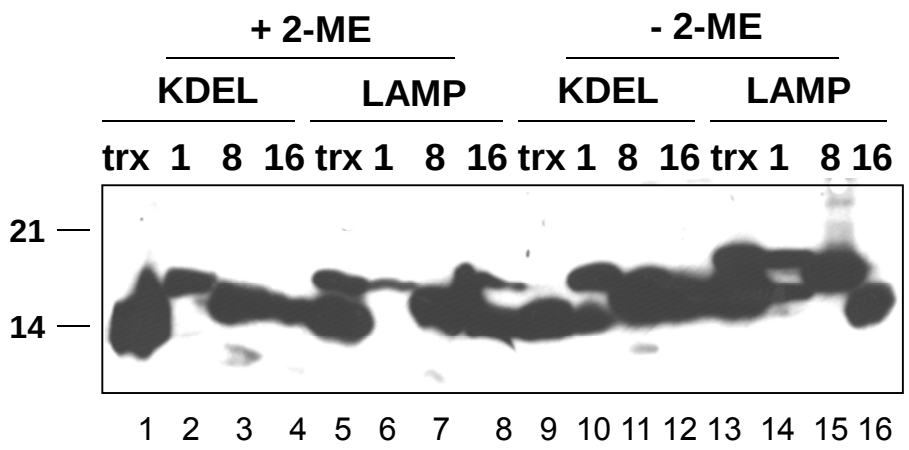

Fig. 38. Analysis of KDEL- and LAMP peptide aptamers under non-reducing conditions. Lysates of N2a cells transiently transfected with KDEL- and LAMP-peptide aptamer constructs were analysed in immunoblot under reducing (+ 2-ME) or non-reducing (- 2-ME) conditions using 4H11 antibody.

Indeed, when comparing the migration of 16-LAMP with or without 2-ME, the non-reduced sample migrates faster (lane 16). Both 1-KDEL (lane 10) and 1-LAMP (lane 14) exhibit double bands that are not visible in samples with 2-ME (lanes 2 and 6, respectively), which might indicate formation of a disulfide bond in a fraction of the expressed protein. 16-KDEL, however, appears not to harbour a disulfide bond since the migration with and without 2-ME is equal.

In conclusion, it is argued that the inconsistent expression of 16-LAMP might be linked to improper formation of a disulfide bond.

5. Discussion

Peptide aptamers have been selected so far against various intracellular targets, including proteins involved in cell-cycle regulation or signal transduction, including some viral proteins. Here, the generation of peptide aptamers targeting the GPI-anchored protein PrP^c using bacterial trxA as a folding scaffold is demonstrated. Interestingly, these molecules retained their binding properties to PrP^c when expressed intracellularly within the secretory pathway. As a functional read-out for their efficacy in cultured cells, their potential to inhibit endogenous PrP^{Sc} conversion was evaluated. Establishing high-affinity peptide aptamers against PrP^c might open new possibilities for designing novel therapeutic agents or help to elucidate the nature of the still enigmatic PrP^c-PrP^{Sc} interaction.

5.1 TrxA is a stable scaffold for presentation of peptide aptamer libraries

Peptides can be useful reagents for the competitive interference with various cellular processes such as signal transduction or protein-protein interactions by covering binding sites or activating domains of target proteins. When selecting peptides for such purposes, one advantage is that no prior structural information about the target protein is required and when compared to classical gene knock-out only one specific function of a protein can be blocked in contrast to completely abolishing its presence within the cell. In order to achieve a stable and consistent folding of a given peptide sequence, they are frequently embedded within a scaffold protein. This manipulation confers a reduced conformational freedom due to the N- and C-terminal constraint which in turn results in an increased binding affinity compared to the unconstrained counterpart of the peptide moiety. For the selection of PrP-binding peptide aptamers, the bacterial thioredoxin A (trxA) protein was employed here as a scaffold to present a combinatorial library of 16mer peptides. The choice of the scaffold protein is critical for the binding of target sequences since it appears to influence the folding of the peptide moiety. Transfer of a known interacting protein selected in a given scaffold to alternative platform proteins can result in the loss of target recognition (Klevenz et al., 2002). TrxA is so far the most frequently used scaffold protein for the selection of peptide aptamers that mainly were selected against cytosolic targets implicated in cell cycle regulation or oncogenic transformation (Butz et al., 2001; Kunz et al., 2006; Zhao & Hoffmann, 2006; Pamonsinlapatham et al., 2008). The peptides are inserted into the active-site loop of trxA and then presented on the surface of the protein. The active center is constituted by 4 residues (Cys-Ser-Pro-Cys) and in the first study describing trxA as a scaffold for

presentation of peptides (Colas et al., 1996) an internal AvaII restriction site was used for subcloning of the random sequences. We decided to create a BamHI restriction site at the identical position by introducing a single nucleotide. Thereby, three additional amino acids are contained since the frame shift by adding a single nucleotide had to be adjusted to the reading frame of trxA by inserting two further nucleotides, resulting in total in nine additional nucleotides. The peptides are then flanked N-terminally by Cys-Gly-Ser and C-terminally by Gly-Asp-Pro-Cys. The residues depicted in red indicate the additional amino acids. These manipulations result in an amino-terminal as well as a carboxy-terminal Gly residue which can improve the individual folding of the peptide moieties due to its conformationally inert character and flexibility (Klevenz et al., 2002).

However, the approach of cloning via one restriction site suffered from several drawbacks. First, concatemers were formed during ligation, and this resulted in the insertion of duplicate or more peptide encoding sequences. This does not necessarily interfere with the binding properties to the target protein since PA1 is such an elongated peptide sequence and was identified in two independent Y2H screens indicating its high affinity. In several other studies also duplicated peptides were described that bound with high affinity to their target proteins (Colas et al., 1996, Borghouts et al., 2008). The major problem elicited was that, for example, insertion of triplicates resulted in a frame shift, which was the case in many of the initially identified positive clones. Although such sequences reproducibly bound to PrP23-231 in Y2H, they were excluded from further analysis since with such sequences fused only N-terminally to the trxA backbone the requirement of a constrained peptide moiety could not be fulfilled anymore. The constrained conformation, however, offers several advantages. These are in particular higher binding affinities, higher stability under biological conditions, the preferred conformation can be helpful for structure determination as a pre-requisite for drug development and finally, hydrophobic residues which are usually buried in the interior of proteins can be exposed (Ladner, 1995). Second, oligonucleotides can be ligated in two orientations when using only one restriction site. For construction of the random library, the sequence $(NNK)_{16}$ was used. N is the code for A, G, C or T, whereas K only allows T or G, which reduces the probability of stop codon formation, since only one out of three stop codons harbours a G at the third position of the triplet. However, by bi-directional cloning the sequence can be reverted, thereby increasing the probability of stop codons compared to the NNK-sequence. However, stop codons within the randomized sequence were only occasionally observed and did not pose a major problem. Nevertheless, for future studies the use of two restriction sites will be preferred.

5.2 Three peptide aptamers interact with PrP23-231

Despite the above discussed drawbacks of our newly designed peptide library, three peptide aptamers (PA1, 8 and 16; **Table 7**) were identified that reproducibly interact with PrP23-231 both in yeast and upon *in vitro* trancription/translation followed by co-immunoprecipitation. Furthermore, when these peptide aptamers were recombinantly expressed and prion-infected cells were treated with the purified proteins, the amount of PrP^{Sc} was significantly reduced. In the used Y2H approaches, three independent reporter genes are activated by the interaction. These conditions correspond to highest stringency and activation of all reporter genes is indicative for high-affinity binding. Using the trxA scaffold enables, in addition to combinatorial peptides, presentation of naturally occurring peptide sequences (Klevenz et al., 2002), which can be exploited for elucidation of natural binding partner of certain proteins. For example, by using peptide aptamer technology a novel interaction of functional importance of the microtubule-associated protein 1B (MAP1B) with Death Associated Protein Kinase (DAPK) was revealed (Stevens & Hupp, 2008). Therefore, primary structures of PrP-binding peptides were analysed for homology with known murine proteins by BLAST search. Only PA8 had some identity with an immunoglobulin heavy chain region (**Table 9**). However, the biological significance of this finding is presently not known and requires further investigations.

Table 9. Homology of PA8 to IgG heavy chain.

PA8	1	ARFEYLRDGYW	11
		ARF+ DGYW	
IgG heavy chain	90	ARFDY--DGYW	98

When analysing the peptide sequences, it is striking that all peptides have a high content of aromatic residues (Trp, Phe and Tyr) clearly above the average frequency found in proteins (Bogan & Thorn, 1998), and also a few charged amino acids (mainly Arg). Algorithms for secondary structure prediction projected a certain content of β-strands for all peptide aptamers. Most interfaces of protein-protein interactions are composed of two protein surfaces and the energy of binding is assumed to directly correlate with the area of hydrophobic surface that is buried by the interaction (Jones & Thornton, 1996). However, this appears to be different when analysing the contribution of single amino acid residues, which are highly uneven distributed (Bogan & Thorn, 1998). Interestingly, the detailed analysis of interfaces constituting natural protein-protein interactions revealed that only three amino acids appear with a frequency of more than 10 %, namely Trp, Arg and Tyr (Bogan & Thorn, 1998). These are exactly those amino acids which are over-represented in the PrP-binding

peptide aptamer sequences. The frequency of aromatic residues can be explained by the contribution of binding energy through the hydrophobic effect (Padlan, 1990). Besides this important force, the aromatic residues can contribute π-interactions, Trp and Tyr in addition hydrogen bonding ability. Arg is also capable of multiple types of interactions. It can form hydrogen bonds and a salt bridge with its guanidinium group. The delocalised electrons of the guanidinium group can mimick aromatic π-interactions. In summary, the amino acid composition of the PrP-binding peptide aptamers appears to strongly support tight binding to its respective protein surface counterpart.

5.3 Inhibition of PrP^{Sc} propagation by purified peptide aptamers

The initial idea was to use peptide aptamers for interference in the prion conversion process. In order to prove that this is indeed possible, peptide aptamers were expressed recombinantly in *E. coli* as poly-His-fusion proteins and were purified by nickel affinity chromatography. Since they were expressed in high amounts in inclusion bodies, denaturing conditions with buffers containing GdnCl or urea were chosen for lysis and purification. Refolding was performed by dialysis against sodium acetate. At neutral pH, high amounts of the protein precipitated during this process. This is presumably mainly due to formation of intermolecular disulfide bonds between the cysteines forming the active site in native trxA leading to oligomerization of the protein. When the Cys residues would be mutated to Gly a significantly higher expression yield and an improved solubility of the proteins could be obtained. This was in turn advantageous for cellular uptake, a process which is crucial for peptide aptamers that might be used as therapeutic agents (Borghouts et al., 2008). In our approach, the pH of the dialysis buffer was reduced to 3,5, and these acidic conditions also efficiently prevented precipitation of proteins during dialysis.

In further experiments purified proteins were added to the culture media of ScN2a cells. All peptide aptamers induced a reduction of the total amount of PrP^{Sc} after 5 days of treatment in a dose-dependent manner. The dissociation constants (K_D) of the PrP-peptide aptamer interaction were not determined here. Instead, the IC_{50} (inhibitory concentration), which is the concentration of peptide aptamer that reduces the PrP^{Sc} content to 50 % compared to control cells was estimated. PA16 induced a 50 % reduction at a concentration of 350 nM, whereas 700 nM of PA1 or PA8 were required to achieve the same effect. The difference between PA1 and PA16 is striking, since both peptide aptamers interact with epitopes within the identical PrP region. One reason for this could be the length of the peptides. PA1 consists of 35 amino acids due to concatemer formation during the ligation. This might result in a more instable folding. In addition, the use of shorter peptides allows the binding to smaller pockets

within the solvent-exposed protein surface (Baines & Colas, 2006). Comparing PA1 and PA16, PA16 might fit more perfectly to the surface of PrP^c due to the smaller size. It would be interesting to determine the K_D-values by classically biochemical methods like surface plasmon resonance (SPR) to have an indication whether the difference in the IC_{50} values are indeed reflected by the binding affinity to recombinant PrP.

The IC_{50} values for the inhibitory activity in prion conversion are below 1 µM, which is in the range of the IC_{50} of many small molecule inhibitors. These are for example 500 nM for quinacrine (Doh-Ura et al., 2004), 0,5 - 1,2 µM for mefloquin dependent on the prion strain used for infection of the cell cultures (Kocisko et al., 2006), or tannic acid, pentosan polysulfate and Fe(III) deuteroporphyrin 2,4-bisethyleneglycol with $\leq$ 5 µM (Kocisko et al., 2005). However, by chemical modification the efficiency of the substances can be improved, as demonstrated for acridines joined with different linkers, resulting in bivalent bis-acridines. The IC_{50} of those quinacrine derivatives was about 10fold lower than that of the monovalent substances (May et al., 2003). Best comparable to peptide aptamers, however, are molecules with similar specificities. Here, RNA aptamer DP7 should be mentioned, the IC_{50} of which was also 700 nM (Proske et al., 2002). In addition, the effects of Fab fragments derived of anti-prion antibodies were evaluated in prion-infected cultured cells, and these had IC_{50} values ~ 20 – 50 fold lower than the peptide aptamers described here (Peretz et al., 2001). The latter are indeed significantly more potent than the peptide aptamers. However, those could be improved by several manipulations. First, this could be tandem fusion of peptide aptamers joined by a flexible linker, e. g. the glycine-rich heptapeptide described for dimerization of PrP (Gilch et al., 2003; Kaiser-Schulz et al., 2007). Such linked peptide aptamers might then be capable of inducing aggregation of PrP^c at the cell surface due to bivalent character, a mechanism that led to a significantly higher anti-prion activity of polyclonal anti-PrP antibodies compared to their corresponding Fab molecules (Gilch et al., 2003). Similarly, chemical compounds that induce aggregation of PrP at the cell surface due to their bivalent character can inhibit prion conversion (Nunziante et al., 2005). Second, binding affinities of peptide aptamers can be improved by affinity maturation using error-prone PCR. After random mutagenesis of the peptide moiety, derivatives of the original sequence can be identified by Y2H screen. By this technology, highest binding affinities can be achieved, as demonstrated for an affinity maturated single-chain antibody against bovine PrP, the final K_D of which was as low as 1 pM (Luginbühl et al., 2006).

The anti-prion effect of the peptide aptamers might be stronger if they in addition to PrP^c also bind PrP^{Sc}. Since this interaction cannot be analysed by Y2H, the question was addressed indirectly by solubility assay of infected or non-infected N2a cells treated with purified peptide aptamers. Provided that PrP^{Sc} is insoluble whereas PrP^c remains soluble in this assay, it was

assumed that peptide aptamers might become insoluble in infected cells due to binding to PrP^{Sc}. However, the major fraction of the purified peptide aptamers was insoluble in infected as well as in non-infected cells. TrxA which was used as a control was hardly detectable in cell lysates indicating a less efficient uptake by the cells. Only PA8 was found in substantial amounts in the soluble fraction of the solubility assay. The insolubility might be an intrinsic property of the peptide aptamers except PA8, since by addition to the cell culture media pH and salt conditions again differed from the refolding protocol. As already mentioned, insolubility and aggregation propensity was described for trxA-based peptide aptamers (Borghouts et al., 2008). Nevertheless, it apparently did not negatively influence the expected impact on PrP^{Sc} propagation.

5.4 Binding sites and possible implications in prion conversion

Mapping studies in order to elucidate the PrP regions recognized by the peptide aptamers were performed by Y2H approach and revealed that PA8 interacts with the carboxy-terminal domain (aa 90 – 231), whereas PA1 and PA16 interact with both the N-terminal (aa 23 – 100) and the C-terminal part of PrP. The mapping of binding sites was continued by H. Anders during her Bachelor thesis. Here, further PrP constructs covering residues 90 – 120, 90 – 150, 90 – 180 and 90 – 210 were tested for binding to the various peptide aptamers. It was found that PA 1 and 16 do not, as initially discussed, bind to the overlapping segment consisting of aa 90 – 100 but that they indeed appear to have two binding sites, one within the N-terminal part and the second between aa 120 – 150 (**Fig. 39**). Alternatively, parts of the amino-terminus and residues 120 – 150 might lie in close proximity in the folded state of the protein and form one epitope.

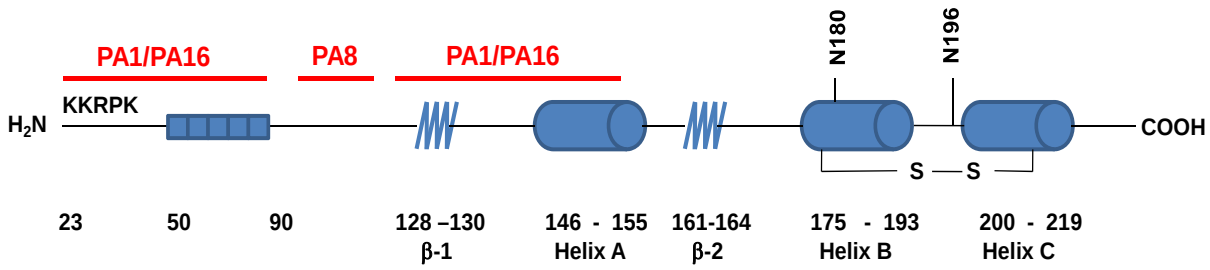

Fig. 39. Schematic representation of peptide aptamer binding sites in PrP^{C}. Secondary structure elements, the two glycosylation sites and the disulfide bond are depicted, amino acid positions are given below. "KKRPK" indicates the stretch of positively charged amino acids at the amino-terminus, followed by the octarepeat region.

For the N-terminal part of PrP, no defined structure could be assigned, indicating that this domain of the protein is highly flexible (Riek et al., 1996). It harbours the octapeptide repeat segment which can bind copper ions (Brown et al., 1997). In human PrP, insertion of up to 9

additional octapeptide sequences are linked with the development of inherited prion diseases (Campbell et al., 1996). The pre-octarepeat domain (aa 23 – 50) has a high content of positively charged amino acids at the extreme N-terminus. The domain appears to be important for post-ER quality control mechanisms recognizing misfolded PrP aggregates (Gilch et al., 2004). The trafficking of PrP through the secretory pathway is also supported by the PrP N-terminus (Nunziante et al., 2003). For internalisation of PrP^c at the plasma membrane, the basic residues are important for co-factor binding (LRP1; Parkyn et al., 2008) and apparently mediate the transfer from lipid rafts to clathrin-coated pits, a step that is crucial for PrP internalisation (Sunyach et al., 2003). Interestingly, enhancing the internalisation rate by treatment with sulphated compounds like PPS or dextran sulfate interferes with prion conversion and can cure persistently infected cells from prion infection (Birkett et al., 2001). Interaction of peptide aptamers with the N-terminal positively charged region might also compete for interaction of PrP^c with glycosaminoglycans (GAGs) which are suspected to be co-receptors in prion infection and to sequester both PrP^c and PrP^{Sc} (Caughey & Race, 1994), thereby offering spatial proximity which is necessary for the interaction of the PrP isoforms. These data indicate that binding of peptide aptamers to the PrP N-terminus can lead to interference by different mechanisms. First, the internalisation might be enhanced, however this appears to be negligible since this usually results in a reduction of total PrP^c within the cell, a phenotype which was not observed upon treatment of cells with peptide aptamers. Second, and this is the more probable explanation, interference with co-factor binding might be responsible for an anti-prion effect elicited by peptide aptamers interacting with the PrP N-terminus.

The binding site of PA8 lies within residues 100 – 120. Interestingly, this region overlaps partially the peptide sequence (aa 90 – 130) chosen for selection of RNA aptamers. The most potent interactor, RNA aptamer DP7 presumably interfered with the formation of PK resistant high-molecular weight PrP^{Sc} aggregates in prion-infected cells (Proske et al., 2000). The sequence is part of the hydrophobic domain (HD; aa 110 – 130) implicated in neurotoxicity (Baumann et al., 2007; Li et al., 2007). According to the 2D-crystal structure forwarded for PrP^{Sc}, within this region the most dramatic structural transitions appear to occur. Whereas in PrP^c the structure of this part of the protein is flexible, it is converted into a domain with high β-sheet content in PrP^{Sc} (Wille et al. 2002, Govaerts et al., 2004). Covering this part of the protein by peptide aptamer binding might prevent the structural transitions.

PA1 and PA16 bind in addition to the PrP N-terminus also an epitope comprised by aa 120 – 150. This region covers a part of the hydrophobic domain and α-helix 1. Within PrP^c, many regions were mapped by peptide or antibody binding and employing motif-grafted antibodies,

respectively, to be important for the interaction between PrP^{c} and PrP^{Sc}. To provide an overview, these are listed in **Table 10**.

However, the significance can hardly be evaluated since for example the use of whole IgG molecules might, despite specific epitope recognition, yield false-positive results due to sterical hindrance of the PrP^{c}-PrP^{Sc} interaction rather than epitope-specific inhibition, a problem that was indeed discussed by Horiuchi et al. (Horiuchi et al., 1999). Nevertheless, this does not exclude the possibility that possibly the binding of PA1 or PA16 to PrP^{c} might cover surfaces implicated in the interaction of the PrP isoforms, which is supported by several mapping studies (**Table 10**)

Table 10. Putative PrP domains implicated in prion conversion.

Method	PrP-region/species	Reference
Peptides	106-141/hamster inhibits *in vitro* conversion	Chabry et al., 1998
	119-136/hamster, mouse inhibits *in vitro* conversion	Chabry et al., 1999
	166-179, 200-223, 119-136/hamster inhibits *in vitro* conversion	Horiuchi et al., 2001
PrP^{Sc} binding peptides	19-30, 100-111, 154-165, 226-237/ human bind vCJD; 23-30 binds native PrP^{Sc} of cattle, sheep, humans, hamster	Lau et al., 2007
Anti-PrP antibodies	epitope 219-232/hamster inhibits *in vitro* conversion;	Horiuchi et al., 1999
	epitopes 144-152 or 59-89/mouse inhibit conversion in 22L-N2a	Perrier et al., 2004
	epitope 159-178/mouse inhibits conversion in RML-N2a	Gilch et al., 2003
	epitopes 89-112, 136-158/mouse inhibit conversion in RML-N2a	Peretz et al., 2001
motif-grafted antibodies	89-112, 136-158 bind PrP^{Sc} of mouse, humans, hamster	Moroncini et al., 2004
	23-33, 98-110, 136-158 bind RML PrP^{Sc}	Solforosi et al., 2007

Overall, the binding sites of PrP identified for the different peptide aptamers suggest two modes of action (**Fig. 40**). First, the interaction might stabilize the native structure of PrP^{c} and prevent structural transitions. Such a mechanism has previously been suggested for the chemical chaperones DMSO or glycerol, which abrogate PrP^{Sc} propagation in infected cell

cultures (Tatzelt et al., 1996). Of note, such a chaperone-like activity has also been described for antibodies (Ermolenko et al., 2004). Second, the PrP^{c}-PrP^{Sc} interaction which is crucial for subsequent conversion might be inhibited, as suggested for numerous other molecules that bind to PrP^{c} and/or PrP^{Sc}.

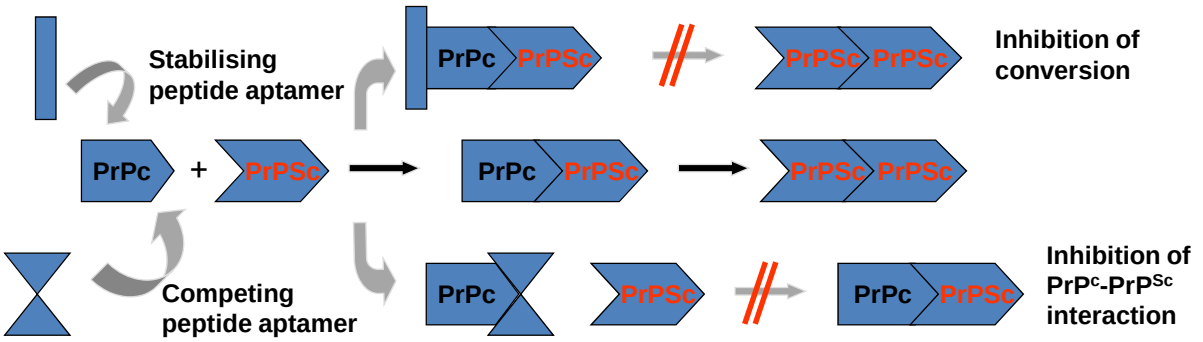

Fig. 40. Schematic depiction of proposed sites of interference. By binding of peptide aptamers to PrP^{c}, the interaction with PrP^{Sc} can be inhibited either by covering the binding sites or by withdrawal of PrP^{c} from the subcellular site of conversion (competing peptide aptamer). Alternatively, PrP^{c}-PrP^{Sc} interaction can take place despite binding of peptide aptamers, but PrP^{c} is overstabilized and not eligible for structural transitions (stabilising peptide aptamer).

5.5 Manipulation of subcellular localization does not alter binding properties of peptide aptamers

Prion diseases are disorders of the central nervous system and therapy requires molecules that can penetrate the brain in case of sporadic prion diseases. During infectiously aquired and genetic manifestations, prophylaxis of disease onset at the periphery might be feasible. However, whereas in infectious prion diseases replication of prions occurs at peripheral sites mainly in the spleen which could be inhibited by substances that do not necessarily have to reach the CNS, genetic forms develop like sporadic disease in the brain. This means that although in these cases prophylaxis is a realistic goal due to the possibility of early diagnosis upon sequencing of the prion protein gene, compounds are required that have access to the CNS.

This requirement is difficult to fulfil and recombinantly expressed peptide aptamers are probably not applicable. Prophylaxis in the periphery could be achieved by intravenous injection of peptide aptamers, although in this case the bacterial trxA will probably elicit an immune reaction resulting in neutralization of the peptide aptamers over time. Of note, this could be overcome by using homologous trx of the respective species for presentation of the peptide moiety. Transfer of peptides isolated in bacterial trxA against a given target protein to human trx does not alter binding properties, although this protein is only 30 % homologous to

E. coli trxA (Borghouts et al., 2008), indicating that this should also be possible with other species. However, transfer of anti-prion peptide aptamers to the brain by lentiviral delivery would be a highly desirable option. Therefore, expression of peptide aptamers in the secretory pathway and binding properties of those derivatives had to be evaluated. So far, peptide aptamers were only generated against cytosolic protein domains and it was completely unclear whether trxA-based peptide aptamers can be subjected to secretory expression at all. However, it could be unambiguously demonstrated here that upon fusion of peptide aptamers to an N-terminal signal peptide for ER entry and a C-terminal signal mediating attachment of a GPI-anchor all proteins were localized at the outer leaflet of the plasma membrane. 8-GPI and 16-GPI appeared to be equally efficiently imported into the ER and transported to the plasma membrane whereas a significant fraction of 1-GPI was located intracellularly. This might be due to an inefficient import into the ER, which was here achieved by the PrP signal peptide. It is established that signal peptides differ in their efficiency of mediating ER import and the PrP signal peptide appears to be not highly efficient in mediating translocation (Rane et al., 2004). Since all peptide aptamers are fused to the PrP signal peptide one would expect an equal translocation of all constructs. However, the import is further influenced by the polypeptide chain following the signal peptide (Hegde & Lingappa, 1996) and this makes it hard to predict whether a protein containing a randomised region is efficiently translocated across the ER membrane. Alternatively, 1-GPI might be folded incorrectly, leading to its retro-translocation into the cytosol and its subsequent proteasomal degradation which is the classical degradation pathway for misfolded proteins recognised by ER quality control mechanisms (Meusser et al., 2005).

Although immunofluorescence studies clearly revealed the correct localisation of the GPI-peptide aptamers at the cell surface, it was not or only slightly possible to release them from the cell surface by PIPLC treatment (data not shown) or trypsin digestion, independent of PrP^c expression within the cells. Since the enzyme might have had no access to the GPI-anchor due to sterical hindrance, treatment with trypsin, an endoprotease that digests all proteins, was performed. Here, also only marginal effects were achieved, although PrP^c was readily digested at the cell surface by the treatment. Comparing the expression levels of PrP^c with that of the peptide aptamers, the latter were in contrast to PrP^c highly overexpressed, and therefore the effects might be less clear for the peptide aptamers. Additionally, significant amounts of all GPI-peptide aptamers are located intracellularly leading to inaccessibility for extracellular enzymes.

Importantly, GPI-peptide aptamers still can bind to PrP^c as demonstrated by co-immunoprecipitation experiments, and also the interaction of all peptide aptamers with the C-terminal domain (aa 90 – 231) could be confirmed. Again, this was unpredictable. This

underlines once more that trxA is a highly stable scaffold protein as already described previously (Klevenz et al., 2002). In addition, the peptide moieties also appear to adopt an intrinsic conformational stability. In the cytosol of yeast, the conditions are reducing, and no disulfide bonds are formed. In contrast, the environment within the ER is oxidizing, and the correct disulfide bond formation is controlled by various enzymes. The peptide aptamers harbour at least two cysteines usually forming the active-site loop of trxA. It is possible that oxidation of these residues, similar to the situation in immunoglobulins (disulfide-closed loop; Ladner 1995), decreases the conformational freedom of the random peptides and thereby enhances their intrinsic stability. PA16 harbours two additional cysteine residues within the PrP-binding sequence. Analysis of reduced and non-reduced samples in immunoblot indicated that at least in 16-LAMP disulfide bonds are formed. However, it is not entirely clear why this has only been observed in the LAMP-version of the peptide aptamer, since thiol-groups are oxidized within the ER, and here also 16-GPI and 16-KDEL are located. One possible explanation for this might be that oxidation occurs in the acidic environment of the lysosomes due to spatial proximity of the two cysteines.

5.6 Raft localization and binding are not sufficient for inhibition of prion conversion

The retained binding affinity of the peptide aptamers with PrP^{c} upon changing their subcellular localization by the addition of a signal peptide for ER translocation and a GPI-anchor provided the basis for a possible inhibition of the prion conversion process in persistently infected cells (3F4-ScN2a). However, only 8-GPI slightly reduced the amount of PrP^{Sc} when expressed transiently for six consecutive days. The direct interaction of PrP^{c} with PrP^{Sc}, possibly in complex with a putative cellular co-factor is a crucial premise for prion conversion. On the cellular level, the trafficking kinetics and localization of PrP^{c}, especially the lipid raft association of PrP^{c}, are important. In prion-infected cell cultures both PrP^{c} and PrP^{Sc} are found in lipid raft fractions of the plasma membrane (Vey et al., 1996). Along this line, perturbation of lipid raft localization by various means has been demonstrated to inhibit prion conversion. In the first study conducted on this issue by Taraboulos and co-workers it was demonstrated that inhibition of cholesterol synthesis which prevents lipid raft formation reduces the PrP^{Sc} content in infected cell cultures. Similarly, a PrP mutant with a transmembrane helix for membrane anchorage that replaced the GPI-anchor and conferred non-raft localization was not converted into PrP^{Sc} (Taraboulos et al., 1995). The findings with mutant PrP can be challenged by the argument that here PrP was significantly mutated by completely exchanging the 3'-region of the coding sequence. These manipulations might

introduce a strong species barrier between PrP^c and the transmembrane form of PrP, since already as little as one amino acid exchange can completely abrogate the convertibility of the respective PrP (Vorberg et al., 2003). In a later study, similar experiments were performed employing a GPI-signal sequence that can be converted into a signal for transmembrane anchoring by exchanging only the last C-terminal amino acid. Here, the GPI-PrP construct was converted whereas the transmembrane form was not (Kaneko et al., 1997). Similar to the inhibition of cholesterol synthesis (Taraboulos et al., 1995), chemical manipulation of lipid rafts by cholesterol complexation (Mange et al., 2000) or extraction from the membrane (Marella et al., 2002) prevented PrP^{Sc} formation. All the studies described above led to the conclusion that lipid rafts might be the compartment of prion conversion. Since the GPI-peptide aptamers harboured the GPI-signal of PrP, it was assumed that they co-localize with PrP^c in lipid rafts. Having found that their anti-prion effects, if present at all, were only marginal extraction of lipid rafts and floatation assays were performed. The raft partitioning of the peptide aptamers could be confirmed, and the proteins were detected in the identical fractions as PrP^c. The finding that GPI-peptide aptamers bind to PrP^c and are located in lipid rafts but do not significantly inhibit PrP^{Sc} propagation appears to contradict the proposed importance of lipid rafts in the conversion process. One point of criticism, though, has to be noted in respect to the interaction of PrP^c with the GPI-peptide aptamers. Co-immunoprecipitation was performed with whole cell lysates and it could not be distinguished in which compartment peptide aptamers bind to PrP^c and at which subcellular stage they dissociate. In order to clarify this issue, co-immunoprecipitation experiments could be performed in fractions of isolated organelles, for example ER, Golgi compartment or lipid rafts. In general, the amounts of peptide aptamers obtained by transient transfection might not be equimolar with the number of PrP^c molecules leaving in case of 100 % binding of peptide aptamer molecules a certain fraction of PrP^c eligible for conversion. In addition, GPI-peptide aptamers are assumed to be competitive inhibitors of conversion, i. e. their binding affinity needs to be higher than that of PrP^{Sc}. If high amounts of recombinantly expressed and purified peptide aptamers are added, this problem can apparently be overcome. Provided an IC_{50} of approximately 350 nM, this allows an estimation of which high expression levels of GPI-peptide aptamers would be required to achieve the same effect. Taking this into account it appears convincing that the anti-prion effect of the GPI-peptide aptamers was not as pronounced as that of the purified proteins added from outside.

5.7 Intracellular retention and re-routing improve anti-prion effect

The rather unsatisfying anti-prion effects of the GPI-peptide aptamers necessitated further improvement of the molecules. This should be achieved by addtion of C-terminal modifications. On the one hand, PrP^c should be retained within the ER by binding to peptide aptamers harbouring a KDEL ER retention motif. On the other hand, it should be guided to lysosomes without reaching the plasma membrane by interaction with peptide aptamers fused to transmembrane and cytosolic domains of LAMP-I. Both KDEL- and LAMP-peptide aptamers partially co-localized with PrP^c and retained their binding properties to the target protein as demonstrated by co-immunoprecipitation. LAMP-peptide aptamers were indeed routed to lysosomes. PIPLC digestion of cells expressing KDEL- or LAMP-peptide aptamers indicated that depending on the peptide moiety and C-terminal modification less PrP^c was located at the cell surface. In particular, 8- and 16-KDEL and 1- and 8-LAMP had this effect. Of note, this was paralled by a significant anti-prion activity of those peptide aptamers in 3F4-ScN2a cells. In addition, expression of 8- and 16-KDEL during *de novo* prion infection of susceptible cells prevented persistent infection with scrapie strain RML.

Trapping of PrP^c within the ER has been performed previously by employing a KDEL-fused version of a single-chain antibody (scFv) derived from the monoclonal anti-PrP antibody 8H4 (Cardinale et al., 2005). This antibody recognizes PrP aa 175 – 185, an epitope embedded in helix B and covering the first glycosylation site. Similar to the effect of KDEL-peptide aptamers, it was demonstrated that maturation and cell surface localisation of PrP^c was prevented to a certain extent (Cardinale et al., 2005). Apparently, also the lysosomal degradation of PrP^c was inhibited by expression of anti-PrP scFv KDEL-8H4 (Vetrugno et al., 2005). For the evaluation of these anti-prion effects, the authors used the rat pheochromocytoma cell line PC12. In contrast to ScN2a cells used in our laboratory, PC12 cells can only be infected with prion strain 139A upon differentiation with nerve growth factor (NGF; Rubenstein et al., 1984). Cardinale et al. did not investigate the effects of KDEL-8H4 in persistently prion-infected cells but compared the amount of accumulated PrP^{Sc} upon differentiation of PC12 cell with NGF, followed by treatment with 139A infected brain homogenate and subsequent cultivation for at least 21 days (Cardinale et al., 2005). Notably, PC12 cells stably expressing KDEL-8H4 were used. Under these experimental conditions which mirror a prophylactic situation, accumulation of PrP^{Sc} and generation of prion infectivity was completely prevented (Cardinale et al., 2005; Vetrugno et al., 2005). In contrast, we demonstrate here for the first time that interference with prion propagation in persistently infected cells by using KDEL-tagged molecules that interact with PrP^c is possible. Of note, in our experiments on inhibition of *de novo* infection by peptide aptamers PrP^{Sc} accumlation was tested upon 2 passages after infection, which equals to 13 days. In contrast to the study

by Cardinale et al., KDEL-peptide aptamers were only expressed transiently during the incubation period with brain homogenate. These are highly restrictive conditions which require a strong interference with the steps of initial prion conversion, whereas during continued expression of KDEL-8H4 it cannot be distinguished whether indeed these steps are completely inhibited or whether a small amount of PrP^{Sc} is newly converted during infection but persistent infection cannot be established due to the permanent presence of KDEL-8H4.

In some aspects, scFv's are more similar to peptide aptamers than full IgG molecules. Their molecular weight is significantly lower and expression is not as complicated as that of IgG since they only consist of one polypeptide chain. They were already used for molecular therapy approaches of other neurodegenerative diseases (Miller & Messer, 2005). In prion diseases, scFv's have further been used as molecules secreted by a producer cell line that was co-cultivated with ScN2a cells. In these experiments, PrP^{Sc} was undetectable after 3 weeks of co-culture (Donofrio et al., 2005). This time period is significantly longer than the 6 consecutive days in which KDEL- and LAMP-peptide aptamers were expressed in 3F4-ScN2a cells, indicating that the peptide aptamers indeed exhibited a very powerful negative effect on PrP^{Sc} propagation, although within an even shorter time frame of 16 hours *de novo* generation of PrP^{Sc} in metabolically labelled cells was not influenced under our experimental conditions.

For LAMP-peptide aptamers, 1-LAMP and 8-LAMP expression induced an abrogation of PrP^{Sc} propagation. As already discussed, 16-LAMP was hardly expressed which might be due to additional cysteine residues and disulfide bond formation. The finding that 1-LAMP was effective whereas 1-KDEL was not allows the conclusion that depending on the peptide sequence a certain compartment is more supportive for their interaction with PrP^{c} than another. This means that 1-LAMP might preferentially bind to PrP^{c} in an environment provided in post-ER compartments.

The fusion of the peptide aptamers to transmembrane and cytosolic domain of the LAMP-1 protein should induce a bypass of the plasma membrane for PrP^{c} which was achieved at least partially. Targeting to lysosomes could additionally increase the degradation rate of PrP^{c} since similar to PrP^{Sc} it is degraded in acidic compartments (Taraboulos et al., 1992). The strategy of direct re-routing of PrP^{c} from the trans-Golgi network to lysosomes has been described previously by us (Gilch et al., 2001). In this former report, aggregation of PrP^{c} was chemically induced by treatment of cell cultures with the naphthyl-urea compound suramin, and these aggregates were apparently recognized by cellular mechanisms to be misfolded. However, in a follow-up study it was shown that N-terminally deleted and aggregated PrP is transported to the cell surface and was also not converted (Gilch et al., 2004). Therefore, it

was difficult to dissect whether the induction of aggregation is most important for the anti-prion effect of suramin and the re-routing might only play a minor role. The experiments described here using LAMP-peptide aptamers for interference in prion conversion clearly demonstrate that the induction of re-routing indeed can be a decisive factor for preventing PrP^{Sc} propagation.

In conclusion, it is demonstrated in this thesis that peptide aptamers can be efficiently selected against membrane proteins and can bind their target protein upon expression within the secretory pathway. In case of anti-PrP^{c} peptide aptamers, they can inhibit the conversion of PrP^{c} to PrP^{Sc} and interfere with prion infection. Here, combination of binding properties and the fusion of targeting motifs has a synergistic inhibitory effect. Exploring the binding sites and structure of the peptide aptamers might open new possibilities for experimental approaches dealing with prion diseases.

5.8 Outlook

In light of the above presented promising results obtained with peptide aptamers as binding partners for PrP^{c} and their negative influence of prion propagation, the project will be continued in several avenues of research dealing with both applied and basic research.

For applied science, the prophylactic and therapeutic properties of the peptide aptamers will be improved. With peptide aptamer 8 the most consistent results were obtained. This construct appears to have the highest intrinsic folding stability since all modifications (GPI, KDEL and LAMP) inhibited PrP^{Sc} propagation at least to a certain extent. However, the binding affinity needs to be improved in order to achieve interference in prion conversion with lower concentrations of the peptide aptamer. This will be obtained by random mutagenesis of this peptide encoding sequence using error-prone PCR and subsequent identification of novel peptide aptamer 8 derivatives that interact with PrP in Y2H. Error-prone PCR has already been established and sequencing of several clones obtained from the PCR product indicates a feasible frequency of mutations (**Table 11**). Subsequent structure determination of a high-affinity binder can then be exploited for the generation of small molecule inhibitors by rational drug design that might be able to cross the blood-brain-barrier.

Table 11. Alignment of PA8-derived clones upon error-prone PCR.

```
PA_8        GGATCCGCTCGTTTTGAGTATTTGCGGGATGGTTATTGGGTTTGGAGGTTTACGGGTCTAGA
EP_Klon_3   GGATCCGCTCGTCTTGAGTGTTTGCGGGATGGCTATCGGGTCTGGAGGTCTACGGGTCTAGA
EP_Klon_4   GGATCCGCCCGCTTTGAGTATTTGCGGGATGGCTATTGGGTTTGGAGGTTTACGGGTCTAGA
EP_Klon_1   GGATCCGCCCGTTCCGAGTACTCGCGGGATGACTGCTGGGCTTGGAGGTCTGCGGGTCTAGA
             ******* **     ****  * ********  *   ***  ******* * **********
```

* - single, fully conserved residue
 - no consensus

For basic research, application of peptide aptamer technology should shed light on the composition of the interface of PrP^{c}-PrP^{Sc} interactions. PrP^{c}-derived peptides will be inserted into the active-site loop of trxA. Experiments using these PrP-aptamers for immunoprecipitation of PrP^{Sc} might shed light on the question which PrP segments are required for the interaction between the PrP isoforms. In contrast to a similar approach by Moroncini et al. employing motif-grafted antibodies for precipitation of human PrP^{Sc} (Moroncini et al., 2004) our intention is to precipitate PrP^{Sc} of different mouse-adapted scrapie strains or species. The working hypothesis here is that possibly the binding sites of various prion strains to PrP^{Sc} are strain-specific, as proposed for some yeast prion strains (Tessier & Lindquist, 2007).

In summary, there is a wide variety of possible applications for peptide aptamers in prion research. Exploring the binding sites and structure of the peptide aptamers might open new possibilities for experimental approaches dealing with prion diseases. Employing peptide aptamers displaying PrP-derived peptides for binding studies with PrP^{Sc}, important novel information can be gained about the possibly strain-specific interface of the PrP^{c}-PrP^{Sc} interaction.

6. References

Adjou KT, Demaimay R, Lasmezas C et al. (1995) MS-8209, a new amphotericin B derivative, provides enhanced efficacy in delaying hamster scrapie. *Antimicrob Agents Chemother* 39: 2810-2812.

Adjou KT, Demaimay R, Lasmezas CI et al. (1996) Differential effects of a new amphotericin B derivative, MS-8209, on mouse BSE and scrapie: implications for the mechanism of action of polyene antibiotics. *Res Virol.* 147: 213-218.

Adjou KT, Demaimay R, Deslys JP, Lasmézas CI, Beringue V, Demart S, Lamoury F, Seman M, Dormont D. (1999) MS-8209, a water-soluble amphotericin B derivative, affects both scrapie agent replication and PrPres accumulation in Syrian hamster scrapie. *J Gen Virol.* 80:1079-85.

Adjou KT, Simoneau S, Salès N, Lamoury F, Dormont D, Papy-Garcia D, Barritault D, Deslys JP, Lasmézas CI. (2003) A novel generation of heparan sulfate mimetics for the treatment of prion diseases. *J Gen Virol.* 84: 2595-603.

Aguib Y, Gilch S, Krammer C, Ertmer A, Groschup MH, Schätzl HM. (2008) Neuroendocrine cultured cells counteract persistent prion infection by down-regulation of PrPc. *Mol Cell Neurosci.* 38: 98-109.

Aguzzi A. (2002) Absence of the prion protein homologue Doppel causes male sterility. *EMBO J.* 21: 3652-8.

Aguzzi A, Polymenidou M. (2004) Mammalian prion biology: one century of evolving concepts. *Cell*. 116: 313-27.

Alper T, Cramp WA, Haig DA, Clarke MC. (1967) Does the agent of scrapie replicate without nucleic acid? *Nature.* 214: 764-6.

Angers RC, Browning SR, Seward TS, Sigurdson CJ, Miller MW, Hoover EA, Telling GC. (2006) Prions in skeletal muscles of deer with chronic wasting disease. *Science* 311: 1117.

Arbel M, Lavie V, Solomon B. (2003) Generation of antibodies against prion protein in wild-type mice via helix 1 peptide immunization. *J Neuroimmunol*. 144: 38-45.

Bainbridge J, Jones N, Walker B. (2004) Multiple antigenic peptides facilitate generation of anti-prion antibodies. *Clin Exp Immunol*. 137: 298-304.

Baines IC & Colas P. (2006) Peptide aptamers as guides for small-molecule drug discovery. *Drug Discov Today.* 11: 334-341.

Barret A, Tagliavini F, Forloni G, Bate C, Salmona M, Colombo L, De Luigi A, Limido L, Suardi S, Rossi G, Auvré F, Adjou KT, Salès N, Williams A, Lasmézas C, Deslys JP. (2003) Evaluation of quinacrine treatment for prion diseases. *J Virol.* 77: 8462-9.

Basler K, Oesch B, Scott M, Westaway D, Wälchli M, Groth DF, McKinley MP, Prusiner SB, Weissmann C. (1986) Scrapie and cellular PrP isoforms are encoded by the same chromosomal gene. *Cell*. 46: 417-28.

Bate C, Salmona M, Diomede L et al. (2004) Squalestatin cures prion-infected neurons and protects against prion neurotoxicity. *J Bio Chem.* 279: 14983-90.

Baumann F, Tolnay M, Brabeck C, Pahnke J, Kloz U, Niemann HH, Heikenwalder M, Rülicke T, Bürkle A, Aguzzi A. (2007) Lethal recessive myelin toxicity of prion protein lacking its central domain. *EMBO J.* 26: 538-47.

Behrens A, Genoud N, Naumann H, Rülicke T, Janett F, Heppner FL, Ledermann B, Aguzzi A. (2002) Absence of the prion protein homologue Doppel causes male sterility. *EMBO J.* 21: 3652-8.

Belay ED. (1999) Transmissible spongiform encephalopathies in humans. *Annu Rev Microbiol.* 53: 283-314.

Bellingham SA, Coleman LA, Masters CL, Camakaris J, Hill AF. (2008) Regulation of prion gene expression by transcription factors SP1 and MTF-1. *J Biol Chem.* Nov 6. [Epub ahead of print]

Bendheim PE, Brown HR, Rudelli RD, Scala LJ, Goller NL, Wen GY, Kascsak RJ, Cashman NR, Bolton DC. (1992) Nearly ubiquitous tissue distribution of the scrapie agent precursor protein. *Neurology*. 42: 149-56.

Benito-León J. (2004) Combined quinacrine and chlorpromazine therapy in fatal familial insomnia. *Clin Neuropharmacol*. 27: 201-3.

Béranger F, Mangé A, Goud B, Lehmann S. (2002) Stimulation of PrP(C) retrograde transport toward the endoplasmic reticulum increases accumulation of PrP(Sc) in prion-infected cells. *J Biol Chem.* 277: 38972-7.

Beringue V, Vilette D, Mallinson G et al. (2004) PrPSc binding antibodies are potent inhibitors of prion replication in cell lines. *J Biol Chem*. 279: 39671-39676.

Bertsch U, Winklhofer KF, Hirschberger T, Bieschke J, Weber P, Hartl FU, Tavan P, Tatzelt J, Kretzschmar HA, Giese A. (2005) Systematic identification of antiprion drugs by high-throughput screening based on scanning for intensely fluorescent targets. *J Virol.* 79: 7785-91.

Bessen RA, Marsh RF. (1992) Identification of two biologically distinct strains of transmissible mink encephalopathy in hamsters. *J Gen Virol*. 73:329-34.

Beste G, Schmidt FS, Stibora T, Skerra A. (1999) Small antibody-like proteins with prescribed ligand specificities derived from the lipocalin fold. *Proc Natl Acad Sci USA* 96: 1898-1903.

Birkett CR, Hennion RM, Bembridge DA, Clarke MC, Chree A, Bruce ME, Bostock CJ. (2001) Scrapie strains maintain biological phenotypes on propagation in a cell line in culture. *EMBO J.* 20: 3351-8.

Bogan AA & Thorn KS. (1998) Anatomy of hot spots in protein interfaces. *J Mol Biol.* 280: 1-9.

Bolton DC, McKinley MP, Prusiner SB. (1982) Identification of a protein that purifies with the scrapie prion. *Science.* 218: 1309-11.

Borchelt DR, Scott M, Taraboulos A, Stahl N, Prusiner SB. (1990) Scrapie and cellular prion proteins differ in their kinetics of synthesis and topology in cultured cells. *J Cell Biol.* 110: 743-52.

Borchelt DR, Taraboulos A, Prusiner SB. (1992) Evidence for synthesis of scrapie prion proteins in the endocytic pathway. *J Biol Chem.*267: 16188-99.

Borghouts C, Kunz C, Groner B. Peptide aptamer libraries. (2008) *Comb Chem High Throughput Screen.* 11: 135-45.

Bosque PJ, Prusiner SB. (2000) Cultured cell sublines highly susceptible to prion infection. *J Virol.* 74: 4377-86.

Brandner S, Isenmann S, Raeber A, Fischer M, Sailer A, Kobayashi Y, Marino S, Weissmann C, Aguzzi A. (1996) Normal host prion protein necessary for scrapie-induced neurotoxicity. *Nature.* 379: 339-43.

Breydo L, Bocharova OV, Baskakov IV. (2005) Semiautomated cell-free conversion of prion protein: applications for high-throughput screening of potential antiprioin drugs. *Anal Biochem.*339: 165-73

Brotherston JG, Renwick CC, Stamp JT, Zlotnik I, Pattison IH. (1968) Spread and scrapie by contact to goats and sheep. *J Comp Pathol*. 78: 9-17.

Brown DR, Besinger A. (1998) Prion protein expression and superoxide dismutase activity. *Biochem J.* 334: 423-9.

Brown DR, Qin K, Herms JW, Madlung A, Manson J, Strome R, Fraser PE, Kruck T, von Bohlen A, Schulz-Schaeffer W, Giese A, Westaway D, Kretzschmar H. (1997) The cellular prion protein binds copper in vivo. *Nature.* 390: 684-7.

Brown DR. (2001) Microglia and prion disease. *Microsc Res Tech.* 54: 71-80.

Brown P, Preece M, Brandel JP, Sato T, McShane L, Zerr I, Fletcher A, Will RG, Pocchiari M, Cashman NR, d'Aignaux JH, Cervenáková L, Fradkin J, Schonberger LB, Collins SJ. (2000) Iatrogenic Creutzfeldt-Jakob disease at the millennium. *Neurology.* 55: 1075-81.

Bruce ME, Fraser H. (1991) Scrapie strain variation and its implications. *Curr Top Microbiol Immunol.* 172: 125-38.

Bruce M, Chree A, McConnell I, Foster J, Pearson G, Fraser H. (1994) Transmission of bovine spongiform encephalopathy and scrapie to mice: strain variation and the species barrier. *Philos Trans R Soc Lond B Biol Sci*. 343: 405-11.

Büeler H, Aguzzi A, Sailer A, Greiner RA, Autenried P, Aguet M, Weissmann C. (1993) Mice devoid of PrP are resistant to scrapie. *Cell.* Jul 2; 73: 1339-47.

Buerger C, Nagel-Wolfrum K, Kunz C, Wittig I, Butz K, Hoppe-Seyler F, Groner B. (2003) Sequence-specific peptide aptamers, interacting with the intracellular domain of the epidermal growth factor receptor, interfere with Stat3 activation and inhibit the growth of tumor cells. *J Biol Chem.* 278: 37610-37621.

Burger D, Hartsough GR. (1965) Encephalopathy of mink. II. Experimental and natural transmission. *J Infect Dis*. 115: 393-9.

Butler DA, Scott MR, Bockman JM, Borchelt DR, Taraboulos A, Hsiao KK, Kingsbury DT, Prusiner SB. (1988) Scrapie-infected murine neuroblastoma cells produce protease-resistant prion proteins. *J Virol.* 62: 1558-64.

Butz K, Denk C, Ullmann A, Scheffner M, Hoppe-Seyler F. (2000) Induction of apoptosis in human papillomaviruspositive cancer cells by peptide aptamers targeting the viral E6 oncoprotein. *Proc Natl Acad Sci USA.* 97: 6693-6697.
Butz K, Denk C, Fitscher B, Crnkovic-Mertens I, Ullmann A, Schroder CH, Hoppe-Seyler F. (2001) Peptide aptamers targeting the hepatitis B virus core protein: a new class of molecules with antiviral activity. *Oncogene.* 20: 6579-6586.

Campbell TA, Palmer MS, Will RG, Gibb WR, Luthert PJ, Collinge J. (1996) A prion disease with a novel 96-base pair insertional mutation in the prion protein gene. *Neurology.* 46: 761-6.

Cardinale A, Filesi I, Vetrugno V et al. (2005) Trapping prion protein in the endoplasmic reticulum impairs PrPC maturation and prevents PrPSc accumulation. *J Biol Chem*. 280: 685-694.

Caspi S, Halimi M, Yanai A et al. (1998) The anti-prion activity of Congo red. Putative mechanism. *J Biol Chem.* 273: 3484-89.

Castilla J, Saá P, Hetz C, Soto C. (2005) In vitro generation of infectious scrapie prions. *Cell*. 121: 195-206.

Cattaneo A & Biocca S. (1999) The selection of intracellular antibodies. *Trends Biotechnol.* 17: 115-121.

Caughey B, Raymond GJ. (1991) The scrapie-associated form of PrP is made from a cell surface precursor that is both protease- and phospholipase-sensitive. *J Biol Chem.* 266: 18217-23.

Caughey B, Race RE. (1992) Potent inhibition of scrapie-associated PrP accumulation by congo red*. J Neurochem*. 59: 768-71.

Caughey B, Ernst D, Race RE. (1993) Congo red inhibition of scrapie agent replication. *J Virol.* 67: 6270-72.

Caughey B, Race RE. (1994) Scrapie-associated PrP accumulation and its inhibition: revisiting the amyloid-glycosaminoglycan connection. *Ann N Y Acad Sci.* 724: 290-5.

Caughey B, Kocisko DA, Raymond GJ, Lansbury PT Jr. (1995) Aggregates of scrapie-associated prion protein induce the cell-free conversion of protease-sensitive prion protein to the protease-resistant state*. Chem Biol*. 2: 807-17.

Caughey WS, Raymond LD, Horiuchi M et al. (1998) Inhibition of protease-resistant prion protein formation by porphyrins and phthalocyanines. *Proc Natl Acad Sci U S A.* 95: 12117-12122.

Chabry J, Caughey B, Chesebro B. (1998) Specific inhibition of in vitro formation of protease-resistant prion protein by synthetic peptides. *J Biol Chem*. 273: 13203-7.

Chabry J, Priola SA, Wehrly K et al. (1999) Species-independent inhibition of abnormal prion protein (PrP) formation by a peptide containing a conserved PrP sequence. *J Virol.* 73: 6245-6250.

Chesebro B, Trifilo M, Race R, Meade-White K, Teng C, LaCasse R, Raymond L, Favara C, Baron G, Priola S, Caughey B, Masliah E, Oldstone M. (2005) Anchorless prion protein results in infectious amyloid disease without clinical scrapie. *Science* 308: 1435-9.

Cohen FE, Pan KM, Huang Z, Baldwin M, Fletterick RJ, Prusiner SB. (1994) Structural clues to prion replication. *Science.* 264: 530-1.

Colas P,Cohen B, Jessen T, Grishina I, McCoy J, Brent, R. (1996) Genetic selection of peptide aptamers that recognize and inhibit cyclin-dependent kinase 2. *Nature.* 380: 548-550.

Colas P, Cohen B, Ko FP, Silver PA, Brent R. (2000) Targeted modification and transportation of cellular proteins. *Proc Natl Acad Sci USA*. 97: 13720-13725.

Colling SB, Collinge J, Jefferys JG. (1996) Hippocampal slices from prion protein null mice: disrupted Ca(2+)-activated K+ currents. *Neurosci Lett*. 209: 49-52.

Collinge J, Beck J, Campbell T, Estibeiro K, Will RG. (1996) Prion protein gene analysis in new variant cases of Creutzfeldt-Jakob disease. *Lancet.* 348: 56.

Collinge J, Rossor M. (1996) A new variant of prion disease. *Lancet*. 347: 916-7.

Collinge J, Sidle KC, Meads J, Ironside J, Hill AF. (1996) Molecular analysis of prion strain variation and the aetiology of 'new variant' CJD. *Nature.* 383: 685-90.

Collinge J. (1997) Human prion diseases and bovine spongiform encephalopathy (BSE).*Hum Mol Genet*. 6:1699-705.

Collinge J. (2001) Prion diseases of humans and animals: their causes and molecular basis. *Annu Rev Neurosci*. 24: 519-50.

Come JH, Fraser PE, Lansbury PT Jr. (1993) A kinetic model for amyloid formation in the prion diseases: importance of seeding. *Proc Natl Acad Sci U S A.* 90: 5959-63.

Creutzfeldt, HG. (1920). Über eine eigenartige herdförmige Erkrankung des zentralen Nervensystems. /. *Ges. Neuro. Psychiatr*. 57, 1-18.

Cronier S, Laude H, Peyrin JM. (2004) Prions can infect primary cultured neurons and astrocytes and promote neuronal cell death. *Proc Natl Acad Sci U S A.* 101: 12271-6.

Cronier S, Beringue V, Bellon A, Peyrin JM, Laude H. (2007) Prion strain- and species-dependent effects of antiprion molecules in primary neuronal cultures. *J Virol.* 81: 13794-800.

Daude N, Marella M, Chabry J. (2003) Specific inhibition of pathological prion protein accumulation by small interfering RNAs. *J Cell Sci.* 116: 2775-2779.

Davanipour Z, Alter M, Sobel E, Asher D, Gajdusek DC. (1985) Creutzfeldt-Jakob disease: possible medical risk factors. *Neurology*. 35: 1483-6.

Demaimay R, Adjou K, Lasmezas C et al. (1994) Pharmacological studies of a new derivative of amphotericin B, MS-8209, in mouse and hamster scrapie. *J Gen Virol* 75: 2499-2503.

Dickinson AG, Stamp JT, Renwick CC. (1974) Maternal and lateral transmission of scrapie in sheep. *J Comp Pathol*. 84:19-25.

Dickinson AG, Meikle VM, Fraser H. (1968) Identification of a gene which controls the incubation period of some strains of scrapie agent in mice. *J Comp Pathol*. 78: 293-9.

Diringer H, Ehlers B. (1991) Chemoprophylaxis of scrapie in mice. *J Gen Virol*. 72: 457-60.

Dlakic WM, Grigg E, Bessen RA. (2007) Prion infection of muscle cells in vitro. *J Virol.* 81: 4615-24.

Doh-Ura K, Iwaki T, Caughey B. (2000) Lysosomotropic agents and cysteine protease inhibitors inhibit scrapie-associated prion protein accumulation. *J Virol*. 74: 4894-4897.

Doh-ura K, Ishikawa K, Murakami-Kubo I, Sasaki K, Mohri S, Race R, Iwaki T. (2004) Treatment of transmissible spongiform encephalopathy by intraventricular drug infusion in animal models. *J Virol.* 78: 4999-5006.

Donnelly CA, Ferguson NM, Ghani AC, Anderson RM. (2002) Implications of BSE infection screening data for the scale of the British BSE epidemic and current European infection levels. *Proc Biol Sci.* 269: 2179-90.

Donofrio G, Heppner FL, Polymenidou M et al. (2005) Paracrine inhibition of prion propagation by anti-PrP single-chain Fv miniantibodies. *J Virol.* 79: 8330-8338.

Dupiereux I, Falisse-Poirrier N, Zorzi W, Watt NT, Thellin O, Zorzi D, Pierard O, Hooper NM, Heinen E, Elmoualij B. (2007) Protective effect of prion protein via the N-terminal region in mediating a protective effect on paraquat-induced oxidative injury in neuronal cells. *J Neurosci Res*. 86: 653-659.

Edenhofer F, Rieger R, Famulok M, Wendler W, Weiss S, Winnacker EL. (1996) Prion protein PrPc interacts with molecular chaperones of the Hsp60 family. *J Virol*. 70: 4724-8.

Enari M, Flechsig E, Weissmann C. (2001) Scrapie prion protein accumulation by scrapie-infected neuroblastoma cells abrogated by exposure to a prion protein antibody. *Proc Natl Acad Sci U S A.* 98: 9295-9.

Ermolenko DN, Zherdev AV, Dzantiev BB. (2004) Antibodies as specific chaperones. *Biochemistry (Mosc.)*. 69: 1233-1238.

Ertmer A, Gilch S, Yun SW, Flechsig E, Klebl B, Stein-Gerlach M, Klein MA, Schätzl HM. (2004) The tyrosine kinase inhibitor STI571 induces cellular clearance of PrPSc in prion-infected cells. *J Biol Chem*. 279: 41918-27.

Ertmer A, Huber V, Gilch S et al. (2007) The anticancer drug imatinib induces cellular autophagy. *Leukemia.* 21: 936-942.

Farquhar CF, Dickinson AG. (1986) Prolongation of scrapie incubation period by an injection of dextran sulphate 500 within the month before or after infection. *J Gen Virol.* 67: 463-73.

Féraudet C, Morel N, Simon S, Volland H, Frobert Y, Créminon C, Vilette D, Lehmann S, Grassi J. (2005) Screening of 145 anti-PrP monoclonal antibodies for their capacity to inhibit PrPSc replication in infected cells. *J Biol Chem*. 280: 11247-58.

Fernandez-Borges N, Brun A, Whitton JL et al. (2006) DNA vaccination can break immunological tolerance to PrP in wild-type mice and attenuates prion disease after intracerebral challenge. *J Virol*. 80: 9970-9976.

Fevrier B, Vilette D, Archer F, Loew D, Faigle W, Vidal M, Laude H, Raposo G. (2004) Cells release prions in association with exosomes. *Proc Natl Acad Sci U S A.* 101:9683-8.

Forloni G, Iussich S, Awan T et al. (2002) Tetracyclines affect prion infectivity. *Proc Natl Acad Sci U S A* 99: 10849-10854.

Gajdusek DC, Zigas V. (1957) Degenerative disease of the central nervous system in New Guinea; the endemic occurrence of kuru in the native population. *N Engl J Med*. 257: 974-8.

Gasset M, Baldwin MA, Fletterick RJ, Prusiner SB. (1993) Perturbation of the secondary structure of the scrapie prion protein under conditions that alter infectivity. *Proc Natl Acad Sci U S A*. 90: 1-5.

Gauczynski S, Nikles D, El-Gogo S, Papy-Garcia D, Rey C, Alban S, Barritault D, Lasmezas CI, Weiss S. (2006) The 37-kDa/67-kDa laminin receptor acts as a receptor for infectious prions and is inhibited by polysulfated glycanes. *J Infect Dis.* 194: 702-9.

Gerstmann J, Sträussler E, Scheinker, I. (1936) Über eine eigenartige hereditär-familiäre Erkrankug des zentralen Nervensystems. Zugleich ein Beitrag zur Frage des vorzeitigen lokalen Alterns. *Z. Ges. Neurol. Psychiat*.154: 736-762.

Geyer CR, Colman-Lerner A, Brent, R. (1999) "Mutagenesis" by peptide aptamers identifies genetic network members and pathway connections. *Proc Natl Acad Sci USA.* 96: 8567-8572.

Geyer CR. (2001) Peptide aptamers: dominant "genetic" agents for forward and reverse analysis of cellular processes. *Curr Protoc Mol Biol.* Chapter 24: Unit 24.4.

Ghani AC, Donnelly CA, Ferguson NM, Anderson RM. (2003) Updated projections of future vCJD deaths in the UK. *BMC Infect Dis*. 3: 4.

Gilch S, Winklhofer KF, Groschup MH, Nunziante M, Lucassen R, Spielhaupter C, Muranyi W, Riesner D, Tatzelt J, Schätzl HM. (2001) Intracellular re-routing of prion protein prevents propagation of PrP(Sc) and delays onset of prion disease. *EMBO J*. 20: 3957-66.

Gilch S, Wopfner F, Renner-Müller I, Kremmer E, Bauer C, Wolf E, Brem G, Groschup MH, Schätzl HM. (2003) Polyclonal anti-PrP auto-antibodies induced with dimeric PrP interfere efficiently with PrPSc propagation in prion-infected cells. *J Biol Chem*. 278: 18524-31.

Gilch S, Nunziante M, Ertmer A, Wopfner F, Laszlo L, Schätzl HM. (2004) Recognition of lumenal prion protein aggregates by post-ER quality control mechanisms is mediated by the preoctarepeat region of PrP. *Traffic*. 5: 300-13.

Gilch S, Kehler C, Schatzl HM. (2006) The prion protein requires cholesterol for cell surface localization. *Mol Cell Neurosci.* 31: 346-353.

Goñi F, Knudsen E, Schreiber F, Scholtzova H, Pankiewicz J, Carp R, Meeker HC, Rubenstein R, Brown DR, Sy MS, Chabalgoity JA, Sigurdsson EM, Wisniewski T. (2005) Mucosal vaccination delays or prevents prion infection via an oral route. *Neuroscience.* 133: 413-21.

Govaerts C, Wille H, Prusiner SB, Cohen FE. (2004) Evidence for assembly of prions with left-handed beta-helices into trimers. *Proc Natl Acad Sci U S A*. 101: 8342-7.

Hadlow WJ, Kennedy RC, Race RE. (1982) Natural infection of Suffolk sheep with scrapie virus. *J Infect Dis.* 146:657-64.

Hadlow WJ, Race RE, Kennedy RC. (1987) Temporal distribution of transmissible mink encephalopathy virus in mink inoculated subcutaneously. *J Virol.* 61: 3235-40.

Haigh CL, Brown DR. (2006) Prion protein reduces both oxidative and non-oxidative copper toxicity. *J Neurochem*.98: 677-89.

Haïk S, Brandel JP, Salomon D, Sazdovitch V, Delasnerie-Lauprêtre N, Laplanche JL, Faucheux BA, Soubrié C, Boher E, Belorgey C, Hauw JJ, Alpérovitch A. (2004) Compassionate use of quinacrine in Creutzfeldt-Jakob disease fails to show significant effects. *Neurology.* 63: 2413-5.

Handisurya A, Gilch S, Winter D et al. (2007) Vaccination with prion peptide-displaying papillomavirus-like particles induces autoantibodies to normal prion protein that interfere with pathologic prion protein production in infected cells. *FEBS J*. 274: 1747-1758.

Head MW, Northcott V, Rennison K, Ritchie D, McCardle L, Bunn TJ, McLennan NF, Ironside JW, Tullo AB, Bonshek RE. (2003) Prion protein accumulation in eyes of patients with sporadic and variant Creutzfeldt-Jakob disease. *Invest Ophthalmol Vis Sci.* 44: 342-6.

Hegde RS, Lingappa VR. (1996) Sequence-specific alteration of the ribosome-membrane junction exposes nascent secretory proteins to the cytosol. *Cell.* 85: 217-28.

Hegde RS, Mastrianni JA, Scott MR, DeFea KA, Tremblay P, Torchia M, DeArmond SJ, Prusiner SB, Lingappa VR. (1998) A transmembrane form of the prion protein in neurodegenerative disease. *Science.* 279: 827-34.

Heikenwalder M, Polymenidou M, Junt T, Sigurdson C, Wagner H, Akira S, Zinkernagel R, Aguzzi A. (2004) Lymphoid follicle destruction and immunosuppression after repeated CpG oligodeoxynucleotide administration. *Nat Med*. 10: 187-92.

Heiseke A, Schöbel S, Lichtenthaler SF, Vorberg I, Groschup MH, Kretzschmar H, Schätzl HM, Nunziante M. (2008) The novel sorting nexin SNX33 interferes with cellular PrP formation by modulation of PrP shedding. *Traffic.* 9: 1116-29.

Heppner FL, Musahl C, Arrighi I, Klein MA, Rülicke T, Oesch B, Zinkernagel RM, Kalinke U, Aguzzi A. (2001) Prevention of scrapie pathogenesis by transgenic expression of anti-prion protein antibodies. *Science.* 294: 178-82.

Hijazi N, Kariv-Inbal Z, Gasset M, Gabizon R. (2005) PrPSc incorporation to cells requires endogenous glycosaminoglycan expression. *J Biol Chem.* 280: 17057-61.

Hill AF, Desbruslais M, Joiner S, Sidle KC, Gowland I, Collinge J, Doey LJ, Lantos P. (1997) The same prion strain causes vCJD and BSE. *Nature*. 389: 448-50, 526.

Hill AF, Butterworth RJ, Joiner S, Jackson G, Rossor MN, Thomas DJ, Frosh A, Tolley N, Bell JE, Spencer M, King A, Al-Sarraj S, Ironside JW, Lantos PL, Collinge J. (1999) Investigation of variant Creutzfeldt-Jakob disease and other human prion diseases with tonsil biopsy samples*. Lancet.* 353: 183-9.

Hill AF, Joiner S, Linehan J, Desbruslais M, Lantos PL, Collinge J. (2000) Species-barrier-independent prion replication in apparently resistant species.*Proc Natl Acad Sci U S A*.97: 10248-53.

Hill AF, Joiner S, Wadsworth JD, Sidle KC, Bell JE, Budka H, Ironside JW,Collinge J. (2003) Molecular classification of sporadic Creutzfeldt-Jakob disease. *Brain*. 126: 1333-46.

Hoppe-Seyler F, Crnkovic-Mertens I, Denk C, Fitscher BA, Klevenz B, Tomai E, Butz K. (2001) Peptide aptamers: new tools to study protein interactions. *. Steroid Biochem Mol Biol.* 78: 105-111.

Hoppe-Seyler F, Crnkovic-Mertens I, Tomai E, Butz K. (2004) Peptide aptamers: specific inhibitors of protein function. *Curr. Mol. Med.* 4: 529-538.

Horiuchi M, Caughey B. (1999) Specific binding of normal prion protein to the scrapie form via a localized domain initiates its conversion to the protease-resistant state. *EMBO J.* 18:3193-203.

Horiuchi M, Baron GS, Xiong LW et al. (2001) Inhibition of interactions and interconversions of prion protein isoforms by peptide fragments from the C-terminal folded domain. *J Biol Chem*. 276: 15489-15497.

Horiuchi M, Baron GS, Xiong LW, Caughey B. (2001) Inhibition of interactions and interconversions of prion protein isoforms by peptide fragments from the C-terminal folded domain. *J Biol Chem.* 276: 15489-97

Horiuchi M. (2001) Prion diseases in animals. *Uirusu*. 51: 145-150.

Hornshaw MP, McDermott JR, Candy JM. (1995) Copper binding to the N-terminal tandem repeat regions of mammalian and avian prion protein. *Biochem Biophys Res Commun*. 207: 621-9.

Horonchik L, Tzaban S, Ben-Zaken O, Yedidia Y, Rouvinski A, Papy-Garcia D, Barritault D, Vlodavsky I, Taraboulos A. (2005) Heparan sulfate is a cellular receptor for purified infectious prions. *J Biol Chem.* 280: 17062-7.

Hundt C, Peyrin JM, Haïk S, Gauczynski S, Leucht C, Rieger R, Riley ML, Deslys JP, Dormont D, Lasmézas CI, Weiss S. (2001) Identification of interaction domains of the prion protein with its 37-kDa/67-kDa laminin receptor. *EMBO J.* 20: 5876-86.

Ingrosso L, Ladogana A, Pocchiari M. (1995) Congo red prolongs the incubation period in scrapie-infected hamsters. *J Virol.* 69: 506-8.

Iwamaru Y, Takenouchi T, Ogihara K, Hoshino M, Takata M, Imamura M, Tagawa Y, Hayashi-Kato H, Ushiki-Kaku Y, Shimizu Y, Okada H, Shinagawa M, Kitani H, Yokoyama T. (2007) Microglial cell line established from prion protein-overexpressing mice is susceptible to various murine prion strains. *J Virol*. 81: 1524-7.

Jakob, AM. (1921) Über eigenartige Erkrankungen des Zentralnervensystems mit bemerkenswerten anatomischen Befunden (Spastische Pseudosklerose-Encephalomyelopathie mit disseminierten Degererationsherden). *Dtsch. Z. Nervenheilk*. 70:132-146.

Johnson S, Evans D, Laurenson S, Paul D, Davies AG, Ferrigno PK, Wälti C. (2008) Surface-immobilized peptide aptamers as probe molecules for protein detection. *Anal Chem.*80: 978-83.

Jones S, Thornton JM. (1996) Principles of protein-protein interactions. *Proc Natl Acad Sci U S A.* 93: 13-20.

Kahn S, Dubé C, Bates L, Balachandran A. (2004) Chronic wasting disease in Canada: Part 1. *Can Vet J.* 45: 397-404.

Kaiser-Schulz G, Heit A, Quintanilla-Martinez L, Hammerschmidt F, Hess S, Jennen L, Rezaei H, Wagner H, Schätzl HM. (2007) Polylactide-coglycolide microspheres co-encapsulating recombinant tandem prion protein with CpG-oligonucleotide break self-tolerance to prion protein in wild-type mice and induce CD4 and CD8 T cell responses. *J Immunol.* 179: 2797-807.

Kaneko K, Vey M, Scott M, Pilkuhn S, Cohen FE, Prusiner SB. (1997) COOH-terminal sequence of the cellular prion protein directs subcellular trafficking and controls conversion into the scrapie isoform. *Proc Natl Acad Sci U S A.* 94: 2333-8.

Karpuj MV, Giles K, Gelibter-Niv S, Scott MR, Lingappa VR, Szoka FC, Peretz D, Denetclaw W, Prusiner SB. (2007) Phosphorothioate oligonucleotides reduce PrP levels and prion infectivity in cultured cells. *Mol Med*. 13: 190-8.

Kim TY, Shon HJ, Joo YS, Mun UK, Kang KS, Lee YS. (2005) Additional cases of Chronic Wasting Disease in imported deer in Korea. *J Vet Med Sci.* 67:753-9.

Klevenz B, Butz K, Hoppe-Seyler F. (2002) Peptide aptamers: exchange of the thioredoxin-A scaffold by alternative platform proteins and its influence on target protein binding. *Cell Mol Life Sci.* 59: 1993-8.

Klöhn PC, Stoltze L, Flechsig E, Enari M, Weissmann C. (2003) A quantitative, highly sensitive cell-based infectivity assay for mouse scrapie prions. *Proc Natl Acad Sci U S A.* 100: 11666-71.

Koller MF, Grau T, Christen P. (2002) Induction of antibodies against murine full-length prion protein in wild-type mice. *J Neuroimmunol*. 132: 113-116.

Kocisko DA, Baron GS, Rubenstein R et al. (2003) New inhibitors of scrapie-associated prion protein formation in a library of 2000 drugs and natural products. *J Virol.* 88: 1062-1067.

Kocisko DA, Engel AL, Harbuck K, Arnold KM, Olsen EA, Raymond LD, Vilette D, Caughey B. (2005) Comparison of protease-resistant prion protein inhibitors in cell cultures infected with two strains of mouse and sheep scrapie. *Neurosci Lett.* 388: 106-11.

Kocisko DA, Caughey B. (2006) Searching for anti-prion compounds: cell-based high-throughput in vitro assays and animal testing strategies. *Methods Enzymol*. 412: 223-34.

Kocisko DA, Vaillant A, Lee KS, Arnold KM, Bertholet N, Race RE, Olsen EA, Juteau JM, Caughey B. (2006) Potent antiscrapie activities of degenerate phosphorothioate oligonucleotides. *Antimicrob Agents Chemother*. 50: 1034-44.

Korth C, May BC, Cohen FE, Prusiner SB. (2001) Acridine and phenothiazine derivatives as pharmacotherapeutics for prion disease. *Proc Natl Acad Sci U S A.* 98: 9836-41.

Kretzschmar HA, Prusiner SB, Stowring LE, DeArmond SJ. (1986) Scrapie prion proteins are synthesized in neurons. *Am J Pathol*. 122: 1-5.

Kunz C, Borghouts C, Buerger C, Groner B. (2006) Peptide aptamers with binding specificity for the intracellular domain of the ErbB2 receptor interfere with AKT signaling and sensitize breast cancer cells to Taxol. *Mol Cancer Res.* 4: 983-98.

Kurschner C, Morgan JI. (1995) The cellular prion protein (PrP) selectively binds to Bcl-2 in the yeast two-hybrid system. *Brain Res Mol Brain Res*. 30: 165-8.

Ladner RC. (1995) Constrained peptides as binding entities. *Trends Biotechnol.* 13: 426-430.
Ladogana A, Casaccia P, Ingrosso L, Cibati M, Salvatore M, Xi YG, Masullo C, Pocchiari M. (1992) Sulphate polyanions prolong the incubation period of scrapie-infected hamsters. *J Gen Virol*. 73: 661-5.

Ladogana A, Casaccia P, Ingrosso L, Cibati M, Salvatore M, Xi YG, Masullo C, Pocchiari M. (1992) Sulphate polyanions prolong the incubation period of scrapie-infected hamsters. *J Gen Virol*. 73: 661-5.

Larramendy-Gozalo C, Barret A, Daudigeos E et al. (2007) comparison of CR36, a new heparan mimetic, and pentosan polysulfate in the treatment of prion diseases. *J Gen Virol.* 88: 1062-67

Lasmézas CI, Deslys JP, Demaimay R, Adjou KT, Lamoury F, Dormont D, Robain O, Ironside J, Hauw JJ. (1996) BSE transmission to macaques. *Nature.* 381: 743-4.

Laszlo L, Lowe J, Self T, Kenward N, Landon M, McBride T, Farquhar C, McConnell I, Brown J, Hope J, et al. (1992) Lysosomes as key organelles in the pathogenesis of prion encephalopathies. *J Pathol.* 166: 333-41.

Lau AL, Yam AY, Michelitsch MM, Wang X, Gao C, Goodson RJ, Shimizu R, Timoteo G, Hall J, Medina-Selby A, Coit D, McCoin C, Phelps B, Wu P, Hu C, Chien D, Peretz D. (2007) Characterization of prion protein (PrP)-derived peptides that discriminate full-length PrPSc from PrPC. *Proc Natl Acad Sci U S A.* 104: 11551-6.

Le Borgne R, Alconada A, Bauer U, Hoflack B. (1998) The mammalian AP-3 adaptor-like complex mediates the intracellular transport of lysosomal membrane glycoproteins. *J Biol Chem.* 273: 29451-61.

Legname G, Baskakov IV, Nguyen HO, Riesner D, Cohen FE, DeArmond SJ, Prusiner SB. (2004) Synthetic mammalian prions. *Science*. 305: 673-6.

Lewis MJ, Pelham HR. (1992) Ligand-induced redistribution of a human KDEL receptor from the Golgi complex to the endoplasmic reticulum. *Cell.* 68: 353-64.

Li A, Christensen HM, Stewart LR, Roth KA, Chiesa R, Harris DA. (2007) Neonatal lethality in transgenic mice expressing prion protein with a deletion of residues 105-125. *EMBO J.* 26: 548-58.

Llewelyn CA, Hewitt PE, Knight RS, Amar K, Cousens S, Mackenzie J, Will RG. (2004) Possible transmission of variant Creutzfeldt-Jakob disease by blood transfusion. *Lancet*. 363: 417-21.

Lueck CJ, McIlwaine GG, Zeidler M. (2000) Creutzfeldt-Jakob disease and the eye. II. Ophthalmic and neuro-ophthalmic features. *Eye.* 14: 291-301.

Lugaresi E, Medori R, Montagna P, Baruzzi A, Cortelli P, Lugaresi A, Tinuper P, Zucconi M, Gambetti P. (1986) Fatal familial insomnia and dysautonomia with selective degeneration of thalamic nuclei. *N Engl J Med*. 315: 997-1003.

Luginbühl B, Kanyo Z, Jones RM, Fletterick RJ, Prusiner SB, Cohen FE, Williamson RA, Burton DR, Plückthun A. (2006) Directed evolution of an anti-prion protein scFv fragment to an affinity of 1 pM and its structural interpretation. *J Mol Biol.* 363: 75-97.

Ma J, Lindquist S. (2002a) Conversion of PrP to a self-perpetuating PrPSc-like conformation in the cytosol. *Science.* 298: 1785-8.

Ma J, Wollmann R, Lindquist S. (2002b) Neurotoxicity and neurodegeneration when PrP accumulates in the cytosol. *Science*. 298: 1781-5.

Maas E, Geissen M, Groschup MH, Rost R, Onodera T, Schätzl H, Vorberg IM. (2007) Scrapie infection of prion protein-deficient cell line upon ectopic expression of mutant prion proteins. *J Biol Chem*.282: 18702-10.

Madore N, Smith KL, Graham CH, Jen A, Brady K, Hall S, Morris R. (1999) Functionally different GPI proteins are organized in different domains on the neuronal surface. *EMBO J*. 18: 6917-26.

Magalhães AC, Baron GS, Lee KS, Steele-Mortimer O, Dorward D, Prado MA, Caughey B. (2005) Uptake and neuritic transport of scrapie prion protein coincident with infection of neuronal cells. *J Neurosci.* 25: 5207-16.

Mallucci G, Dickinson A, Linehan J, Klöhn PC, Brandner S, Collinge J. (2003) Depleting neuronal PrP in prion infection prevents disease and reverses spongiosis. *Science.* 302: 871-4.

Mangé A, Nishida N, Milhavet O, McMahon HE, Casanova D, Lehmann S. (2000) Amphotericin B inhibits the generation of the scrapie isoform of the prion protein in infected cultures. *J Virol*. 74: 3135-40.

Manson JC, Clarke AR, Hooper ML, Aitchison L, McConnell I, Hope J. (1994) 129/Ola mice carrying a null mutation in PrP that abolishes mRNA production are developmentally normal. *Mol Neurobiol*. 8: 121-7.

Marella M, Lehmann S, Grassi J, Chabry J. (2002) Filipin prevents pathological prion protein accumulation by reducing endocytosis and inducing cellular PrP release. *J Biol Chem.* 277: 25457-64.

Mathiason CK, Powers JG, Dahmes SJ, Osborn DA, Miller KV, Warren RJ, Mason GL, Hays SA, Hayes-Klug J, Seelig DM, Wild MA, Wolfe LL, Spraker TR, Miller MW, Sigurdson CJ, Telling GC, Hoover EA. (2006) Infectious prions in the saliva and blood of deer with chronic wasting disease. *Science.* 314: 133-6.

May BC, Fafarman AT, Hong SB et al. (2003) Potent inhibition of scrapie prion replication in cultured cells by bis-acridines. *Proc Natl Acad Sci U S A.* 100: 3416-3421.

McGowan, JP. (1914) Investigation into the disease of sheep called „scrapie“ with special reference to its association with sarcospoidiosis. *Rept.* 232.

McKenzie D, Kaczkowski J, Marsh R, Aiken J. (1994) Amphotericin B delays both scrapie agent replication and PrP-res accumulation early in infection. *J Virol*. 68: 7534-6.

Mead S. (2006) Prion disease genetics. *Eur J Hum Genet*. 14: 273-81.

Meusser B, Hirsch C, Jarosch E, Sommer T. (2005) ERAD: the long road to destruction. *Nat Cell Biol.* 7: 766-72.

Miller MW, Williams ES. (2003) Prion disease: horizontal prion transmission in mule deer. *Nature.* 425: 35-6.

Miller TW, Messer A. (2005) Intrabody applications in neurological disorders: progress and future prospects. *Mol Ther*. 12: 394-401.

Mironov A Jr, Latawiec D, Wille H, Bouzamondo-Bernstein E, Legname G, Williamson RA, Burton D, DeArmond SJ, Prusiner SB, Peters PJ. (2003) Cytosolic prion protein in neurons. *J Neurosci*. 23: 7183-93.

Moore RC, Lee IY, Silverman GL, Harrison PM, Strome R, Heinrich C, Karunaratne A, Pasternak SH, Chishti MA, Liang Y, Mastrangelo P, Wang K, Smit AF, Katamine S, Carlson GA, Cohen FE, Prusiner SB, Melton DW, Tremblay P, Hood LE, Westaway D. (1999) Ataxia in prion protein (PrP)-deficient mice is associated with upregulation of the novel PrP-like protein doppel. *J Mol Biol*. 292: 797-817.

Morel E, Andrieu T, Casagrande F, Gauczynski S, Weiss S, Grassi J, Rousset M, Dormont D, Chambaz J. (2005) Bovine prion is endocytosed by human enterocytes via the 37 kDa/67 kDa laminin receptor. *Am J Pathol.* 167: 1033-42.

Moroncini G, Kanu N, Solforosi L, Abalos G, Telling GC, Head M, Ironside J, Brockes JP, Burton DR, Williamson RA. (2004) Motif-grafted antibodies containing the replicative interface of cellular PrP are specific for PrPSc. *Proc Natl Acad Sci U S A.* 101: 10404-9.

Mouillet-Richard S, Ermonval M, Chebassier C, Laplanche JL, Lehmann S, Launay JM, Kellermann O. (2000) Signal transduction through prion protein. *Science*. 289: 1925-8.

Nauenburg S, Zwerschke W, Jansen-Durr P (2001) Induction of apoptosis in cervical carcinoma cells by peptide aptamers that bind to the HPV-16 E7 oncoprotein. *FASEB J.* 15: 592-594.

Nelson JA, Groudine M. (1986) Transcriptional regulation of the human cytomegalovirus major immediate-early gene is associated with induction of DNase I-hypersensitive sites. *Mol Cell Biol.* 6: 452-61.

Nikles D, Bach P, Boller K et al. (2005) Circumventing tolerance to the prion protein (PrP): vaccination with PrP-displaying retrovirus particles induces humoral immune responses against the native form of cellular PrP. *J Virol*. 79: 4033-4042.

Nishimura T, Sakudo A, Hashiyama Y, Yachi A, Saeki K, Matsumoto Y, Ogawa M, Sakaguchi S, Itohara S, Onodera T. (2007) Serum withdrawal-induced apoptosis in ZrchI prion protein (PrP) gene-deficient neuronal cell line is suppressed by PrP, independent of Doppel. *Microbiol Immunol*. 51: 457-66.

Nord K, Gunneriusson E, Ringdahl J, Stahl S, Uhlen M, Nygren PA. (1997) Binding proteins selected from combinatorial libraries of an alpha-helical bacterial receptor domain. *Nat Biotechnol.* 15: 772-777.

Novitskaya V, Bocharova OV, Bronstein I, Baskakov IV. (2006) Amyloid fibrils of mammalian prion protein are highly toxic to cultured cells and primary neurons. *J Biol Chem.* 281: 13828-36.

Nunziante M, Gilch S, Schätzl HM. (2003) Essential role of the prion protein N terminus in subcellular trafficking and half-life of cellular prion protein. *J Biol Chem*. 278: 3726-34.

Nunziante M, Kehler C, Maas E, Kassack MU, Groschup M, Schätzl HM. (2005) Charged bipolar suramin derivatives induce aggregation of the prion protein at the cell surface and inhibit PrPSc replication. *J Cell Sci.* 118: 4959-73.

Oboznaya MB, Gilch S, Titova MA et al. (2007) Antibodies to a Nonconjugated Prion Protein Peptide 95-123 Interfere with PrP(Sc) Propagation in Prion-Infected Cells. *Cell Mol Neurobiol.*

Oesch B, Westaway D, Wälchli M, McKinley MP, Kent SB, Aebersold R, Barry RA, Tempst P, Teplow DB, Hood LE, et al. (1985) A cellular gene encodes scrapie PrP 27-30 protein. *Cell.* 40: 735-46.

Orci L, Stamnes M, Ravazzola M, Amherdt M, Perrelet A, Söllner TH, Rothman JE. (1997) Bidirectional transport by distinct populations of COPI-coated vesicles. *Cell.* 90: 335-49.

Otto M, Cepek L, Ratzka P, Doehlinger S, Boekhoff I, Wiltfang J, Irle E, Pergande G, Ellers-Lenz B, Windl O, Kretzschmar HA, Poser S, Prange H. (2004) Efficacy of flupirtine on cognitive function in patients with CJD: A double-blind study. *Neurology*. 62: 714-8.

Padlan EA. (1990) On the nature of antibody combining sites: unusual structural features that may confer on these sites an enhanced capacity for binding ligands. *Proteins.* 7: 112-24.

Pamonsinlapatham P, Hadj-Slimane R, Raynaud F, Bickle M, Corneloup C, Barthelaix A, Lepelletier Y, Mercier P, Schapira M, Samson J, Mathieu AL, Hugo N, Moncorgé O, Mikaelian I, Dufour S, Garbay C, Colas P. (2008) A RasGAP SH3 peptide aptamer inhibits RasGAP-Aurora interaction and induces caspase-independent tumor cell death. *PLoS ONE.*

Pan KM, Baldwin M, Nguyen J, Gasset M, Serban A, Groth D, Mehlhorn I, Huang Z, Fletterick RJ, Cohen FE, et al. (1993) Conversion of alpha-helices into beta-sheets features in the formation of the scrapie prion proteins. *Proc Natl Acad Sci U S A.* 90: 10962-6.

Pan T, Wong BS, Liu T, Li R, Petersen RB, Sy MS. (2002) Cell-surface prion protein interacts with glycosaminoglycans. *Biochem J.* 368: 81-90.

Pankiewicz J, Prelli F, Sy MS, Kascsak RJ, Kascsak RB, Spinner DS, Carp RI, Meeker HC, Sadowski M, Wisniewski T. (2006) Clearance and prevention of prion infection in cell culture by anti-PrP antibodies. *Eur J Neurosci*. 23: 2635-47.

Parchi P, Castellani R, Capellari S, Ghetti B, Young K, Chen SG, Farlow M, Dickson DW, Sima AA, Trojanowski JQ, Petersen RB, Gambetti P. (1996) Molecular basis of phenotypic variability in sporadic Creutzfeldt-Jakob disease. *Ann Neurol.* 39: 767-78.

Parchi P, Capellari S, Chen SG, Petersen RB, Gambetti P, Kopp N, Brown P, Kitamoto T, Tateishi J, Giese A, Kretzschmar H. (1997) Typing prion isoforms. *Nature*. 386: 232-4.

Parchi P, Giese A, Capellari S, Brown P, Schulz-Schaeffer W, Windl O, Zerr I, Budka H, Kopp N, Piccardo P, Poser S, Rojiani A, Streichemberger N, Julien J, Vital C, Ghetti B, Gambetti P, Kretzschmar H. (1999) Classification of sporadic Creutzfeldt-Jakob disease based on molecular and phenotypic analysis of 300 subjects. *Ann Neurol*. 46: 224-33.

Parchi P, Zou W, Wang W, Brown P, Capellari S, Ghetti B, Kopp N, Schulz-Schaeffer WJ, Kretzschmar HA, Head MW, Ironside JW, Gambetti P, Chen SG. (2000) Genetic influence on the structural variations of the abnormal prion protein. *Proc Natl Acad Sci U S A.* 97: 10168-72.

Parkin ET, Watt NT, Turner AJ, Hooper NM. (2004) Dual mechanisms for shedding of the cellular prion protein. *J Biol Chem.* 279: 11170-8.

Parkyn CJ, Vermeulen EG, Mootoosamy RC, Sunyach C, Jacobsen C, Oxvig C, Moestrup S, Liu Q, Bu G, Jen A, Morris RJ. (2008) LRP1 controls biosynthetic and endocytic trafficking of neuronal prion protein. *J Cell Sci.* 121: 773-83.

Parry A, Baker I, Stacey R, Wimalaratna S. (2007) Long term survival in a patient with variant Creutzfeldt-Jakob disease treated with intraventricular pentosan polysulphate. *J Neurol Neurosurg Psychiatry.* 78: 733-4.

Pattison IH. (1965) Scrapie in the welsh mountain breed of sheep and its experimental transmission to goats. *Vet Rec*. 77: 1388-90.

Pauly PC, Harris DA. (1998) Copper stimulates endocytosis of the prion protein. *J Biol Chem.* 273: 33107-10.

Peden AH, Head MW, Ritchie DL, Bell JE, Ironside JW. (2004) Preclinical vCJD after blood transfusion in a PRNP codon 129 heterozygouspatient. *Lancet.* 364: 527-9.

Peelle B, Lorens J, Li W, Bogenberger J, Payan DG, Anderson DC. (2001) Intracellular protein scaffold-mediated display of random peptide libraries for phenotypic screens in mammalian cells. *Che. Biol.* 8: 521-534.

Peretz D, Williamson RA, Kaneko K, Vergara J, Leclerc E, Schmitt-Ulms G, Mehlhorn IR, Legname G, Wormald MR, Rudd PM, Dwek RA, Burton DR, Prusiner SB. (2001) Antibodies inhibit prion propagation and clear cell cultures of prion infectivity. *Nature*. 412: 739-43.

Perovic S, Pergande G, Ushijima H, Kelve M, Forrest J, Müller WE. (1995) Flupirtine partially prevents neuronal injury induced by prion protein fragment and lead acetate. *Neurodegeneration.* 4: 369-74.

Perrier V, Solassol J, Crozet C, Frobert Y, Mourton-Gilles C, Grassi J, Lehmann S. (2004) Anti-PrP antibodies block PrPSc replication in prion-infected cell cultures by accelerating PrPC degradation. *J Neurochem*. 89: 454-63.

Perry VH. (2004) The influence of systemic inflammation on inflammation in the brain: implications for chronic neurodegenerative disease. *Brain Behav Immun.* 18: 407-13.

Peters PJ, Mironov A Jr, Peretz D, van Donselaar E, Leclerc E, Erpel S, DeArmond SJ, Burton DR, Williamson RA, Vey M, Prusiner SB. (2003) Trafficking of prion proteins through a caveolae-mediated endosomal pathway. *J Cell Biol.* 162: 703-17.

Pfeifer A, Eigenbrod S, Al Khadra S et al. (2006) Lentivector-mediated RNAi efficiently suppresses prion protein and prolongs survival of scrapie-infected mice. *J Clin Invest.* 116: 3204-3210.

Pfeifer A. (2006) Lentiviral transgenesis--a versatile tool for basic research and gene therapy. *Curr Gene Ther.* 6: 535-542.

Pocchiari M, Casaccia P, Ladogana A. (1989) Amphotericin B: a novel class of antiscrapie drugs. *J Infect Dis.* 160: 795-802.

Poli G, Ponti W, Carcassola G, Ceciliani F, Colombo L, Dall'Ara P, Gervasoni M, Giannino ML, Martino PA, Pollera C, Villa S, Salmona M. (2003) In vitro evaluation of the anti-prionic activity of newly synthesized congo red derivatives. *Arzneimittelforschung* 53: 875-88.

Polymenidou M, Heppner FL, Pellicioli EC, Urich E, Miele G, Braun N, Wopfner F, Schätzl HM, Becher B, Aguzzi A. (2004) Humoral immune response to native eukaryotic prion protein correlates with anti-prion protection. *Proc Natl Acad Sci U S A.* 101:14670-6.

Prado MA, Alves-Silva J, Magalhães AC, Prado VF, Linden R, Martins VR, Brentani RR. (2004) PrPc on the road: trafficking of the cellular prion protein. *J Neurochem*. 88: 769-81.

Premzl M, Sangiorgio L, Strumbo B, Marshall Graves JA, Simonic T, Gready JE. (2003) Shadoo, a new protein highly conserved from fish to mammals and with similarity to prion protein. *Gene*. 314: 89-102.

Priola SA. (1999) Prion protein and species barriers in the transmissible spongiform encephalopathies. *Biomed Pharmacother*. 5: 27-33.

Priola SA, Raines A, Caughey WS. (2000) Porphyrin and phthalocyanine antiscrapie compounds. *Science.*;287: 1503-1506.

Priola SA, Chabry J, Chan K. (2001) Efficient conversion of normal prion protein (PrP) by abnormal hamster PrP is determined by homology at amino acid residue 155. *J Virol.* 75: 4673-80.

Priola SA, Raines A, Caughey W. (2003) Prophylactic and therapeutic effects of phthalocyanine tetrasulfonate in scrapie-infected mice. *J Infect Dis*. 188: 699-705.

Proske D, Gilch S, Wopfner F, Schätzl HM, Winnacker EL, Famulok M. (2002) Prion-protein-specific aptamer reduces PrPSc formation. *Chembiochem.* 3: 717-25.

Prusiner SB. (1982) Novel proteinaceous infectious particles cause scrapie. *Science.* 216: 136-44.

Prusiner SB, Groth DF, Bolton DC, Kent SB, Hood LE. (1984) Purification and structural studies of a major scrapie prion protein. *Cell.* 38: 127-34.

Prusiner SB, Scott M, Foster D, Pan KM, Groth D, Mirenda C, Torchia M, Yang SL, Serban D, Carlson GA, et al. (1990) Transgenetic studies implicate interactions between homologous PrP isoforms in scrapie prion replication. *Cell.* 63: 673-86.

Prusiner SB. (1998) Prions. *Proc Natl Acad Sci U S A.* 95: 13363-83.

Prusiner SB. (2001) Shattuck lecture--neurodegenerative diseases and prions. *N Engl J Med*. 344: 1516-26.

Race RE, Fadness LH, Chesebro B. (1987) Characterization of scrapie infection in mouse neuroblastoma cells. *J Gen Virol*. 68: 1391-9.

Rambold AS, Miesbauer M, Rapaport D, Bartke T, Baier M, Winklhofer KF, Tatzelt J. (2006) Association of Bcl-2 with misfolded prion protein is linked to the toxicpotential of cytosolic PrP. *Mol Biol Cell*. 17: 3356-68.

Rambold AS, Müller V, Ron U, Ben-Tal N, Winklhofer KF, Tatzelt J. (2008) Stress-protective signalling of prion protein is corrupted by scrapie prions. *EMBO J*. 27: 1974-84.

Rane NS, Yonkovich JL, Hegde RS. (2004) Protection from cytosolic prion protein toxicity by modulation of protein translocation. *EMBO J.* 23: 4550-9.

Rangel A, Burgaya F, Gavín R, Soriano E, Aguzzi A, Del Río JA. (2007) Enhanced susceptibility of Prnp-deficient mice to kainate-induced seizures, neuronal apoptosis, and death: Role of AMPA/kainate receptors. *J Neurosci Res*. 85: 2741-55.

Raymond GJ, Olsen EA, Lee KS, Raymond LD, Bryant PK 3rd, Baron GS, Caughey WS, Kocisko DA, McHolland LE, Favara C, Langeveld JP, van Zijderveld FG, Mayer RT, Miller MW, Williams ES, Caughey B. (2006) Inhibition of protease-resistant prion protein formation in a transformed deer cell line infected with chronic wasting disease. *J Virol.* 80: 596-604.

Rieger R, Edenhofer F, Lasmézas CI, Weiss S. (1997) The human 37-kDa laminin receptor precursor interacts with the prion protein in eukaryotic cells. *Nat Med.* 3: 1383-8.

Riek R, Hornemann S, Wider G, Billeter M, Glockshuber R, Wüthrich K. (1996) NMR structure of the mouse prion protein domain PrP(121-321).*Nature.* 382: 180-2.

Riek R, Hornemann S, Wider G, Glockshuber R, Wüthrich K. (1997) NMR characterization of the full-length recombinant murine prion protein, mPrP(23-231). *FEBS Lett.* 413: 282-8.

Riesner D. (2003) Biochemistry and structure of PrP(C) and PrP(Sc). *Br Med Bull.* 66: 21-33
Rivera-Milla E, Stuermer CA, Málaga-Trillo E. (2003) An evolutionary basis for scrapie disease: identification of a fish prion mRNA. *Trends Genet*. 19: 72-5.

Robakis NK, Devine-Gage EA, Jenkins EC, Kascsak RJ, Brown WT, Krawczun MS, Silverman WP. (1986) Localization of a human gene homologous to the PrP gene on the p arm of chromosome 20 and detection of PrP-related antigens in normal human brain. *Biochem Biophys Res Commun*. 140: 758-65.

Roucou X, Guo Q, Zhang Y, Goodyer CG, LeBlanc AC. (2003) Cytosolic prion protein is not toxic and protects against Bax-mediated cell death in human primary neurons. *J Biol Chem.* 278: 40877-81.

Roucou X, Giannopoulos PN, Zhang Y, Jodoin J, Goodyer CG, LeBlanc A. (2005) Cellular prion protein inhibits proapoptotic Bax conformational change in human neurons and in breast carcinoma MCF-7 cells. *Cell Death Differ*. 12: 783-95.

Rubenstein R, Carp RI, Callahan SM. (1984) In vitro replication of scrapie agent in a neuronal model: infection of PC12 cells. *J Gen Virol*. 65 : 2191-8.

Safar J, Wille H, Itri V, Groth D, Serban H, Torchia M, Cohen FE, Prusiner SB. (1998) Eight prion strains have PrP(Sc) molecules with different conformations. *Nat Med*. 4: 1157-65.

Sakudo A, Lee DC, Nakamura I, Taniuchi Y, Saeki K, Matsumoto Y, Itohara S, Ikuta K, Onodera T. (2005) Cell-autonomous PrP-Doppel interaction regulates apoptosis in PrP gene-deficient neuronal cells. *Biochem Biophys Res Commun.* 333: 448-54.

Schätzl HM, Da Costa M, Taylor L, Cohen FE, Prusiner SB. (1995) Prion protein gene variation among primates. *J Mol Biol*. 254: 362-74.

Schätzl HM, Laszlo L, Holtzman DM, Tatzelt J, DeArmond SJ, Weiner RI, Mobley WC, Prusiner SB. (1997) A hypothalamic neuronal cell line persistently infected with scrapie prions exhibits apoptosis. *J Virol.* 71: 8821-31.

Schettler E, Steinbach F, Eschenbacher-Kaps I, Gerst K, Muessdoerffer F, Risch K, Streich WJ, Frölich K. (2006) Surveillance for prion disease in cervids, Germany. *Emerg Infect Dis.* 12: 319-22.

Schmitt-Ulms G, Legname G, Baldwin MA, Ball HL, Bradon N, Bosque PJ, Crossin KL, Edelman GM, DeArmond SJ, Cohen FE, Prusiner SB. (2001) Binding of neural cell adhesion molecules (N-CAMs) to the cellular prion protein. *J Mol Biol*. 314: 1209-25.

Schonberger O, Horonchik L, Gabizon R, Papy-Garcia D, Barritault D, Taraboulos A. (2003) Novel heparan mimetics potently inhibit the scrapie prion protein and its endocytosis. *Biochem Biophys Res Commun*. 312: 473-9.

Schwarz A, Kratke O, Burwinkel M et al. (2003) Immunisation with a synthetic prion protein-derived peptide prolongs survival times of mice orally exposed to the scrapie agent. *Neurosci Lett.* 350: 187-189.

Scott M, Foster D, Mirenda C, Serban D, Coufal F, Wälchli M, Torchia M, Groth D, Carlson G, DeArmond SJ, et al. (1989) Transgenic mice expressing hamster prion protein produce species-specific scrapie infectivity and amyloid plaques. *Cell.* 59: 847-57.

Scott MR, Köhler R, Foster D, Prusiner SB. (1992) Chimeric prion protein expression in cultured cells and transgenic mice*. Protein Sci.* 1: 986-97.

Scott M, Groth D, Foster D, Torchia M, Yang SL, DeArmond SJ, Prusiner SB. (1993) Propagation of prions with artificial properties in transgenic mice expressing chimeric PrP genes. *Cell.* 73: 979-88.

Scott MR, Groth D, Tatzelt J, Torchia M, Tremblay P, DeArmond SJ, Prusiner SB. (1997) Propagation of prion strains through specific conformers of the prion protein. *J Virol.* 71: 9032-44.

Sethi S, Lipford G, Wagner H, Kretzschmar H. (2002) Postexposure prophylaxis against prion disease with a stimulator of innate immunity. *Lancet*.360: 229-30.

Shyng SL, Heuser JE, Harris DA. (1994) A glycolipid-anchored prion protein is endocytosed via clathrin-coated pits. *J Cell Biol.* 125: 1239-50.

Shyng SL, Lehmann S, Moulder KL et al. (1995) Sulfated glycans stimulate endocytosis of the cellular isoform of the prioni protein, PrPC, in cultured cells. *J Biol Chem.* 270: 30221-29

Sigurdson CJ, Williams ES, Miller MW, Spraker TR, O'Rourke KI, Hoover EA. (1999) Oral transmission and early lymphoid tropism of chronic wasting disease PrPres in mule deer fawns (Odocoileus hemionus). *J Gen Virol.* 80: 2757-64.

Sigurdson CJ, Spraker TR, Miller MW, Oesch B, Hoover EA. (2001) PrP(CWD) in the myenteric plexus, vagosympathetic trunk and endocrine glands of deer with chronic wasting disease. *J Gen Virol.* 82: 2327-34.

Sigurdsson EM, Brown DR, Daniels M et al. (2002) Immunization delays the onset of prion disease in mice. *Am J Pathol*. 161: 13-17.

Sigurdsson EM, Brown DR, Daniels M, Kascsak RJ, Kascsak R, Carp R, Meeker HC, Frangione B, Wisniewski T. (2002) Immunization delays the onset of prion disease in mice. *Am J Pathol*. 161: 13-7.

Silveira JR, Raymond GJ, Hughson AG, Race RE, Sim VL, Hayes SF, Caughey B. (2005) The most infectious prion protein particles. *Nature*. 437: 257-61.

Simoneau S, Rezaei H, Salès N, Kaiser-Schulz G, Lefebvre-Roque M, Vidal C, Fournier JG, Comte J, Wopfner F, Grosclaude J, Schätzl H, Lasmézas CI. (2007) In vitro and in vivo neurotoxicity of prion protein oligomers. *PLoS Pathog.* 3:e125.

Solassol J, Crozet C, Perrier V et al. (2004) Cationic phosphorus-containing dendrimers reduce prion replication both in cell culture and in mice infected with scrapie. *J Gen Virol.* 85: 1791-1799.

Solforosi L, Bellon A, Schaller M, Cruite JT, Abalos GC, Williamson RA. (2007) Toward molecular dissection of PrPC-PrPSc interactions. *J Biol Chem.* 282: 7465-71.

Solforosi L, Criado JR, McGavern DB, Wirz S, Sánchez-Alavez M, Sugama S, DeGiorgio LA, Volpe BT, Wiseman E, Abalos G, Masliah E, Gilden D, Oldstone MB, Conti B, Williamson RA. (2004) Cross-linking cellular prion protein triggers neuronal apoptosis in vivo. *Science*. 303: 1514-6.

Soto C, Kascsak RJ, Saborio GP et al. (2000) Reversion of prion protein conformational changes by synthetic beta-sheet breaker peptides. *Lancet*. 355: 192-197.

Souan L, Tal Y, Felling Y et al. (2001) Modulation of proteinase-K resistant prion protein by prion peptide immunization. *Eur J Immunol*. 31: 2338-2346.

Sparkes RS, Simon M, Cohn VH, Fournier RE, Lem J, Klisak I, Heinzmann C, Blatt C, Lucero M, Mohandas T, et al. (1986) Assignment of the human and mouse prion protein genes to homologous chromosomes. *Proc Natl Acad Sci U S A.* 83: 7358-62.

Spielhaupter C, Schätzl HM. (2001) PrPC directly interacts with proteins involved in signaling pathways. *J Biol Chem*. 276: 44604-12.

Stahl N, Baldwin MA, Hecker R, Pan KM, Burlingame AL, Prusiner SB. (1992) Glycosylinositol phospholipid anchors of the scrapie and cellular prion proteins contain sialic acid. *Biochemistry.* 31: 5043-53.

Stevens C, Hupp TR. (2008) Novel insights into DAPK autophagic signalling using peptide aptamer combinatorial protein-interaction screens. *Autophagy.* 4: 531-3.

Strumbo B, Ronchi S, Bolis LC, Simonic T. (2001) Molecular cloning of the cDNA coding for Xenopus laevis prion protein. *FEBS Lett*. 508: 170-4.

Sunyach C, Jen A, Deng J, Fitzgerald KT, Frobert Y, Grassi J, McCaffrey MW, Morris R. (2003) The mechanism of internalization of glycosylphosphatidylinositol-anchored prion protein. *EMBO J.* 22: 3591-601.

Supattapone S, Nguyen HO, Cohen FE et al. (1999) Elimination of prions by branched polyamines and implications for therapeutics. *Proc Natl Acad Sci U S A.* 96: 14529-14534.
Supattapone S, Wille H, Uyechi L et al. (2001) Branched polyamines cure prion-infected neuroblastoma cells. *J Virol*. 75: 3453-3461.

Suzuki T, Kurokawa T, Hashimoto H, Sugiyama M. (2002) cDNA sequence and tissue expression of Fugu rubripes prion protein-like: a candidate for the teleost orthologue of tetrapod PrPs. *Biochem Biophys Res Commun*. 294: 912-7.

Taraboulos A, Raeber AJ, Borchelt DR, Serban D, Prusiner SB. (1992) Synthesis and trafficking of prion proteins in cultured cells. *Mol Biol Cell*. 3: 851-63.

Taraboulos A, Scott M, Semenov A, Avrahami D, Prusiner SB. (1994) Biosynthesis of the prion proteins in scrapie-infected cells in culture. *Braz J Med Biol Res*. 27: 303-7.

Taraboulos A, Scott M, Semenov A, Avrahami D, Laszlo L, Prusiner SB. (1995) Cholesterol depletion and modification of COOH-terminal targeting sequence of the prion protein inhibit formation of the scrapie isoform. *J Cell Biol.* 129: 121-32.

Tatzelt J, Prusiner SB, Welch WJ. (1996) Chemical chaperones interfere with the formation of scrapie prion protein. *EMBO J.* 15: 6363-73.

Telling GC, Scott M, Hsiao KK, Foster D, Yang SL, Torchia M, Sidle KC, Collinge J, DeArmond SJ, Prusiner SB. (1994) Transmission of Creutzfeldt-Jakob disease from humans to transgenic mice expressing chimeric human-mouse prion protein. *Proc Natl Acad Sci U S A.* 91: 9936-40.

Telling GC, Scott M, Mastrianni J, Gabizon R, Torchia M, Cohen FE, DeArmond SJ, Prusiner SB. (1995) Prion propagation in mice expressing human and chimeric PrP transgenes implicates the interaction of cellular PrP with another protein. *Cell.* 83: 79-90.

Telling GC, Parchi P, DeArmond SJ, Cortelli P, Montagna P, Gabizon R, Mastrianni J, Lugaresi E, Gambetti P, Prusiner SB. (1996) Evidence for the conformation of the pathologic

isoform of the prion protein enciphering and propagating prion diversity. *Science.* 274: 2079-82.

Tessier PM, Lindquist S. (2007) Prion recognition elements govern nucleation, strain specificity and species barriers. *Nature.* 447: 556-61.

Tilly G, Chapuis J, Vilette D et al. (2003) Efficient and specific down-regulation of prion protein expression by RNAi. *Biochem Biophys Res Commun*. 305: 548-551.

Tobler I, Gaus SE, Deboer T, Achermann P, Fischer M, Rülicke T, Moser M, Oesch B, McBride PA, Manson JC. (1996) Altered circadian activity rhythms and sleep in mice devoid of prion protein. *Nature*.380: 639-42.

Todd NV, Morrow J, Doh-ura K, Dealler S, O'Hare S, Farling P, Duddy M, Rainov NG. (2005) Cerebroventricular infusion of pentosan polysulphate in human variant Creutzfeldt-Jakob disease. *J Infect.* 50: 394-6.

Tomai E, Butz K, Lohrey C, von Weizsäcker F, Zentgraf H, Hoppe-Seyler F. (2006) Peptide aptamer-mediated inhibition of target proteins by sequestration into aggresomes. *J Biol Chem.* 281: 21345-52.

Trahtenherts A, Gal-Tanamy M, Zemel R, Bachmatov L, Loewenstein S, Tur-Kaspa R, Benhar I. (2008) Inhibition of hepatitis C virus RNA replicons by peptide aptamers. *Antiviral Res.* 77: 195-205.

Vella LJ, Sharples RA, Lawson VA, Masters CL, Cappai R, Hill AF. (2007) Packaging of prions into exosomes is associated with a novel pathway of PrP processing. *J Pathol.* 211: 582-90.

Vetrugno V, Cardinale A, Filesi I et al. (2005) KDEL-tagged anti-prion intrabodies impair PrP lysosomal degradation and inhibit scrapie infectivity. *Biochem Biophys Res Commun.* 338: 1791-1797.

Vey M, Pilkuhn S, Wille H, Nixon R, DeArmond SJ, Smart EJ, Anderson RG, araboulos A, Prusiner SB. (1996) Subcellular colocalization of the cellular and scrapie prion proteins in aveolae-like membranous domains. *Proc Natl Acad Sci U S A.* 93: 14945-9.

Vilette D, Andreoletti O, Archer F, Madelaine MF, Vilotte JL, Lehmann S, Laude H. (2001) Ex vivo propagation of infectious sheep scrapie agent in heterologous epithelial cells expressing ovine prion protein. *Proc Natl Acad Sci U S A*. 98: 4055-9.

Vorberg I, Groschup MH, Pfaff E, Priola SA. (2003) Multiple amino acid residues within the rabbit prion protein inhibit formation of its abnormal isoform. *J Virol.* 77: 2003-9.

Vorberg I, Raines A, Priola SA. (2004) Acute formation of protease-resistant prion protein does not always lead to persistent scrapie infection in vitro. *J Biol Chem*. 279: 29218-25.

Vorberg I, Raines A, Story B, Priola SA. (2004) Susceptibility of common fibroblast cell lines to transmissible spongiform encephalopathy agents. *J Infect Dis.* 189: 431-9.

Wadsworth JD, Joiner S, Hill AF, Campbell TA, Desbruslais M, Luthert PJ, Collinge J. (2001) Tissue distribution of protease resistant prion protein in variant Creutzfeldt-Jakob disease using a highly sensitive immunoblotting assay. *Lancet.* 358: 171-80.

Wadsworth JD, Hill AF, Beck JA, Collinge J. (2003) Molecular and clinical classification of human prion disease. *Br Med Bull*. 66: 241-54.

Wadsworth JD, Collinge J. (2007) Update on human prion disease. *Biochim Biophys Acta.* 1772: 598-609.

Watts JC, Drisaldi B, Ng V, Yang J, Strome B, Horne P, Sy MS, Yoong L, Young R, Mastrangelo P, Bergeron C, Fraser PE, Carlson GA, Mount HT, Schmitt-Ulms G, Westaway D. (2007) The CNS glycoprotein Shadoo has PrP(C)-like protective properties and displays reduced levels in prion infections. *EMBO J.* 26: 4038-50.

Wells GA, Scott AC, Johnson CT, Gunning RF, Hancock RD, Jeffrey M, Dawson M, Bradley R. (1987) A novel progressive spongiform encephalopathy in cattle.*Vet Rec.* 121: 19-20.

Westaway D, Cooper C, Turner S, Da Costa M, Carlson GA, Prusiner SB. (1994) Structure and polymorphism of the mouse prion protein gene. *Proc Natl Acad Sci U S A.* 91: 418-22.

White AR, Enever P, Tayebi M, Mushens R, Linehan J, Brandner S, Anstee D, Collinge J, Hawke S. (2003) Monoclonal antibodies inhibit prion replication and delay the development of prion disease. *Nature.* 422: 80-3.

White MD, Farmer M, Mirabile I, Brandner S, Collinge J, Mallucci GR. (2008) Single treatment with RNAi against prion protein rescues early neuronal dysfunction and prolongs survival in mice with prion disease. *Proc Natl Acad Sci U S A.* 105: 10238-43.

Whittle IR, Knight RS, Will RG. (2006) Unsuccessful intraventricular pentosan polysulphate treatment of variant Creutzfeldt-Jakob disease. *Acta Neurochir (Wien).* 148: 677-9.

Wilesmith JW, Wells GA. (1991) Bovine spongiform encephalopathy. *Curr Top Microbiol Immunol*. 172: 21-38.

Will RG, Ironside JW, Zeidler M, Cousens SN, Estibeiro K, Alperovitch A, Poser S, Pocchiari M, Hofman A, Smith PG. (1996) A new variant of Creutzfeldt-Jakob disease in the UK. *Lancet.* 347: 921-5.

Wille H, Michelitsch MD, Guenebaut V, Supattapone S, Serban A, Cohen FE, Agard DA, Prusiner SB. (2002) Structural studies of the scrapie prion protein by electron crystallography. *Proc Natl Acad Sci U S A.* 99: 3563-8.

Williams ES, Young S. (1980) Chronic wasting disease of captive mule deer: a spongiform encephalopathy. *J Wildl Dis.* 16: 89-98.

Wilson R, Bate C, Boshuizen R et al. (2007) Squalestatin alters the intracellular trafficking of a neurotoxic prion peptide. *BMC Neurosci.* 8: 99.

Winklhofer KF and Tatzelt J. (2000) Cationic lipopolyamines induce degradation of PrPSc in scrapie-infected mouse neuroblastoma cells. *Biol Chem.* 381: 463-469.

Wisniewski T and Sigurdsson EM. (2002) Immunization treatment approaches in Alzheimer's and prion diseases. *Curr Neurol Neurosci Rep*. 2: 400-404.

Woodman R, Yeh JT, Laurenson S, Ko Ferrigno P. (2005) Design and validation of a neutral protein scaffold for the presentation of peptide aptamers. *J Mol Biol.* 352: 1118-33.

Wopfner F, Weidenhöfer G, Schneider R, von Brunn A, Gilch S, Schwarz TF, Werner T, Schätzl HM. (1999) Analysis of 27 mammalian and 9 avian PrPs reveals high conservation of flexible regions of the prion protein. *J Mol Biol*. 289: 1163-78.

Wyatt JM, Pearson GR, Smerdon TN, Gruffydd-Jones TJ, Wells GA, Wilesmith JW. (1991) Naturally occurring scrapie-like spongiform encephalopathy in five domestic cats. *Vet Rec.* 129: 233-6.

Yun SW, Ertmer A, Flechsig E et al. (2007) The tyrosine kinase inhibitor imatinib mesylate delays prion neuroinvasion by inhibiting prion propagation in the periphery. *J Neurovirol.* 13: 328-337.

Zeidler M, Johnstone EC, Bamber RW, Dickens CM, Fisher CJ, Francis AF, Goldbeck R, Higgo R, Johnson-Sabine EC, Lodge GJ, McGarry P, Mitchell S, Tarlo L, Turner M, Ryley P, Will RG. (1997) New variant Creutzfeldt-Jakob disease: psychiatric features. *Lancet.* 350: 908-10.

Zhang X, Li L, Jung J, Xiang S, Hollmann C, Choi YS. (2001) The distinct roles of T cell-derived cytokines and a novel follicular dendritic cell-signaling molecule 8D6 in germinal center-B cell differentiation. *J Immunol*. 167: 49-56.

Zhao BM, Hoffmann FM. (2006) Inhibition of transforming growth factor-beta1-induced signaling and epithelial-to-mesenchymal transition by the Smad-binding peptide aptamer Trx-SARA. *Mol Biol Cell.* 17: 3819-31.

Zigas V, Gajdusek DC. (1957) Kuru: clinical study of a new syndrome resembling paralysis agitans in natives of the Eastern Highlands of Australian New Guinea. *Med J Aust.* 44: 745-54.

Appendix

Publications since 2000

1. **Gilch S**, Krammer C, Schätzl HM. Targeting prion proteins in neurodegenerative disease. *Expert Opin Biol Ther*. **2008** 8:923-40.
2. Aguib Y, **Gilch S**, Krammer C, Ertmer A, Groschup MH, Schätzl HM. Neuroendocrine cultured cells counteract persistent prion infection by down-regulation of PrPc.*Mol Cell Neurosci.* **2008** 38:98-109.
3. Diemer C, Schneider M, Seebach J, Quaas J, Frösner G, Schätzl HM, **Gilch S**. Cell type specific cleavage of nucleocapsid protein by effector caspases during SARS coronavirus infection. *J Mol Biol*. **2008** 376:23-34.
4. **Gilch S**, Schmitz F, Aguib Y, Kehler C, Bülow S, Bauer S, Kremmer E, Schätzl HM. CpG and LPS can interfere negatively with prion clearance in macrophage and microglial cells *FEBS J*. **2007** 274:5834-44.
5. Yun SW, Ertmer A, Flechsig E, **Gilch S**, Riederer P, Gerlach M, Schätzl HM, Klein MA The tyrosine kinase inhibitor imatinib mesylate delays prion neuroinvasion by inhibiting prion propagation in the periphery. *J Neurovirol*. **2007** 13:328-37.
6. **Gilch S**, Kehler C, Schätzl HM. Peptide aptamers expressed in the secretory pathway interfere with cellular PrPSc formation. *J Mol Biol*. **2007** 371:362-73.
7. **Gilch S**, Nunziante M, Ertmer A, Schätzl HM. Strategies for eliminating PrP(c) as substrate for prion conversion and for enhancing PrP(Sc) degradation. *Vet Microbiol*. **2007** 123:377-86.
8. Ertmer A, Huber V, **Gilch S**, Yoshimori T, Erfle V, Duyster J, Elsässer HP, Schätzl HM. The anticancer drug imatinib induces cellular autophagy. *Leukemia*. **2007** 21:936-42.
9. Handisurya A, **Gilch S**, Winter D, Shafti-Keramat S, Maurer D, Schätzl HM, Kirnbauer R. Vaccination with prion peptide-displaying papilloma virus-like particles induces autoantibodies to normal prion protein that interfere with pathologic prion protein production in infected cells. *FEBS J*. **2007** 274:1747-58.
10. Oboznaya MB, **Gilch S**, Titova MA, Koroev DO, Volkova TD, Volpina OM, Schätzl HM. Antibodies to a nonconjugated prion protein peptide 95-123 interfere with PrP(Sc) propagation in prion-infected cells. *Cell Mol Neurobiol*. **2007** 27:271-84.
11. Stengel A, Bach C, Vorberg I, Frank O, **Gilch S**, Lutzny G, Seifarth W, Erfle V, Maas E, Schätzl H, Leib-Mösch C, Greenwood AD. Prion infection influences murine endogenous retrovirus expression in neuronal cells. *Biochem Biophys Res Commun*. **2006** 343:825-31.
12. **Gilch S**, Kehler C, Schätzl HM. The prion protein requires cholesterol for cell surface localization. *Mol Cell Neurosci*. **2006** 31:346-53.
13. Ertmer A, **Gilch S**, Yun SW, Flechsig E, Klebl B, Stein-Gerlach M, Klein MA, Schätzl HM. The tyrosine kinase inhibitor STI571 induces cellular clearance of PrPSc in prion-infected cells. *J Biol Chem*. **2004** 279:41918-27.
14. **Gilch S**, Nunziante M, Ertmer A, Wopfner F, Laszlo L, Schätzl HM. Recognition of lumenal prion protein aggregates by post-ER quality control mechanisms is mediated by the preoctarepeat region of PrP. *Traffic*. **2004** 5:300-13.
15. Nunziante M, **Gilch S**, Schätzl HM. Prion diseases: from molecular biology to intervention strategies. *Chembiochem*. **2003** 4:1268-84.
16. **Gilch S**, Schätzl HM. Promising developments bringing prion diseases closer to therapy and prophylaxis. *Trends Mol Med*. **2003** 9:367-9.
17. **Gilch S**, Wopfner F, Renner-Müller I, Kremmer E, Bauer C, Wolf E, Brem G, Groschup MH, Schätzl HM. Polyclonal anti-PrP auto-antibodies induced with dimeric PrP interfere efficiently with PrPSc propagation in prion-infected cells. *J Biol Chem*. **2003** 278:18524-31.

18. Nunziante M, **Gilch S**, Schätzl HM. Essential role of the prion protein N terminus in subcellular trafficking and half-life of cellular prion protein. *J Biol Chem*. **2003** 278:3726-34.
19. Proske D*, **Gilch S***, Wopfner F, Schätzl HM, Winnacker EL, Famulok M. Prion-protein-specific aptamer reduces PrPSc formation. *Chembiochem*. **2002** 3:717-25.
*: authors contributed equally
20. **Gilch S**, Winklhofer KF, Groschup MH, Nunziante M, Lucassen R, Spielhaupter C, Muranyi W, Riesner D, Tatzelt J, Schätzl HM. Intracellular re-routing of prion protein prevents propagation of PrP(Sc) and delays onset of prion disease. *EMBO J*. **2001** 20:3957-66.
21. **Gilch S**, Spielhaupter C, Schätzl HM. Shortest known prion protein allele in highly BSE-susceptible lemurs. *Biol Chem*. **2000** 381:521-3.

Manuscripts in press

1. Krammer C, Vorberg I, Schätzl HM, **Gilch S**. Prion proteins as targets in neurodegenerative disease. *Infectious Disorders – Dug Targets*. **2008** (*in press*).
2. Diemer C, Schneider M, Schätzl HM, **Gilch S**. Modulation of cell death by SARS-CoV structural and accessory proteins. **2008** in Molecular Biology of the SARS-Coronavirus (ed. Sunil Lal) (in press)

Danksagung

Mein herzlichster Dank geht an Herrn Prof. Hermann M. Schätzl für die Möglichkeit, meine Doktorarbeit über das spannende Thema „Prionen“ schreiben zu können und für seine wertvolle Unterstützung über viele Jahre hinweg. Ohne ihn wäre vieles nicht möglich gewesen!

Für die freundliche Übernahme der Betreuung meiner Promotion möchte ich mich bei Herrn Prof. Dr. J. Bauer, Lehrstuhl für Tierhygiene am Wissenschaftszentrum Weihenstephan der TUM, bedanken.

Für die tatkräftige Unterstützung auf der Suche nach wirksamen Peptid-Aptameren, und für die gute Laune und Fröhlichkeit, die sie stets verbreitet hat, bedanke ich mich Claudia Kehler.

Ein herzliches Dankeschön an alle Kollegen der AGs Schätzl und Vorberg für die Kollegialität und die angenehme Atmosphäre im Labor, besonders an Claudia Wex und Carmen Krammer, die immer auch für Party im und ausserhalb des Labors zu begeistern waren, und an meinen langjährigsten Kollegen Max Nunziante.

Für Hilfe in allen organisatorischen Belangen bedanke ich mich bei Doris Pelz, sowie bei Kata Masic für die Sorge um unser aller Wohl.

Vielen Dank an Franziska Hammerschmidt und Alexa Ertmer, deren Freundschaft ich nicht mehr missen möchte. Die beiden „treuen Seelen“ hatten immer ein offenes Ohr für Probleme in Zeiten der Frustration.